Electronic Supplementary Material (ESI) for Inorganic Chemistry Frontiers.

Supplementary information for

Vegard's Law in Multivariate Libraries of Porous Interpenetrated Zirconia-Organic Frameworks

Jacob I. Furst,[1,2,‡] Jacob T. Bryant, [1,2,‡] Kyle R. Langlois, [1,2] Shea D. Myers,[3] Azina Rahmani, [1,2] David C. Fairchild, [1,2] Rishabh Mehta, [1,2] Titel Jurca, [1,2] Jason B. Benedict,[3*] Fernando J. Uribe-Romo[1,2*]

[1]Department of Chemistry and [2]Renewable Energy and Chemical Transformations Cluster, University of Central Florida, Orlando, FL 32816 United States.

[3]Department of Chemistry, University at Buffalo, Natural Sciences Complex, Buffalo, 14260-3000, USA

‡ These authors contributed equally to this work.

* To whom all correspondence should be addressed:

Prof. Uribe-Romo: fernando@ucf.edu

Prof. Benedict: jbb6@buffalo.edu

Contents

Section S1. **Materials and methods.**

All starting materials, reagents, and solvents were obtained from commercial sources (Aldrich, Fisher, VWR) and used without further purification unless otherwise specified. All reactions were performed at ambient laboratory conditions, and no precautions were taken to exclude oxygen or atmospheric moisture unless otherwise specified. Anhydrous *N,N*-dimethylformamide (DMF), toluene, tetrahydrofuran (THF), and dichloromethane (CH_2Cl_2) were purified using a custom-built alumina-column based solvent purification system (Innovative Technology). Triethylamine and *N,N*-diisopropylamine were bubbled with N_2 gas for 30 minutes before use. 1,2-dichlorobenzene was dried for over 4 Å under N_2 for 24 h. Deuterated solvents ($CDCl_3$, DMSO-d_6) were obtained from Cambridge Isotope Lab. 20 wt% DCl in D_2O was obtained from Sigma-Aldrich. Linkers **H_2QPDC-Me**[S1], and **H_2PEPEP-Me**[S2], **PEPEP-OMe**[S3], **PEPEP-Fc**[S3], **PPP-Me**[S4], **S1**[S5], **S3**[S6], **S9**[S7], and **S10**[S2], were synthesized according to previously published procedures.

High-resolution solution ^{1}H, ^{13}C, and ^{19}F nuclear magnetic resonance (NMR) spectra were collected at RT using a Bruker AVANCE-III 400 MHz spectrometer. The chemical shifts were reported relative to tetramethyl silane at 0 ppm, using the solvent residual signal. NMR data was processed using MestReNova package (v. 10.0.2).

Fourier-transform infrared (FT-IR) spectra were recorded using a Perkin Elmer Spectrum ONE universal FT-IR ATR. 32 scans were collected for each sample from 4000-400 cm^{-1}. Data was corrected using the spectra analysis software.

In house laboratory powder X-ray diffraction (PXRD) was collected using a Rigaku MiniFlex 600 θ-2θ diffractometer in Bragg-Brentano geometry with a 300 mm goniometer diameter, Ni-filtered CuKα radiation (λ = 1.5418 Å), at 600 W power (40 kV, 15 mA), equipped with a high-resolution D/tex 250 detector, 5.0º incident and receiving Soller slits, a 0.625º divergent slit, a 1.25º scattering slit, a 0.3 mm receiving slit, a Ni-CuKβ filter, and an antiscattering blade. Samples were analyzed from 3 to 40 2θ-degrees with 0.02º per step and a scan rate of 0.25 2θ-degrees min^{-1} with spinning. Samples were prepared by dropping the powder sample in a zero-background sample holder and gently tapping the powder with a razor blade spatula forming a smooth surface.

PXRD Data for indexing and refinement was collected using a Panalytical Empyrean diffractometer in Bragg-Brentano geometry with a 240 mm goniometer radius, Ni-filtered CuKα radiation (λ = 1.540598 Å), at 1800 W power (45 kV, 40 mA), 0.02 rad incident slit and 0.02º receiving Soller slit, a 0.125º divergent slit, a 0.5º anti-scattering slit, a fixed 4 mm mask, and a Ni-CuKβ filter. Samples were analyzed from 2 to 40 2θ-degrees with 0.0501º per step and a scan rate of 3.8 2θ-degrees min^{-1} with spinning. The diffractometer was equipped with an X'Cellerator detector. Samples were prepared by dropping the powder sample in a zero-background sample holder and gently tapping the powder with a razor blade spatula forming a smooth surface.

A single crystal suitable for X-ray diffraction was selected from each sample and mounted on the tip of a glass fiber with oil and placed on a Bruker SMART APEX II CCD diffractometer installed with a rotating anode source (Mo-Kα radiation, λ = 0.71073 Å) with a detector distance of 40.00 mm from the crystal and a 2θ-angle of -10°. For samples 40% and 60% mol input of **PEPEP-Me** data was collected at room temperature (298K). For samples 20% and 80% mol input of **PEPEP-Me** data was collected at 90(1)K using an Oxford cryostream nitrogen gas-flow apparatus. For each sample, a total of 1800 frames were collected using five 180° ω-scans (0.5° scan width) at different φ-angles (φ = 0° to 288° in 72° increments), nominally covering complete reciprocal space. Data reduction was completed using SAINT version 8.40A, and a multi-scan absorption correction was applied using SADABS version 2016 included in the Bruker APEX4 software suite.[S8] Space-group determination was performed using the XPREP utility included in the SHELXTL software package.

Liquid chromatography with mass spectrometry time of flight (LC-MS-TOF) measurements were performed using an Agilent Technologies 6230 TOF LC/MS instrument with 1260 Infinity quad pump.

Scanning electron microscopy images and energy dispersive X-ray spectroscopy (EDS) were collected using a Zeiss Ultra 55 SEM equipped with a Noran System 7 EDXS system with a Silicon Drift Detector X-ray detector.

Scanning electron microscopy (SEM) was obtained with a HITACHI Tabletop Microscope TM3000 The samples were loaded on carbon tape for imaging.

Gas adsorption analysis was performed using a Micromeritics ASAP 2020 surface area and porosimetry analyzer. Measurements were performed at 77 K (liquid N_2 bath) for N_2(*g*) on thermally activated samples. Brunauer-Emmet-Teller (BET) surface areas were obtained by performing a Rouquerol analysis over the linear isotherm to determine the upper limits of the BET model from the N_2 isotherms. Pore size distribution plots were obtained by fitting the experimental isotherms with non-local density functional theory (NLDFT) models using N_2 at 77 K cylindrical oxide-surface kernel. Plots are shown in differential pore volume versus pore diameter.[S9, S10]

Raman spectroscopy measurements were performed using a Horiba Scientific LabRAM HR Evolution Raman Spectrometer equipped with a Toppica Photonics XTRA II high power single frequency 785 nm diode laser, and Horiba Scientific Synapse+ plus detector. Spectra were collected using a 600 groove diffraction grating with acquisition time and laser power optimized for the highest quality spectra from sample to sample. All samples were measured using three spectrum accumulations to provide optimal signal to noise ratios.

Thermogravimetric analysis (TGA) of all materials was conducted on an ISI TGA-1000 instrument, housed inside a nitrogen-atmosphere glovebox, using Pt sample pans and a 5 cm^3 min^{-1} flow of UHP N_2. The following protocol was conducted for all TGA experiments: 25-900 °C at a ramp rate of 10 °C min^{-1}.

Section S2. **Synthetic procedures.**

Scheme S1. Synthesis of **PEPEP-F** link.

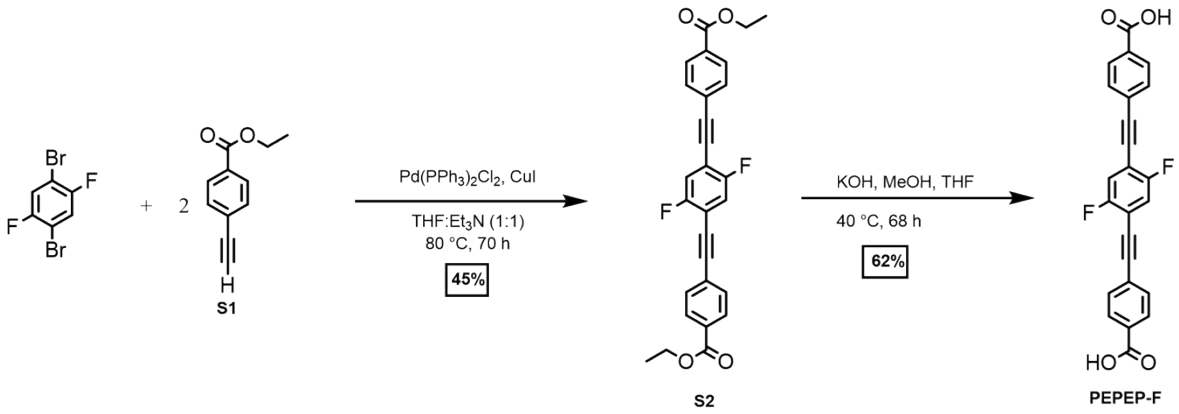

Scheme S2. Synthesis of **PEPEP-TMS** and **PEPEP-I** link.

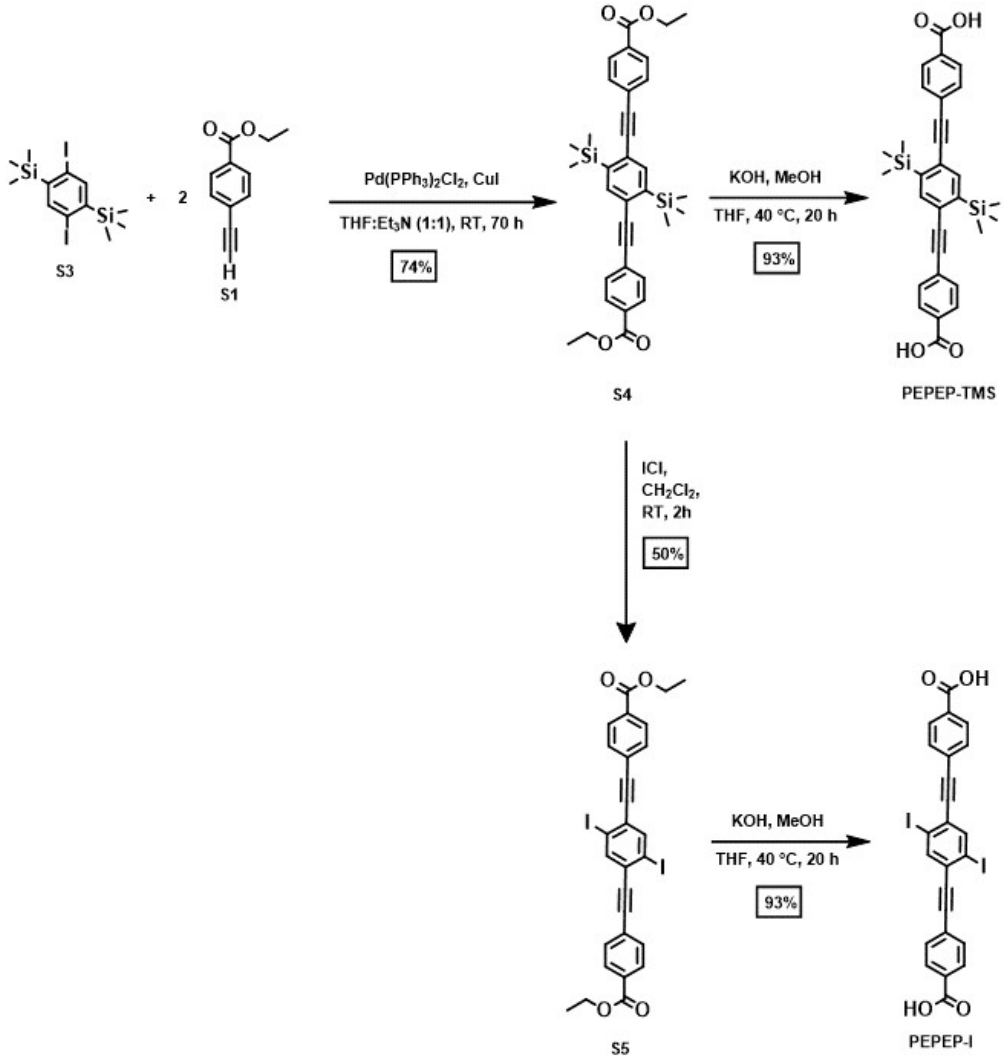

Scheme S3. Synthesis of **PEPEP-Cl** link.

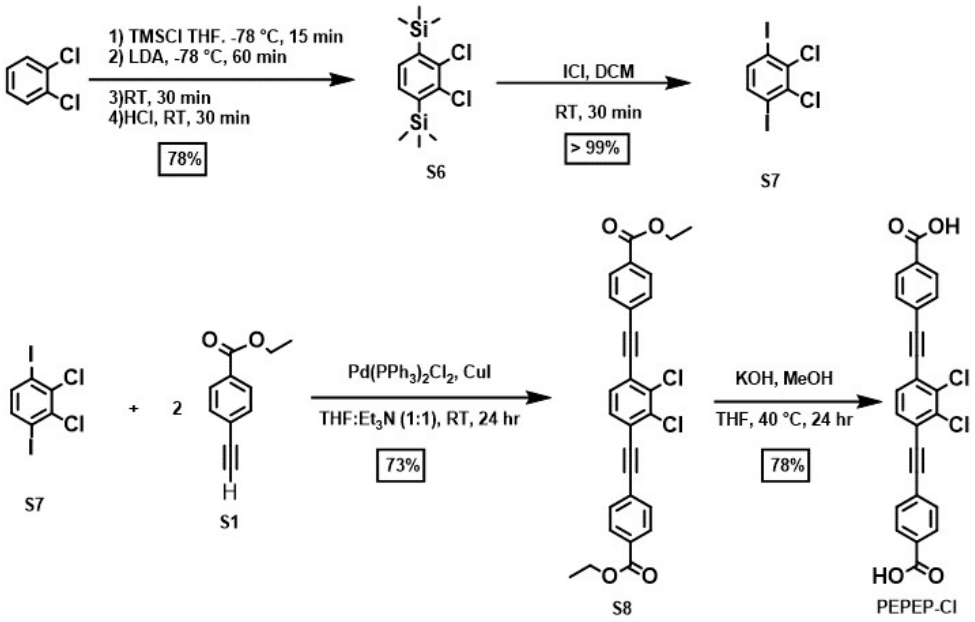

Scheme S4. Synthesis of **PEPEP-Br** link.

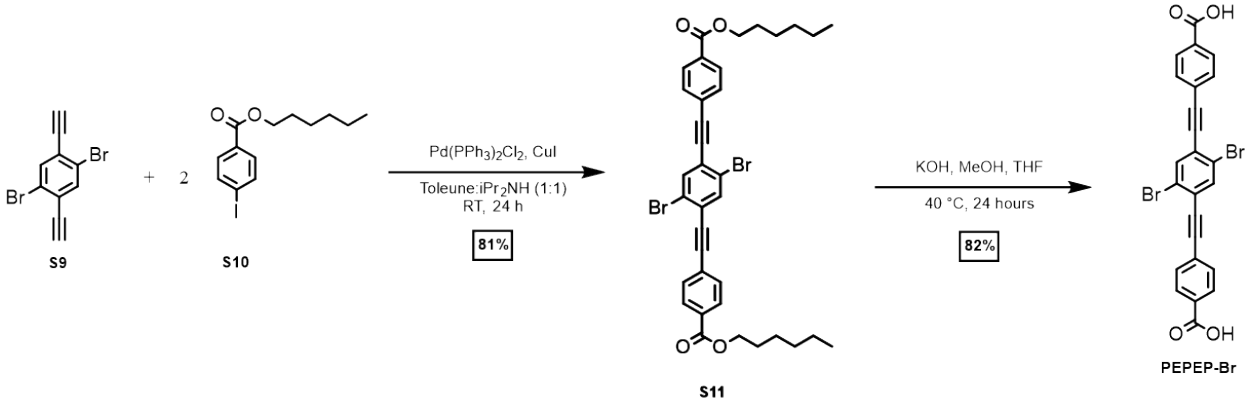

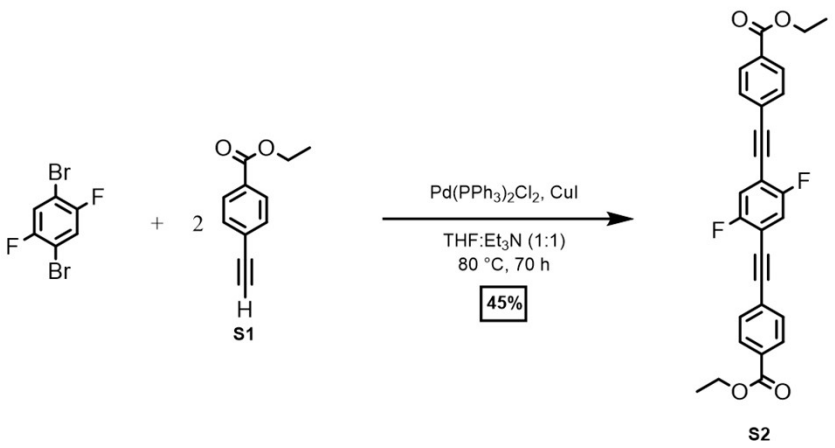

4,4'-[(2,5-difluoro-1,4-phenylene)di-2,2-ethynediyl]bis-1,1'-diethylester benzoic acid (S2): 1,4-Dibromo-2,5-difluorobenzene (600 mg, 2.21 mmol, 1 eq), $Pd(PPh_3)_2Cl_2$ (77.45 mg, 0.11 mmol, 0.05 eq), and CuI (42.03 mg, 0.22 mmol, 0.1 eq) were loaded into an oven-dried 100 mL Schlenk flask equipped with a stir bar and fitted with a condenser. The apparatus was evacuated to an internal pressure of 100 mTorr and backfilled with N_2 three times. Anhydrous THF (10 mL) and degassed triethylamine (10 mL) were added via syringe, followed by **S1** (0.78 mL, 4.85 mmol, 2.2 eq). The reaction was heated to 80 °C for 70 h. The reaction mixture was cooled to RT, quenched with 1 M HCl (10 mL) and extracted with CH_2Cl_2 (2 x 15 mL). The combined organic extracts were washed with water (20 mL), brine (20 mL), and dried over anhydrous Na_2SO_4. Activated charcoal (0.6 g) was added to the solution and sonicated for 10 min. The mixture was then filtered through a silica plug, eluting with CH_2Cl_2, and the solvent was removed in a rotary evaporator at 45 °C. The residue was recrystallized in MeOH and dried under high vacuum (<100 mTorr), resulting in **S2** as a yellow solid. Yield: 453 mg, 45%. ^{1}H NMR (400 MHz, $CDCl_3$, 25 °C) δ (ppm) 8.05 (d, *J* = 8.4 Hz, 4H), 7.62 (d, *J* = 8.4 Hz, 4H), 7.28 (t, *J* = 7.2 Hz, 2H), 4.40 (q, *J* = 7.1 93 Hz, 4H), 1.41 (t, *J* = 7.1 Hz, 6H). ^{19}F NMR (376 MHz, $CDCl_3$, 25 °C) δ (ppm) -118.34 (s, 2F). ^{13}C NMR (400 MHz, CDCl3, 25 °C) δ (ppm) 166.04 (2C), 159.64 [d, $J(^{13}C,^{19}F)$ = 3.7 Hz, 2C], 157.15 [d, $J(^{13}C,^{19}F)$ = 3.6 Hz, 2C], 131.84 (4C), 130.85 (2C), 129.71 (4C), 126.75 (2C), 119.66 [q, $J(^{13}C,^{19}F)$ = 9.1 Hz, 2H], 96.42 (2C), 84.29 (2C), 61.42 (2C), 14.46 (2C). HRMS (ESI-TOF) *m/z*: $[M+H]^+$ Calculated for $C_{28}H_{20}O_4F_2$ 459.1402; Found 459.1404.

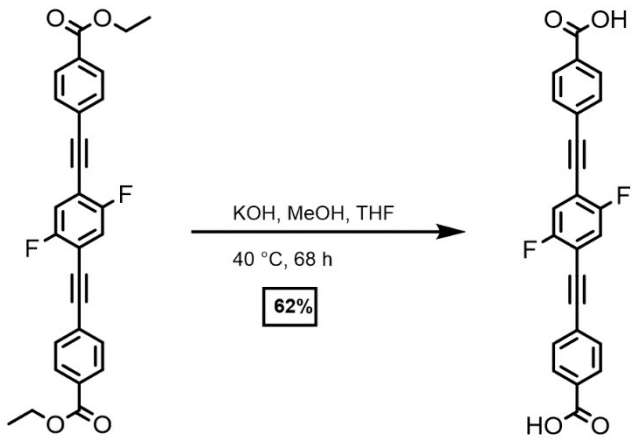

4,4'-[(2,5-difluoro-1,4-phenylene)di-2,2-ethynediyl]bis-1,1'-bis-benzoic acid (PEPEP-F): **S2** (3.50 g, 7.6 mmol, 1 eq) was loaded into a 500 mL round-bottom flask equipped with a stir bar and fitted with a condenser. THF (200 mL) was added, followed by 5 M KOH in MeOH (60 mL, 305 mmol, 40 eq), and the reaction was heated to 40 °C for 72 h. After reaction, the solvent was removed in a rotary evaporator at 50 °C and the crude product was dissolved in water and acidified with 1 M HCl until complete precipitation occurred. The solid was collected via filtration using a Nylon filter paper (Omicron, 0.45 µm). The solid was then dissolved in DMSO and filtered again through Nylon. Water was then added to the DMSO filtrate and the solid was recovered by filtration. The solid was then recrystallized from acetone and dried under high vacuum (<50 mTorr), resulting in **PEPEP-F** as a tan-yellow solid. Yield: 1.9 g, 62%. ^{1}H NMR (400 MHz, DMSO-d_6, 25 °C) δ (ppm) 8.01 (d, J = 8.3 Hz, 4H), 7.79 (t, J = 7.6 Hz, 2H), 7.72 (d, J = 8.3 Hz, 4H). ^{19}F NMR (376 MHz, DMSO-d_6, 25 °C) δ (ppm) -117.35 (s, 2F). ^{13}C NMR (400 MHz, DMSO-d_6, 25 °C) δ (ppm) 166.57 (2C), 158.99 (2C), 156.52 (2C), 131.81 (4C), 131.46 (2C), 129.69 (4C), 125.28 (2C), 120.02 [q, J(^{13}C,^{19}F) = 9.1 Hz, 2C], 96.20 (2C), 83.76 (2C). *m/z*: $[M+H]^+$ Calculated for $C_{24}H_{12}F_2O_4$ 379.0776; Found 379.2404.

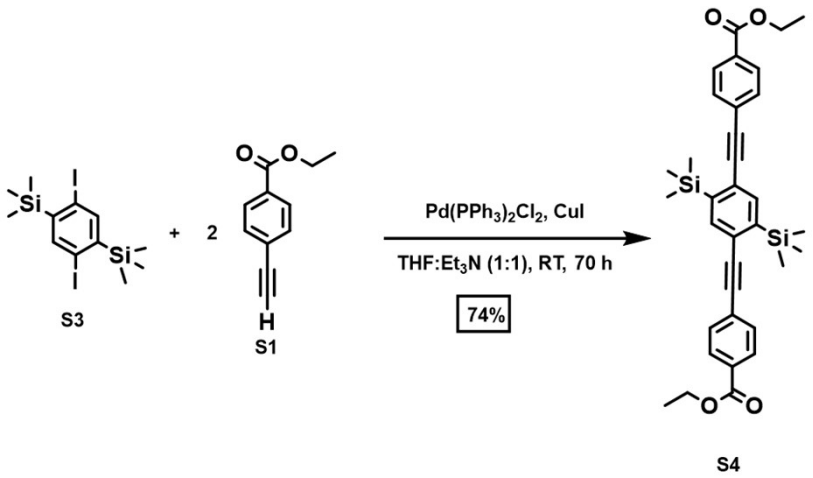

4,4'-[(2,5-bis(trimethylsilyl)-1,4-phenylene)di-2,2-ethynediyl]bis-1,1'-diethylester benzoic acid (S4): **S3** (6.00 g, 12.65 mmol, 1 eq), $Pd(PPh_3)_2Cl_2$ (444 mg, 0.63 mmol, 0.05 eq), and CuI (241 mg, 1.27 mmol, 0.1 eq) were loaded into an oven-dried 250 mL Schlenk flask equipped with a stir bar and fitted with a condenser. The apparatus was evacuated to an internal pressure of 100 mTorr and backfilled with N_2 three times. Anhydrous THF (65 mL) and degassed triethylamine (65 mL) were added via syringe, followed by **S1** (4.5 mL, 28 mmol, 2.2 eq). The reaction was stirred at RT for 70 h. The reaction was quenched with 1 M HCl (60 mL) and extracted with CH_2Cl_2 (2 x 50 mL). The combined organic phases were washed with water (40 mL), brine (40 mL), and dried over anhydrous Na_2SO_4. Activated charcoal (6 g) was added to the solution and sonicated for 10 min. The mixture was then filtered through a silica plug eluting with CH_2Cl_2, and the solvent was removed in a rotary evaporator at 45 °C. The solid was recrystallized from MeOH and dried under high vacuum (<100 mTorr) resulting in **S4** as a pale-yellow solid. Yield: 5.3 g, 74%. ^{1}H NMR (400 MHz, $CDCl_3$, 25 °C) δ (ppm) 8.05 (d, *J* = 8.4 Hz, 4H), 7.71 (s, 2H), 7.59 (d, *J* = 8.5 Hz, 4H), 4.40 (q, *J* = 7.2 Hz, 4H), 1.41 (t, *J* = 7.1 Hz, 6H), 0.44 (s, 18H). ^{13}C NMR (400 MHz, $CDCl_3$, 25 °C) δ (ppm) 166.19 (2C), 143.30 (2C), 138.18 (2C), 131.26 (4C), 130.16 (2C), 129.77 (4C), 127.95 (2C), 127.26 (2C), 94.25 (2C), 93.19 (2C), 61.33 (2C), 14.48 (2C), -0.97 (6C). MS (ESI-TOF) *m/z*: $[M+H]^+$ Calculated for $C_{34}H_{38}O_4Si_2$ 567.2381; Found 566.8785.

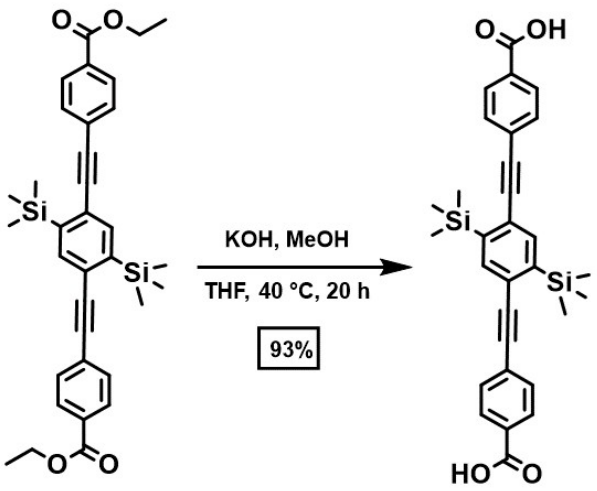

4,4'-[(2,5-bis(trimethylsilyl)-1,4-phenylene)di-2,2-ethynediyl]bis-1,1'-bis-benzoic acid (PEPEP-TMS): **S4** (400 mg, 0.71 mmol, 1 eq) was loaded into a 50 mL round-bottom flask equipped with a stir bar and fitted with a condenser. THF (18 mL) was added, followed by 5 M KOH in MeOH (5.65 mL, 28.23 mmol, 40 eq) and the reaction was heated to 40 °C for 20 h. The solvent was removed in a rotary evaporator at 50 °C and the crude product was dissolved in water and acidified with 1 M HCl until complete precipitation occurred. The solid was collected via filtration using a Nylon filter paper (Omicron, 0.45 µm). The solid was then dissolved in DMF and filtered through nylon. Water was then added to the filtrate and the solid was isolated by filtration. The solid was then recrystallized from acetone and dried under high vacuum (<50 mTorr), resulting in **PEPEP-TMS** as a white solid. Yield: 340 mg, 93%. ^{1}H NMR (400 MHz, DMSO-d_6, 25 °C) δ (ppm) 8.01 (d, 4H), 7.70 (s, 2H), 7.67 (d, 4H), 0.42 (s, 18H). ^{13}C NMR (400 MHz, DMSO-d_6, 25 °C) δ (ppm) 166.65 (2C), 143.03 (2C), 137.75 (2C), 131.17 (4C), 130.86 (2C), 129.79 (4C), 126.59 (2C), 126.37 (2C), 93.30 (2C), 93.15 (2C), -1.29 (6C). HRMS (ESI-TOF) *m/z*: $[M]^+$ Calculated for $C_{30}H_{30}O_4Si_2$ 510.1677; Found 510.1680.

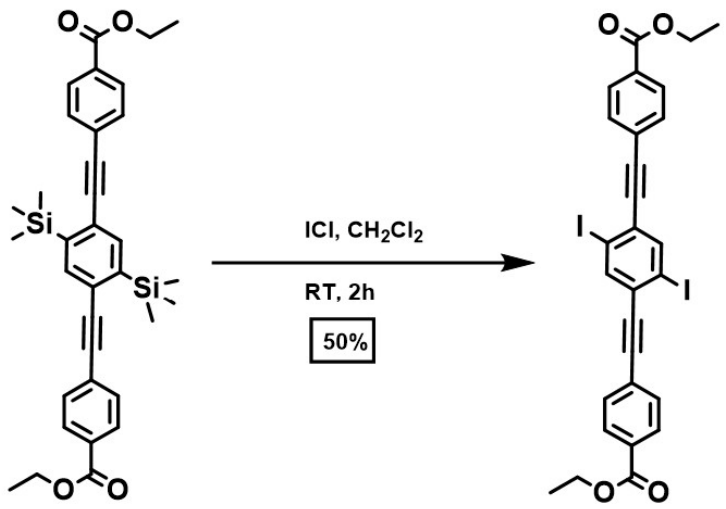

S4 S5

4,4'-[(2,5-diiodo-1,4-phenylene)di-2,2-ethynediyl]bis-1,1'-diethylester benzoic acid (S5): S4 (4.00 g, 7.06 mmol, 1 eq) was loaded into a 500 mL round-bottom flask equipped with a stir bar. CH_2Cl_2 (140 mL) was added, followed by ICl (1.85 mL, 35.3 mmol, 5.0 eq). The reaction was stirred at RT for 2 h, then quenched with 1 M KOH (40 mL) and saturated $NaHSO_3$ (40 mL). The reaction was stirred until the mixture became colorless and then extracted with CH_2Cl_2 (2 x 50 mL). The combined organic phases were washed with water (2 x 30 mL), brine (30 mL), and dried over anhydrous Na_2SO_4, and the solvent was removed in a rotary evaporator at 45 °C. The solid was recrystallized from MeOH and dried under high vacuum (<100 mTorr), resulting in **S5** as a white solid. Yield: 2.40 g, 50%. 1H NMR (400 MHz, $CDCl_3$, 25 °C) δ (ppm) 8.11 (d, *J* = 8.3 Hz, 4H), 7.92 (s, 2H), 7.59 (d, *J* = 8.0 Hz, 4H), 4.41 (q, *J* = 7.1 Hz, 4H), 1.42 (t, *J* = 7.1 Hz, 6H). ^{13}C NMR (400 MHz, $CDCl_3$, 25 °C) δ (ppm) 166.01 (2C), 147.90 (2C), 145.27 (2C), 140.07 (2C), 131.01 (2C), 130.77 (2C), 129.87 (4C), 128.89 (4C), 97.83 (2C), 97.41 (2C), 61.38 (2C), 14.49 (2C). MS (ESI-TOF) *m/z*: $[M+H]^+$ Calculated for $C_{28}H_{22}O_4I_2$ 674.9524; Found 675.5110.

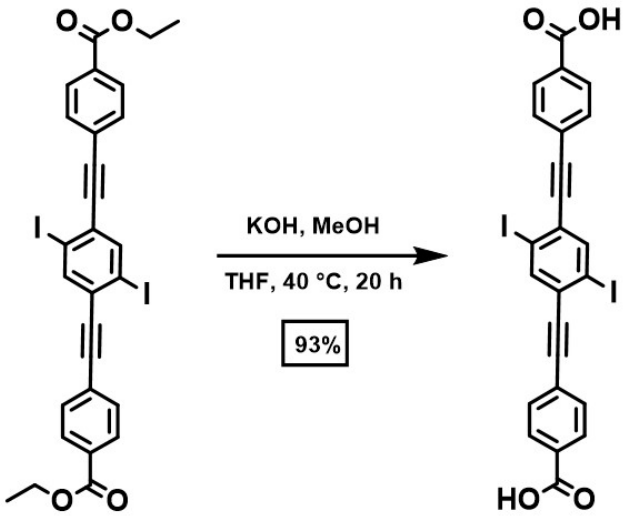

4,4'-[(2,5-diiodo-1,4-phenylene)di-2,2-ethynediyl]bis-1,1'-bis-benzoic acid (PEPEP-I): **S5** (2.30 g, 3.41 mmol, 1 eq) was loaded into a 300 mL round-bottom flask equipped with a stir bar and fitted with a condenser. THF (85 mL) was added, followed by 5 M KOH in MeOH (27.29 mL, 136.44 mmol, 40 eq), and the reaction was heated to 40 °C for 48 h. The solvent was removed in a rotary evaporator at 50 °C and the crude product was dissolved in water and acidified with 1 M HCl until complete precipitation occurred. The solid was collected via filtration using a Nylon filter paper (Omicron, 0.45 µm). The solid was then dissolved in DMF and filtered through nylon. Water was then added to the filtrate and the solid was filtered. The solid was then recrystallized from acetone, and dried under high vacuum (<50 mTorr), resulting in **PEPEP-I** as a tan solid. Yield: 774 mg, 37%. ^{1}H NMR (400 MHz, DMSO-d_6, 25 °C) δ (ppm) 8.19 (s, 2H), 8.02 (d, 4H), 7.72 (d, 4H). ^{13}C NMR (400 MHz, DMSO-d_6, 25 °C) δ (ppm) 166.61 (2C), 141.32 (2C), 131.59 (4C), 131.32 (2C), 129.94 (2C), 129.71 (4C), 125.71 (2C), 101.07 (2C), 94.54 (2C), 92.43 (2C). MS (ESI-TOF) *m/z*: $[M]^+$ Calculated for $C_{24}H_{12}O_4I_2$ 617.8819; Found 617.4603.

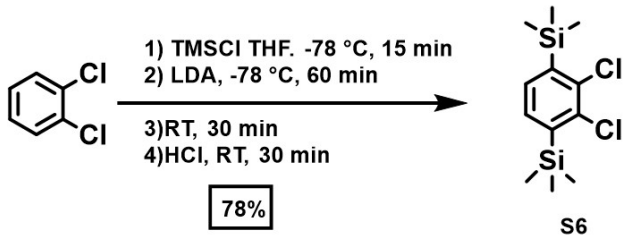

(2,3-dichloro-1,4-phenylene)bis(trimethylsilane) (S6): A 50 mL Schlenk flask equipped with a stir bar was evacuated to an internal pressure of 100 mTorr and backfilled with N_2 three times. Dry 1,2-dichlorobenzene (0.71 mL, 6.25 mmol, 1 eq), andhydrous THF (10 mL) followed by TMSCl (2.65 mL, 21 mmol, 3.3 eq) were the flask under N_2. The mixture was cooled in a dry ice/acetone bath to -78 °C for 15 min. Lithium diisopropylamide (2 M in hexanes, 10.5 mL, 20.88 mmol, 3.3 eq) was added to the mixture via syringe under N_2. The reaction mixture was a -78 °C 1 h. The reaction mixture was slowly warmed to RT for 30 min. 3 M HCl (5 mL) was added to quench the reaction, and let it stir for 30 min and the organic layers were extracted with diethyl ether (3 x 5 mL). The combined organic phases were washed with with brine (3 x 5 mL) and with anhydrous Na_2SO_4, filtered, and the solvent was removed in a rotary evaporator at RT obtaining a yellow oil that was recrystallized from ethanol to give pale-yellow needles. The solid was dried under high vacuum (<50 mTorr), resulting in **S6** as a yellow powder. Yield: 1.41 g, 78%. ^{1}H NMR (400 MHz, $CDCl_3$, 25 °C) δ (ppm) 7.31 (s, 2H), 0.37 (s, 18H). ^{13}C NMR (400 MHz, $CDCl_3$, 25 °C) δ (ppm) 142.61 (2C), 139.06 (2C), 133.07 (2C), -0.62 (6C). MS (ESI-TOF) *m/z*: $[M+H]^+$ Calculated for $C_9H_{20}Cl_2Si_2$ 255.0553; Found 255.1631.

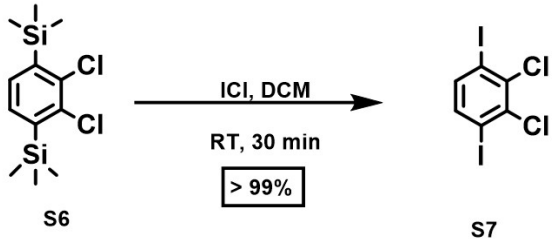

2,3-dichloro-1,4-diiodobenzene (S7): S6 (250 mg, 0.86, 1.0 eq) was loaded into a 20 mL round-bottom flask equipped with a stir bar. Anhdyrous CH_2Cl_2 (10 mL) was then added to the flask. ICl (0.31 mL. 960 mg, 5.9 mmol, 6.9 eq) was added to the reaction mixture and stirred for 30 min followed by TLC. After 30 min the reaction was quenched with 2 M NaOH and 2 M $NaHSO_3$, and the organic layers were extracted with CH_2Cl_2 (3 x 10 mL). The combined organic layers were washed with $NaHSO_3$ (3 x 5 mL) and brine (3 x 3 mL) and dried over anhydrous Na_2SO_4 and filtered. The solvent was removed in a rotary evaporator at 45 °C obtaining **S7** as a white powder. Yield: 385 mg, 99%. ^{1}H NMR (400 MHz, $CDCl_3$, 25 °C) δ (ppm) 7.44 (s, 2H). ^{13}C NMR (400 MHz, $CDCl_3$, 25 °C) δ (ppm) 139.4 (2C), 137.06 (2C), 98.98 (2C). MS (ESI-TOF) *m/z*: $[M+H]^+$ Calculated for $C_6H_2Cl_2$ 398.7696; Found 398.0050.

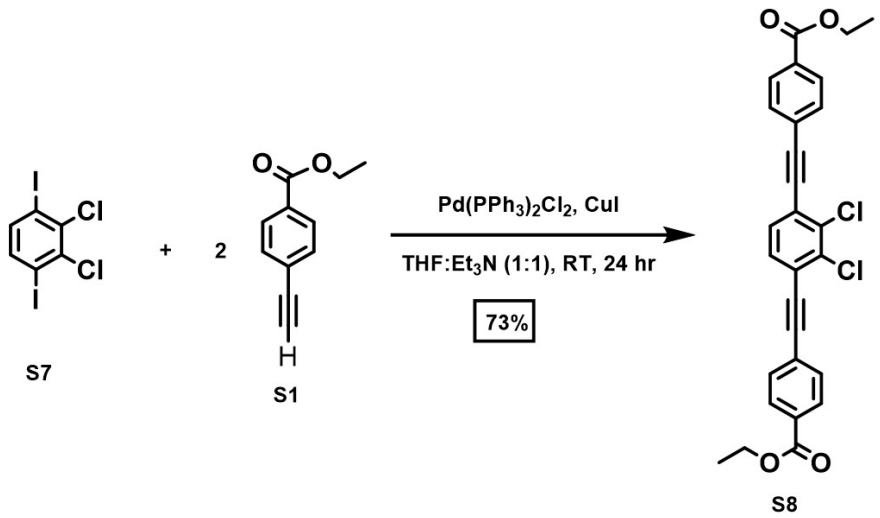

diethyl 4,4'-((2,3-dichloro-1,4-phenylene)bis(ethyne-2,1-diyl))dibenzoate (S8): S7 (280 mg, 0.70 mmol, 1 eq), $Pd(PPh_3)_2Cl_2$ (25 mg, 0.036 mmol, 0.05 eq), and CuI (13 mg, 0.08 mmol, 0.1 eq) were loaded into an 100 mL oven-dried Schlenk flask equipped with a stir bar and fitted with a condenser. The apparatus was evacuated to an internal pressure of 100 mTorr and backfilled with N_2 three times. Anhydrous THF (1.4 mL) and degassed triethylamine (1.4 mL) were added via syringe, followed by **S1** (0.27 mL, 4.85 mmol, 2.2 eq). The reaction was stirred at RT for 24 h. The reaction was quenched with 1 M HCl (10 mL), and the organic layers were extracted using CH_2Cl_2 (3 x 10 mL). The combined organic layers were washed with water (3 x 20 mL) and brine (3 x 20 mL). The organic layer was passed through a plug of silica eluting with CH_2Cl_2. A solid formed in the organic layer after 24 h, and the solid was filtered obtaining **S8** as an off-white compound. Yield: 280 mg, 81%. ^{1}H NMR (600 MHz, $CDCl_3$, 25 °C) δ (ppm) 8.04 (d, 4H), 7.64 (d, 4H), 7.47 (s, 2H), 4.40 (q, 4H), 1.41 (t, 6H). ^{13}C NMR (600 MHz, $CDCl_3$, 25 °C) δ (ppm) 166.07 (2C), 135.33 (2C), 131.85 (2C), 130.78 (2C), 129.70 (4C), 127.84 (2C), 126.9 (2C), 124.78 (2C), 88.58 (2C), 61.41 (2C), 40.22 (2C), 31.07 (2C), 14.45 (2C). MS (ESI-TOF) *m/z*: $[M+H]^+$ Calculated for $C_{28}H_{20}Cl_2O_4$ 491.0811; Found 491.3986.

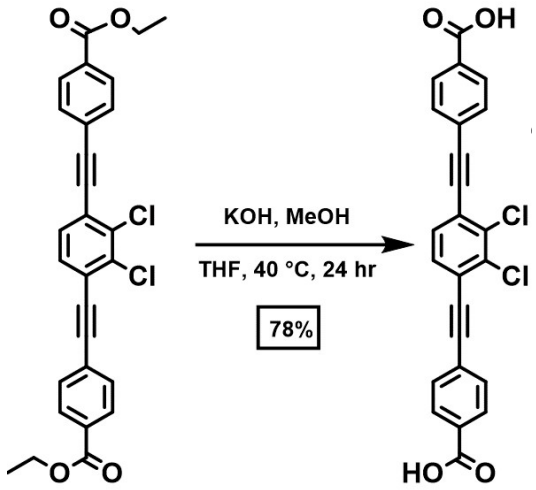

4,4'-((2,3-dichloro-1,4-phenylene)bis(ethyne-2,1-diyl))dibenzoic acid (PEPEP-Cl): S8 (250 mg, 0.51 mmol, 1.0 eq) was loaded into a 20 mL round-bottom flask equipped with a stir bar and fitted with a condenser. THF (3.5 mL) was added, followed by 5 M KOH in MeOH (5.0 mL, 25 mmol, 50 eq), and the reaction was heated to 40 °C for 48 h. The solvent was removed in a rotary evaporator at 50 °C and the crude product was dissolved in water and acidified with 1 M HCl until complete precipitation occurred. The solid was collected via filtration and dried under high vacuum (<50 mTorr), resulting in **PEPEP-Cl** as a light-yellow solid. Yield: 173 mg, 78%. ^{1}H NMR (600 MHz, DMSO-d_6, 25 °C) δ (ppm)13.24 (s, 2H), 8.01 (d, 4H), 7.76 (d, 4H), 7.73 (s, 2H). ^{13}C NMR (600 MHz, DMSO-d_6, 25 °C) δ (ppm) 166.57 (2C), 133.89 (2C), 131.84 (2C), 131.69 (2C), 129.69 (4C), 124.44 (2C), 123.98 (2C), 96.11 (2C), 87.90 (2C). MS (ESI-TOF) *m/z*: $[M-H]^-$ Calculated for $C_{24}H_{12}O_4Cl_2$ 433.004; Found 433.0311.

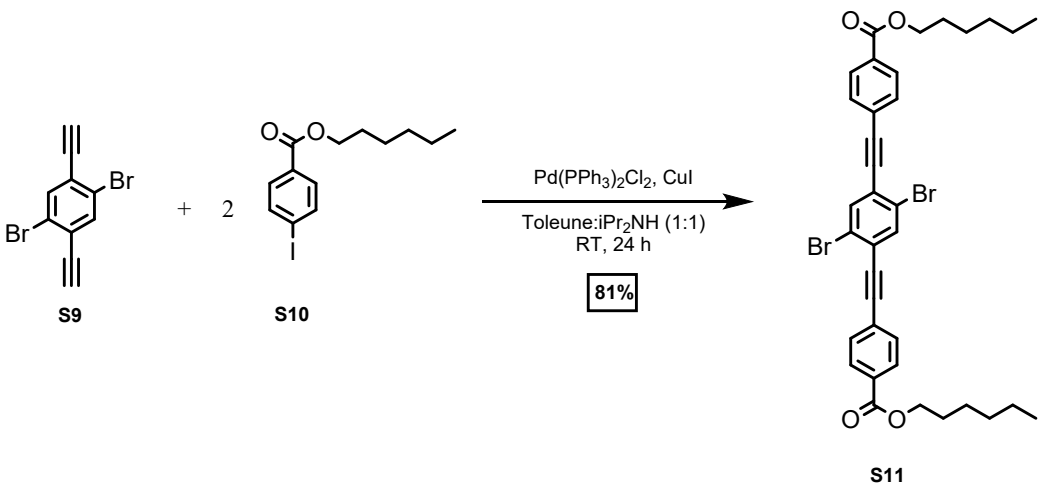

S9 S10 S11

dihexyl 4,4'-((2,5-dibromo-1,4-phenylene)bis(ethyne-2,1-diyl))dibenzoate (S11): S9 (1.10 g, 3.874 mmol, 1 eq), **S10** (2.83 g, 8.523 mmol, 2.2 eq), $Pd(PPh_3)_2Cl_2$ (82 mg, 0.116 mmol, 0.03 eq), and CuI (4.4 mg, 0.232 mmol, 0.06 eq) were loaded into an oven-dried 100 mL Schlenk flask equipped with a stir bar and fitted with a condenser. The apparatus was evacuated to an internal pressure of 100 mTorr and backfilled with N_2 three times. Anhydrous Toluene (19.4 mL) and degassed diisopropylamine (19.4 mL) were added via syringe. The reaction was stirred at RT for 24 h. The reaction was quenched with 1 M HCl (10 mL) and extracted with CH_2Cl_2 (3 x 10 mL). The combined organic phases were washed with 1 M HCl (5 mL), water (5 mL), brine (10 mL), and dried over anhydrous Na_2SO_4. Activated charcoal (6 g) was added to the solution and sonicated for 10 min. The mixture was then filtered through a silica plug eluting with CH_2Cl_2, and the solvent was removed in a rotary evaporator at 45 °C. The solid was recrystallized from EtOH and dried under high vacuum (<100 mTorr) resulting in **S11** as a pale-yellow solid. Yield: 2.1593 g, 81 ^{1}H NMR (600 MHz, $CDCl_3$, 25 °C) δ (ppm) 8.04 (d, 4H) , 7.81 (s, 2H), 7.63 (d, 4H), 4.33 (t, 4H), 1.41 (qui, 4H), 1.45 (m, 4H), 1.35 (m, 8H), 0.91 (t, 6H). ^{13}C NMR (600 MHz, $CDCl_3$, 25 °C) δ (ppm) 166.12 (2C), 136.42 (2C), 131.85 (2C), 130.90 (2C), 129.73 (4C), 126.81 (2C), 126.54 (2C), 124.07 (2C), 96.08 (2C), 89.37 (2C), 65.62 (2C), 31.61 (2C), 28.80 (2C), 25.85 (2C), 22.71 (2C), 14.16 (2C), 1.17 (2C). %. MS (ESI-TOF) m/z: $(M+H)^+$ Calculated for $C_{36}H_{36}Br_2O_4$ 691.9232; Found 691.1053.

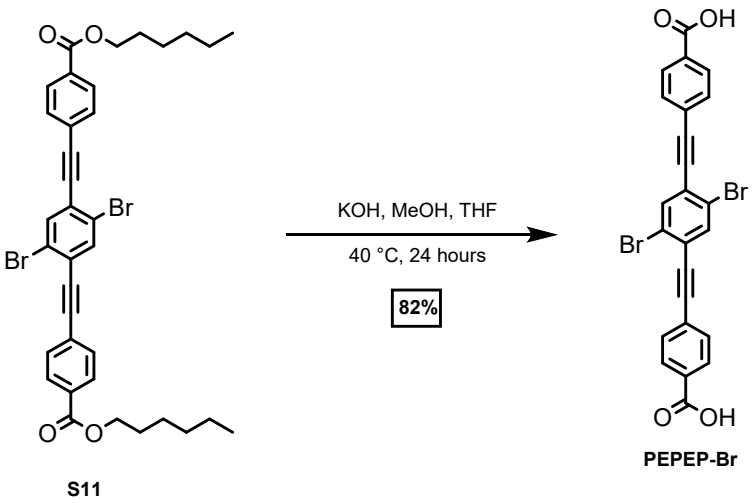

S11 **PEPEP-Br**

4,4'-((2,5-dibromo-1,4-phenylene)bis(ethyne-2,1-diyl))dibenzoic acid (PEPEP-Br): S11 (2.16 g, 3.12 mmol, 1.0 eq) was loaded into a 150 mL round-bottom flask equipped with a stir bar and fitted with a condenser. THF (39 mL) was added, followed by 5 M KOH in MeOH (25.0 mL, 125 mmol, 40.1 eq), and the reaction was heated to 40 °C for 24 h. The solvent was removed in a rotary evaporator at 50 °C and the crude product was dissolved in water and acidified with 1 M HCl until complete precipitation occurred. The solid was collected via filtration, recrystallized in DMF, and dried under high vacuum (<50 mTorr), resulting in **PEPEP-Br** as a light-brown solid. Yield: 1.34 g, 82%. ^{1}H NMR (600 MHz, DMSO-d_6, 25 °C) δ (ppm) 8.13 (s, 2H), 8.01 (d, 4H), 7.72 (s, 2H). ^{13}C NMR (600 MHz, DMSO-d_6, 25 °C) δ (ppm) 166.12 (2C), 136.37 (2C), 131.97 (2C), 131.82 (2C), 131.44 (2C), 129.74 (2C), 129.62 (2C), 125.82 (2C), 125.82 (2C), 125.50 (2C), 123.78 (2C), 95.85 (2C), 88.95 (2C). MS (ESI-TOF) m/z: $(M+H)^+$ Calculated for $C_{24}H_{12}Br_2O_4$ 521.9097; Found 521.4622.

Section S3: General MTV MOF synthetic procedures: Stock solutions of the links **QPDC-Me, PEPEP-Me, PEPEP-OMe, PEPEP-F, PEPEP-TMS, PEPEP-Br,** and **PEPEP-I** were prepared at different concentrations in anhydrous DMF (See tables **S1-S7**). The links at varied molar ratios were added in aliquots alongside anhydrous DMF, toluene, and acetic acid into a conical glass reaction vessel fitted with a ground glass stopper and mixed in an ultrasonic bath for 10 min. $ZrCl_4$ (13.5 mg, 0.045 mmol, 1.1 eq) was added and mixed in an ultrasonic bath for 5 min. The mixture was bubbled with N_2(*g*) for 1 min, capped with a glass stopper and a metal clip and placed in an isothermal oven at 120 ºC for 3 d. The vessel was removed from the oven and allowed to cool to RT, the solids were isolated by filtration, rinsed with DMF (~20 mL) and CH_2Cl_2 (3 x ~10 mL). The obtained crystals were immersed in THF and stored for two days in a desiccator, replacing the exchange solvent three times during this period. The solvent was removed by decantation and the solvent wet crystals was dried under dynamic vacuum (50 mTorr) for 6 h at RT affording clear crystals. See tables S#-S# for conditions and yields. MTV MOFs containing **PEPEP-Fc** were prepared via loading the reaction precursors, solvents, and additives into an 18.5 cm borosilicate glass tube (1 cm o.d., 0.8 cm i.d.) that had been flame-sealed at one end. The tubes were then sonicated, followed by a Schlenk adapter being attached to the open side of the tube using vacuum tubing and the tube was flash frozen in liquid nitrogen up to the solvent level. The tube was evacuated to an internal pressure of 100 mTorr and flame-sealed to a length of 12.5 cm with a torch under static vacuum. The sample tubes were then allowed to thaw and sonicated again. Then, the tubes were placed into sand baths in an isothermal oven at 120 ºC for 3 d. The obtained crystals were immersed in solvent exchange was done first with using DMF for two days (about 5-6 exchanges), followed by exchange by THF to remove the excess DMF for 3 days (5-6 exchanges).. The solvent was removed by decantation and the solvent wet crystals was dried under dynamic vacuum (50 mTorr) for 6 h at RT affording clear crystals. The percent yields were calculated based on the molecular formula of each MTV MOF at their corresponding link ratios.

Table S1: Reaction conditions for $Zr_6O_4(OH)_4((\textbf{QPDC-Me})_{1-x}(\textbf{PEPEP-Me})_x)_6$

x (%mol **PEPEP-Me**)	0.018 M **PEPEP-Me** mL (mmol)	0.027 M **QPDC-Me** mL (mmol)	$ZrCl_4$ (mmol)	DMF mL	Toluene mL	Acetic Acid mL	Yield (mg/ %)
10	0.250 (0.0045)	1.5 (0.0405)	0.05	2.31	0.1875	0.464	18.2 (
20	0.500 (0.009)	1.333 (0.036)	0.05	2.31	0.1875	0.464	8.4 (36.1%)
30	0.750 (0.0135)	1.167 (0.0315)	0.05	2.31	0.450	0.464	13.6 (55.6%)
40	1.000 (0.018)	1.000 (0.027)	0.05	2.31	0.1875	0.464	10.3 (42.4%)
50	1.250 (0.045)	0.833 (0.045)	0.05	4.875	0.375	0.464	11.0 (45.8%)
60	1.500 (0.027)	0.667 (0.018)	0.05	2.31	0.1875	0.464	9.6 (39.5%)
80	2.000 (0.036)	0.333 (0.009)	0.05	2.31	0.1875	0.464	13.4 (54%)
100	5.000 (0.09)	0	0.0995	0	0.425	0.958	18.2 (80.2%)

Table S2: Reaction conditions for $Zr_6O_4(OH)_4((\textbf{QPDC})_{1-x}(\textbf{PEPEP-Ome})_x)_6$

x (%mol **PEPEP-OME**)	0.018 **PEPEP-OMe** mL (mmol)	0.027 M **QPDC-Me** mL (mmol)	$ZrCl_4$ (mmol)	DMF mL	Toluene mL	Acetic Acid mL	Yield (mg/ %)
20	0.500 (0.009)	1.333 (0.036)	0.05	2.31	0.1875	0.464	14.1 (56.2%)
40	1.000 (0.018)	1.000 (0.027)	0.05	2.31	0.1875	0.464	17.0 (68.3%)
60	1.500 (0.027)	0.667 (0.018)	0.05	2.31	0.1875	0.464	14.6 (59.1%)
80	2.000 (0.036	0.333 (0.009)	0.05	2.31	0.1875	0.464	15.2 (62%)

Table S3: Reaction conditions for $Zr_6O_4(OH)_4((\mathbf{QPDC})_{1-x}(\mathbf{PEPEP\text{-}F})_x)_6$

x (%mol **PEPEP-F**)	0.027 M **PEPEP-F** mL (mmol)	0.027 M **QPDC-Me** mL (mmol)	$ZrCl_4$ (mmol)	DMF mL	Toluene mL	Acetic Acid mL	Yield (mg/ %)
1	0.0167 (0.00045)	1.650 (0.04455)	0.05	2.31	0.187	0.464	9.8 (42.2%)
5	0.0833 (0.00225)	1.583 (0.04275)	0.05	2.31	0.187	0.464	8.9 (38.2%)
10	0.167 (0.0045)	1.5 (0.0405)	0.05	2.31	0.187	0.464	10.4 (44.4%)
20	0.333 (0.009)	1.333 (0.036)	0.05	2.31	0.187	0.464	14.8 (61%)
40	0.667 (0.018)	1.000 (0.027)	0.05	2.31	0.187	0.464	10.8 (44.6%)
60	1.000 (0.027)	0.667 (0.018)	0.05	2.31	0.187	0.464	12.4 (51.2%)
80	1.333 (0.036)	0.333 (0.009)	0.05	2.31	0.187	0.464	17.4 (71.4%)
100	1.67 (0.045)	0	0.05	2.31	0.187	0.464	22.8 (91.6%)

Table S4: Reaction conditions for $Zr_6O_4(OH)_4((\mathbf{QPDC})_{1-x}(\mathbf{PEPEP\text{-}TMS})_x)_6$

x (%mol **PEPEP-TMS**)	0.027 M **PEPEP-TMS** mL (mmol)	0.027 M **QPDC** mL (mmol)	$ZrCl_4$ (mmol)	Total DMF mL	Toluene mL	Acetic Acid mL	Yield (mg/ %)
3	0.0500 (0.0014)	1.617 (0.0437)	0.05	2.4	0.125	0.464	9.1 (32.6%)
5	0.0833 (0.0023)	1.583 (0.0428)	0.05	2.4	0.125	0.464	10.5 (37.6%)
10	0.167 (0.0045)	1.500 (0.0405)	0.05	2.4	0.125	0.464	7.9 (29%)
15	0.250 (0.0068)	1.417 (0.0383)	0.05	2.4	0.125	0.464	8.5 (30.8%)
20	0.333 (0.009)	1.333 (0.036)	0.05	2.4	0.125	0.464	4.7 (17.2%)
30	1.000 (0.0270)	2.333 (0.0631)	0.099	4.75	0.25	0.928	5.3 (19.5%)
40	1.333 (0.036)	2.000 (0.054)	0.099	4.75	0.25	0.928	6.2 (23%)

Table S5: Reaction conditions for $Zr_6O_4(OH)_4((\mathbf{QPDC})_{1-x}(\mathbf{PEPEP\text{-}Fc})_x)_6$

x (%mol **PEPEP-FC**)	**PEPEP-Fc** mg (mmol)	**QPDC** mg (mmol)	$ZrCl_4$ (mmol)	DMF mL	Toluene mL	Acetic Acid mL	Yield (mg/ %)
10	4.6 (0.007)	32.1 (0.063)	0.040	1.9	0.10	0.40	22.0 (52.4%)
20	9.2 (0.014)	26.0 (0.058)	0.040	1.9	0.10	0.40	22.0 (50.8%)
30	13.8 (0.022)	22.7 (0.050)	0.040	1.9	0.10	0.40	22.0 (49.3%)
40	18.40 (0.029)	19.5 (0.043)	0.040	1.9	0.10	0.40	22.0 (47.8%)
60	27.58 (0.043)	13.0 (0.029)	0.040	1.9	0.10	0.40	22.0 (45.1%)
80	36.77 (0.058)	6.48 (0.014)	0.040	1.9	0.10	0.40	22.0 (42.7%)

Table S6: Reaction conditions for $Zr_6O_4(OH)_4((\mathbf{QPDC})_{1-x}(\mathbf{PEPEP\text{-}Cl})_x)_6$

x (%mol **PEPEP-Cl**)	**PEPEP-Cl** mg (mmol)	0.027 M **QPDC** mL (mmol)	$ZrCl_4$ (mmol)	DMF mL	Toluene mL	Acetic Acid mL	Yield (mg/ %)
20	3.9 (0.009)	1.333 (0.036)	0.05	2.4	0.125	0.417	10.5 (43%)
40	7.8 (0.018)	1.000 (0.027)	0.05	2.4	0.125	0.417	2.4 (9.7%)
100	19.6 (0.0045)		0.05	2.4	0.125	0.417	13.4 (53%)

Table S7: Reaction conditions for $Zr_6O_4(OH)_4((\mathbf{QPDC})_{1-x}(\mathbf{PEPEP\text{-}Br})_x)_6$

x (%mol **PEPEP-Br**)	0.009 M **PEPEP-Br** mL (mmol)	0.027 M **QPDC** mL (mmol)	$ZrCl_4$ (mmol)	Total DMF mL	Toluene mL	Acetic Acid mL	Yield (mg/ %)
1	0.050 (0.00045)	1.65 (0.04455)	0.05	2.4	0.125	0.464	12.2 (43%)
3	0.150 (0.00135)	1.617 (0.0437)	0.05	2.4	0.125	0.464	10.1 (36%)
5	0.250 (0.00225)	1.583 (0.0428)	0.05	2.4	0.125	0.464	13.7 (49%)
7.5	0.375 (0.00338)	1.5412 (0.0416)	0.05	2.4	0.125	0.464	8.4 (30%)
10	0.5 (0.0045)	1.500 (0.0405)	0.05	2.4	0.125	0.464	17.1 (61%)
15	0.750 (0.0068)	1.417 (0.0383)	0.05	2.4	0.125	0.464	15.2 (54%)

Section S4. **Composition analysis.**

General procedure for MOF digestion: In triplicate, ~5.0 mg of MOF sample was suspended in 10 µL of a 20 wt% DCl in D_2O solution. The suspension was sonicated for five min and then diluted to 0.4 mL with DMSO-d_6 followed by an additional 10 min of sonication. The mixture was transferred to an NMR tube before data collection.

In triplicate, MTV MOFs using **PEPEP-Fc** were suspended using 0.6 mL DMSO-d_6 and 50 µL of a 2.5 M KF in D_2O with ~4 mg of MOF sample. The suspensions were sonicated for 2 min and put in an oven at 120 °C for 2 min. The mixtures were transferred to an NMR tube and the tube was heated with a heat gun to allow for solids to move to bottom of the tube before data collection.

I/O composition plots were fitted with linear functions using excel. **PEPEP-Me, PEPEP-F,** and **PEPEP-Fc** were also fitted using logistic functions in python of the form:

$$y = \frac{100}{1 + Ae^{-B(x-C)}}$$ (equation S1) where A, B, and C are fitting parameters.

Figure S1. NMR spectra of **PEPEP-Me** System (^{1}H NMR, DMSO-d_6, 25 °C). Quantification done using ratios of signals at δ = 7.42 ppm (**PEPEP-Me**) and δ = 6.93 ppm (**QPDC-Me**)

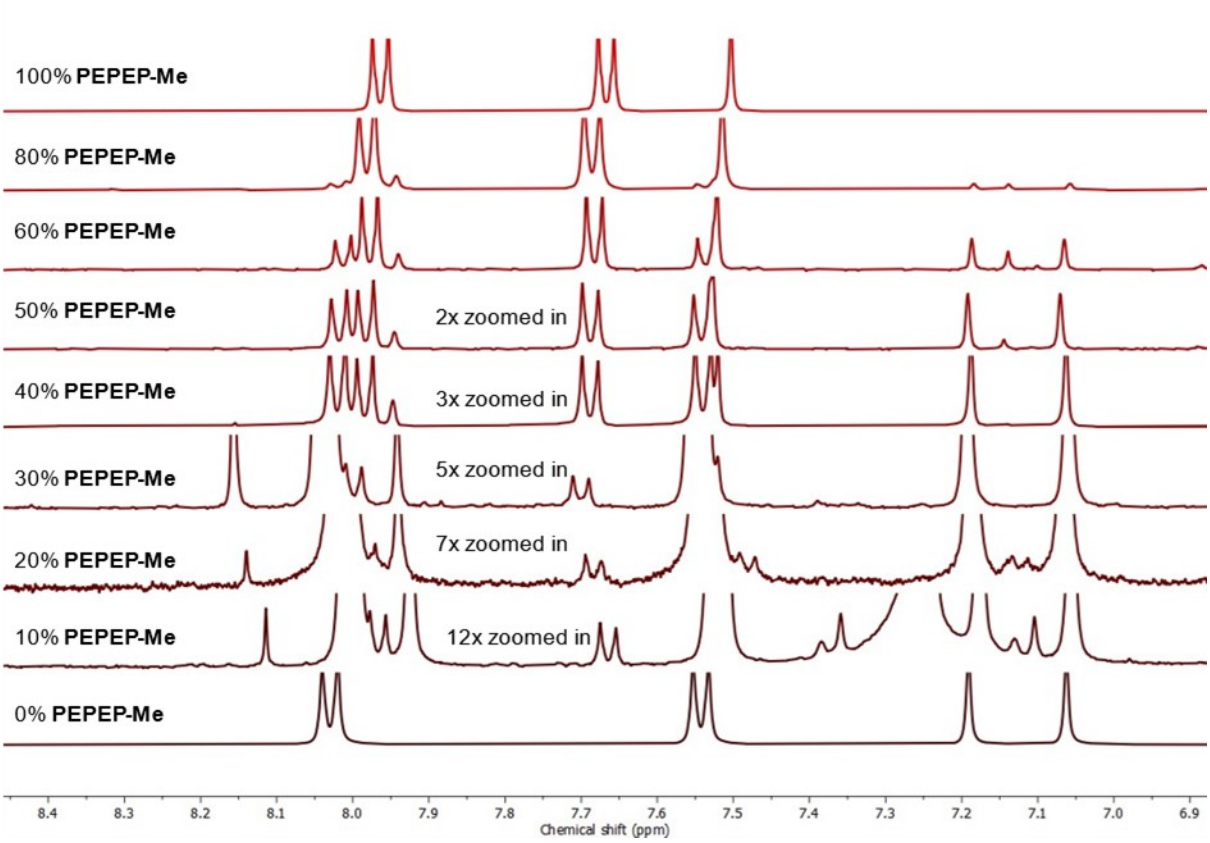

Figure S2. I/O composition plot determined by acid digested samples for **PEPEP-Me**. Error bars are shown for triplicates.

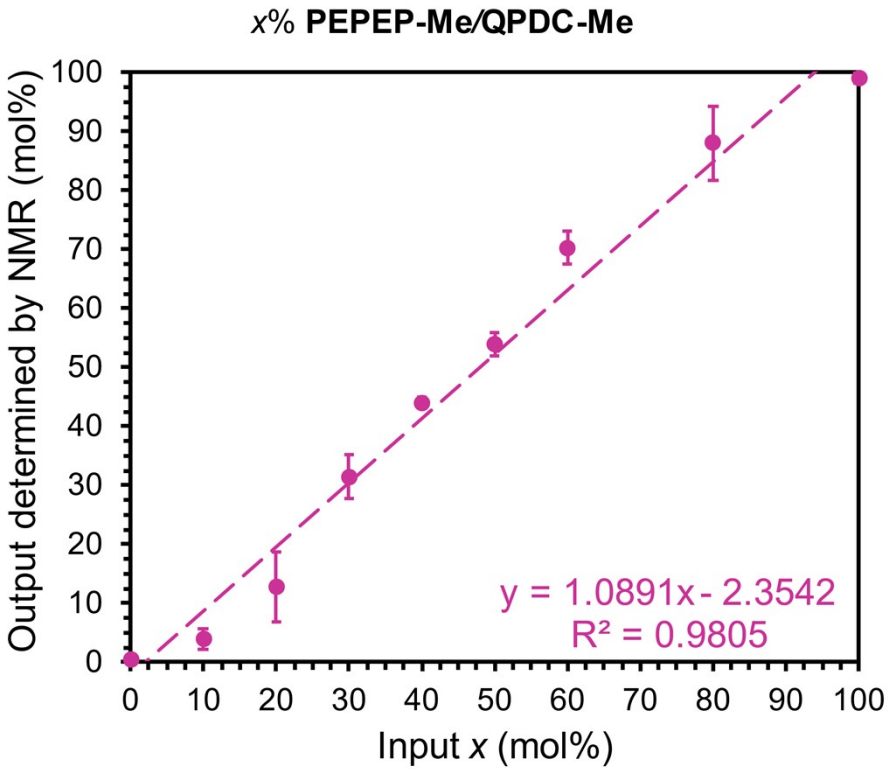

Figure S3. I/O composition plot determined by acid digested **PEPEP-Me** samples using logistic function. A, B, and C parameters for equation **S1** shown.

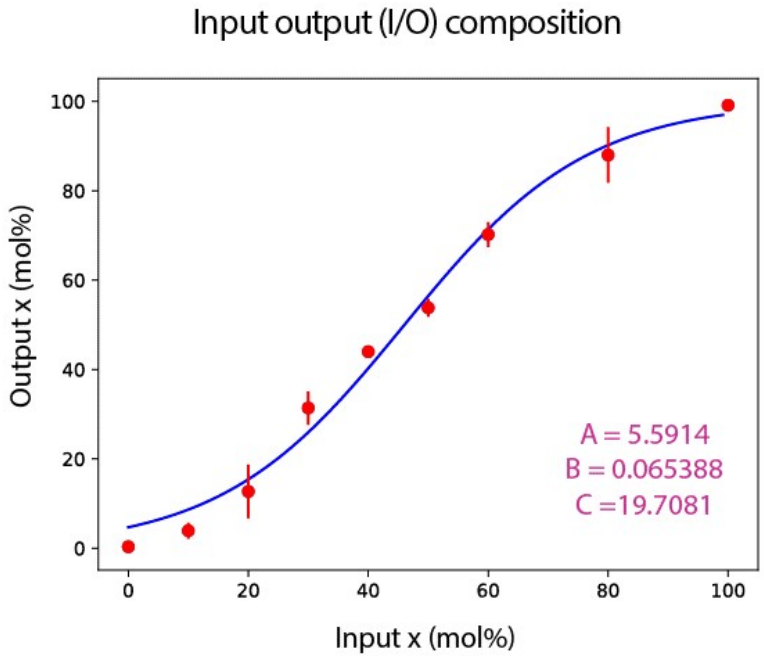

Figure S4. NMR spectra of **PEPEP-OMe** System (^{1}H NMR, DMSO-d_6, 25 °C). Quantification done using ratios of signals at δ = 7.62 ppm (**PEPEP-OMe**) and δ = 7.51 ppm (**QPDC-Me**)

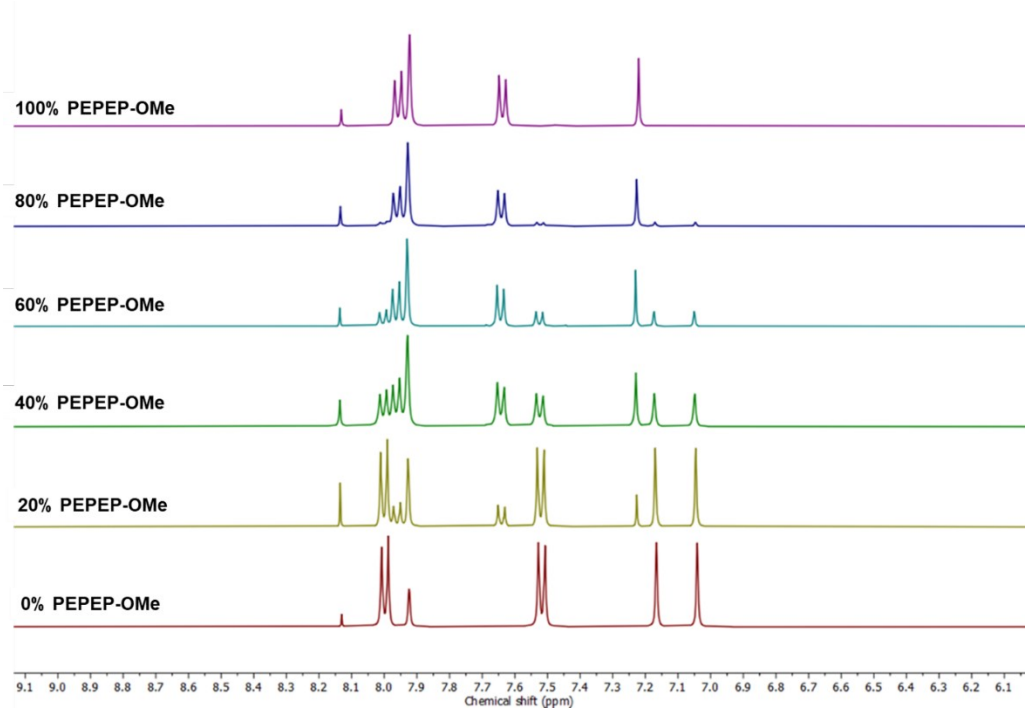

Figure S5. I/O composition plot determined by acid digested samples for **PEPEP-OMe**. Error bars are shown for triplicates. Linear fitting is indicated (broken lines)

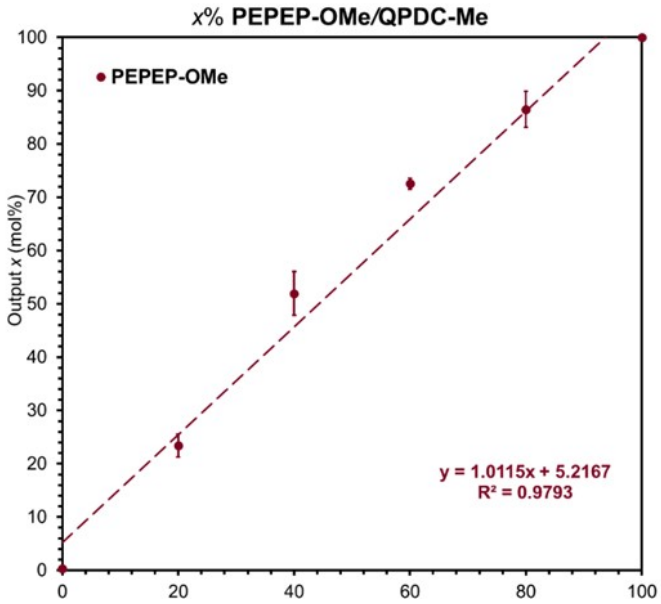

Figure S6. NMR spectra of **PEPEP-F** (^{1}H NMR, DMSO-d_6, 25 °C). Quantification done using ratios of signals at δ = 7.67 ppm (**PEPEP-F**) and δ = 7.50 ppm (**QPDC-Me**)

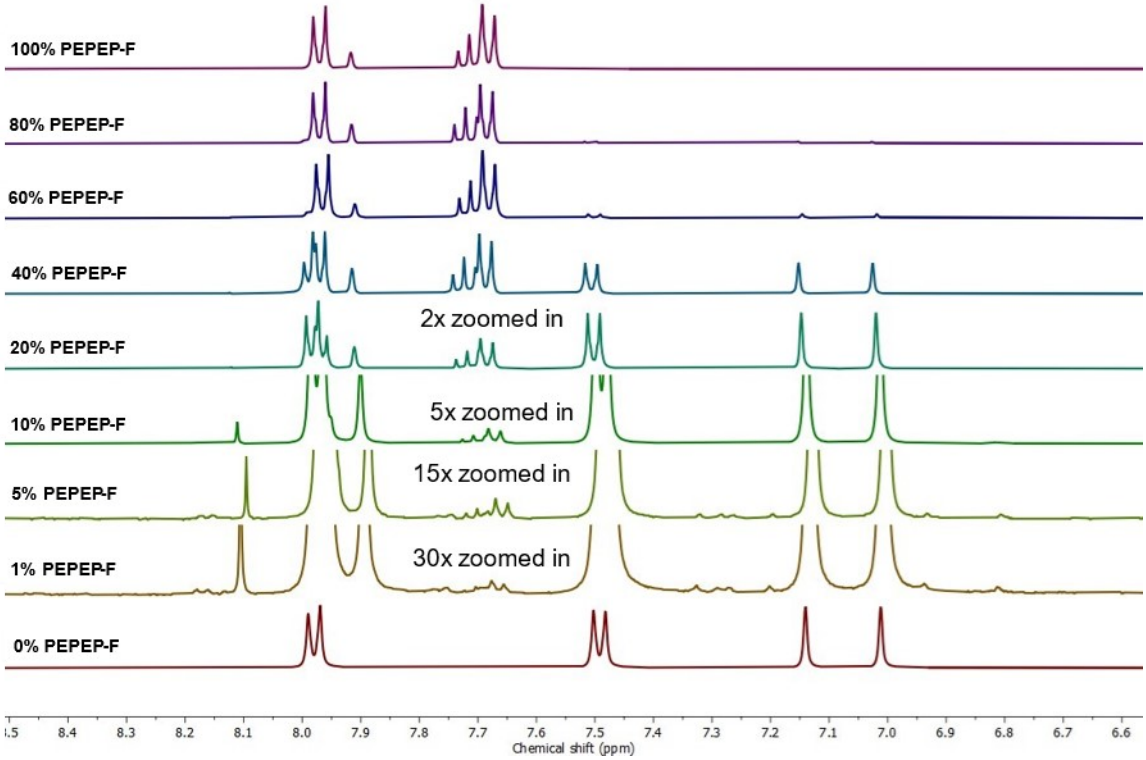

Figure S7. I/O composition plot determined by acid digested **PEPEP-F** samples.

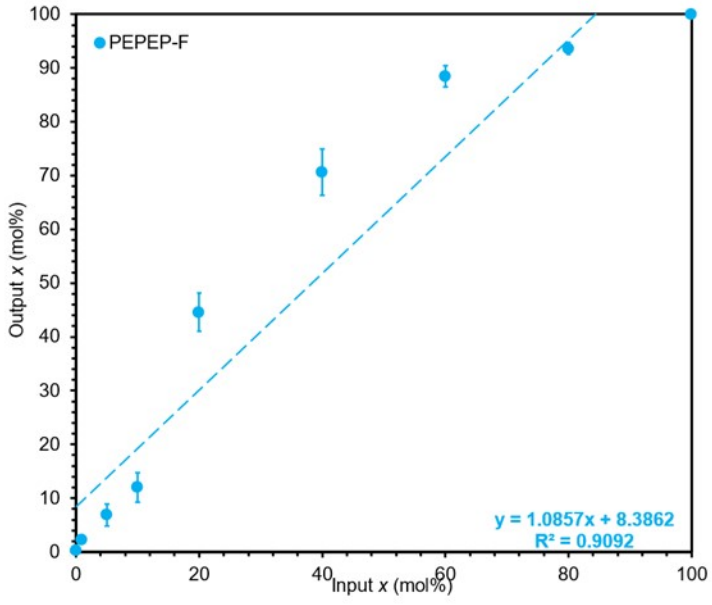

Figure S8. I/O composition plot determined by acid digested **PEPEP-F** samples using logistic function. A, B, and C parameters for equation **S1** shown.

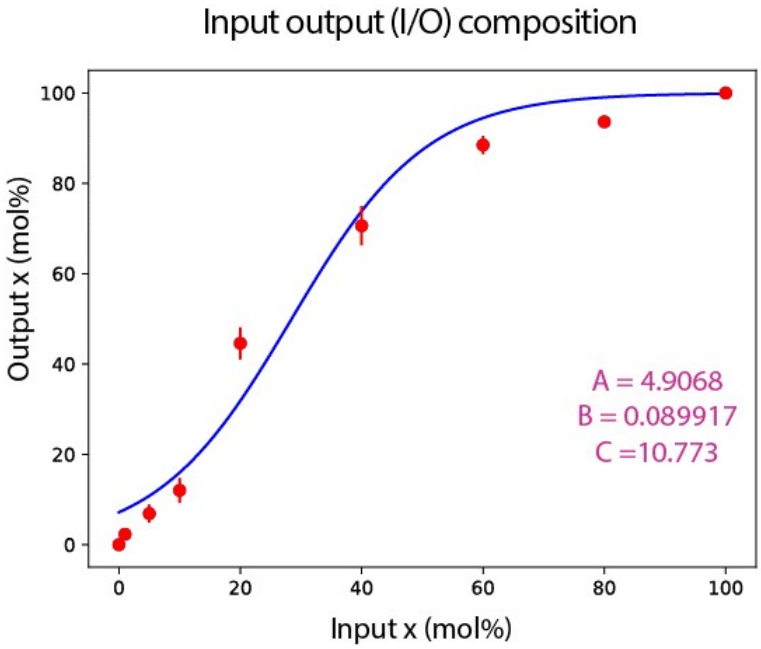

Figure S9. NMR spectra of **PEPEP-TMS**. Quantification done using ratios of signals at δ = 7.66 ppm (**PEPEP-F**) and δ = 7.53 ppm (**QPDC-Me**)

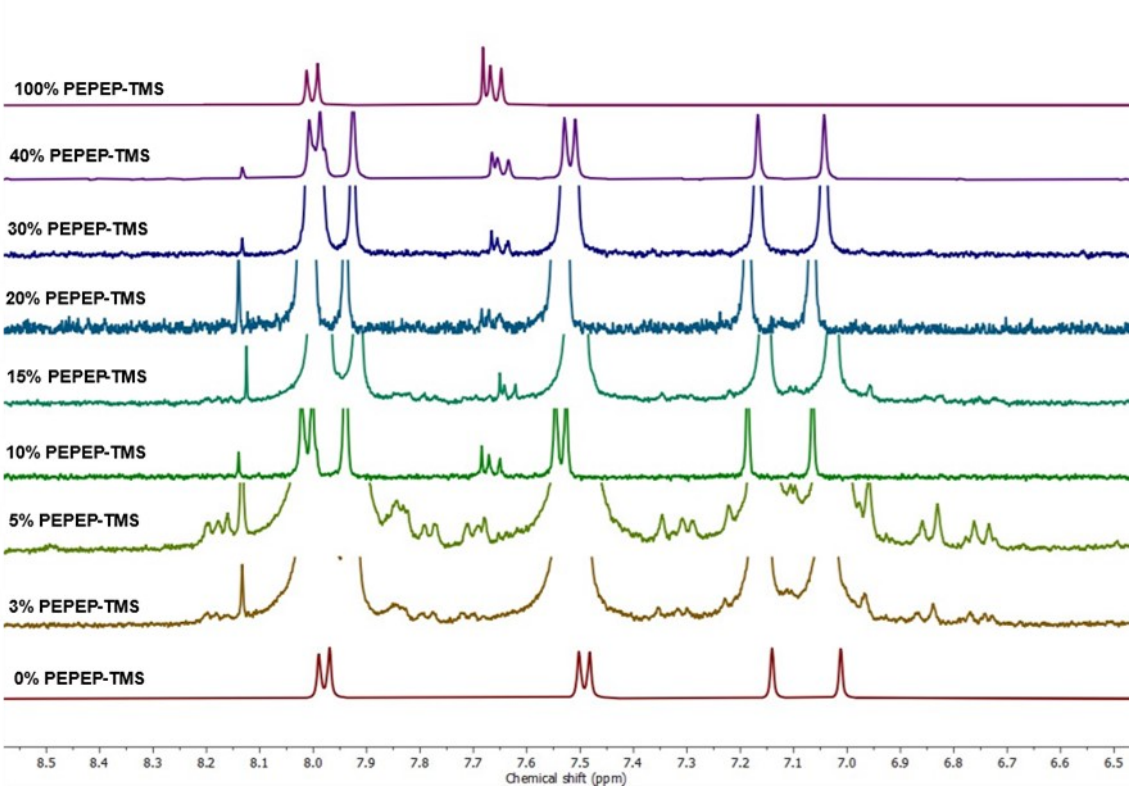

Figure S10. I/O composition plot of **PEPEP-TMS** determined by acid digested samples. Linear fitting is shown.

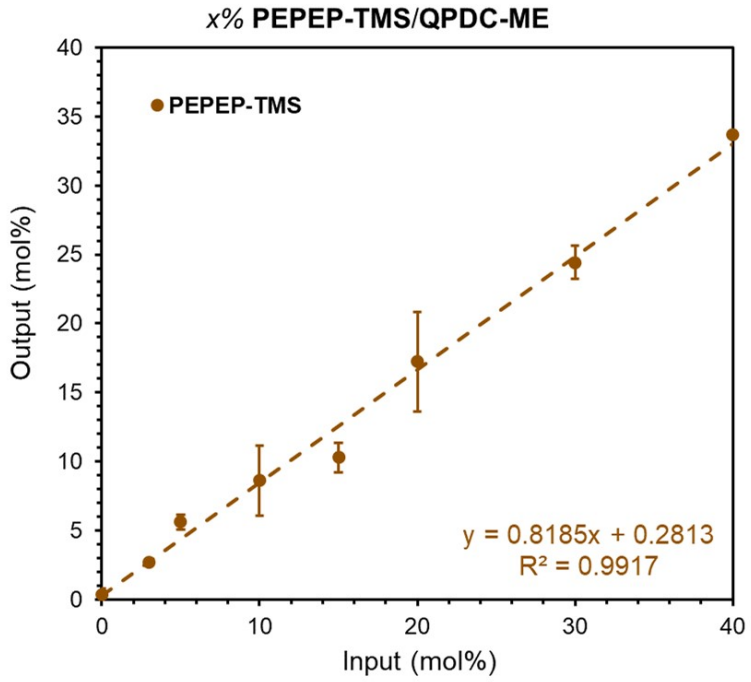

Figure S11. NMR spectra of **PEPEP-Fc** (^{1}H NMR, DMSO-d_6, 25 °C). Quantification done using ratios of signals at δ = 6.94 ppm (**PEPEP-Fc**) and δ = 6.78 ppm (**QPDC-Me**)

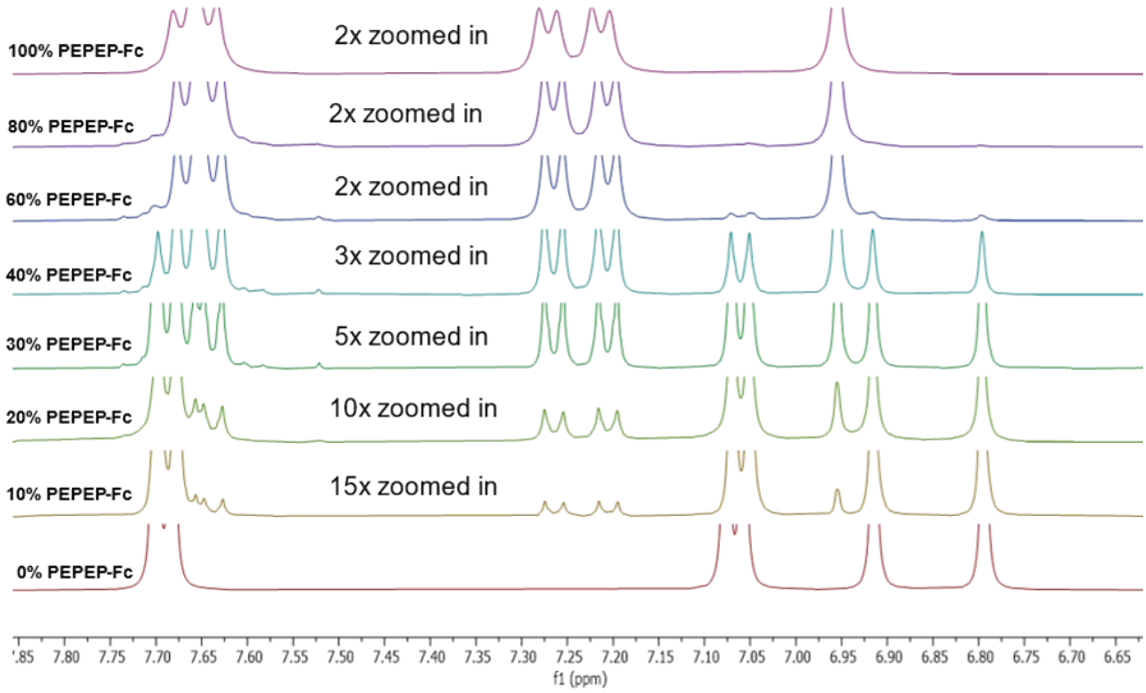

Figure S12. I/O composition plot of **PEPEP-Fc** determined by base digested samples with linear fitting.

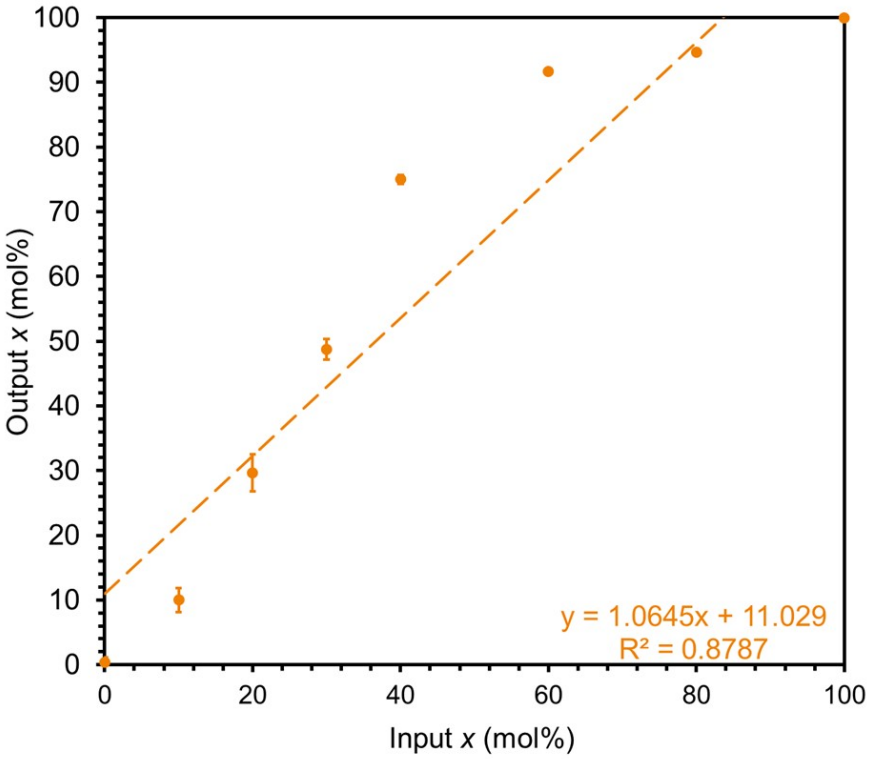

Figure S13. I/O composition plot of **PEPEP-Fc** using logistic function. A, B, and C parameters for equation **S1** shown.

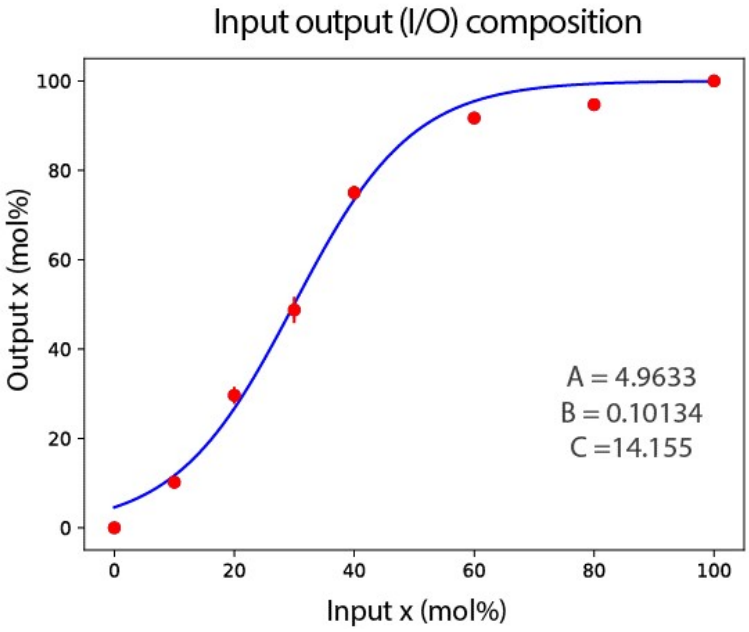

Figure S14. NMR spectra of **PEPEP-Cl** (^{1}H NMR, DMSO-d_6, 25 °C). Quantification done using ratios of signals at δ = 7.67 ppm (**PEPEP-Cl**) and δ = 7.47 ppm (**QPDC-Me**).

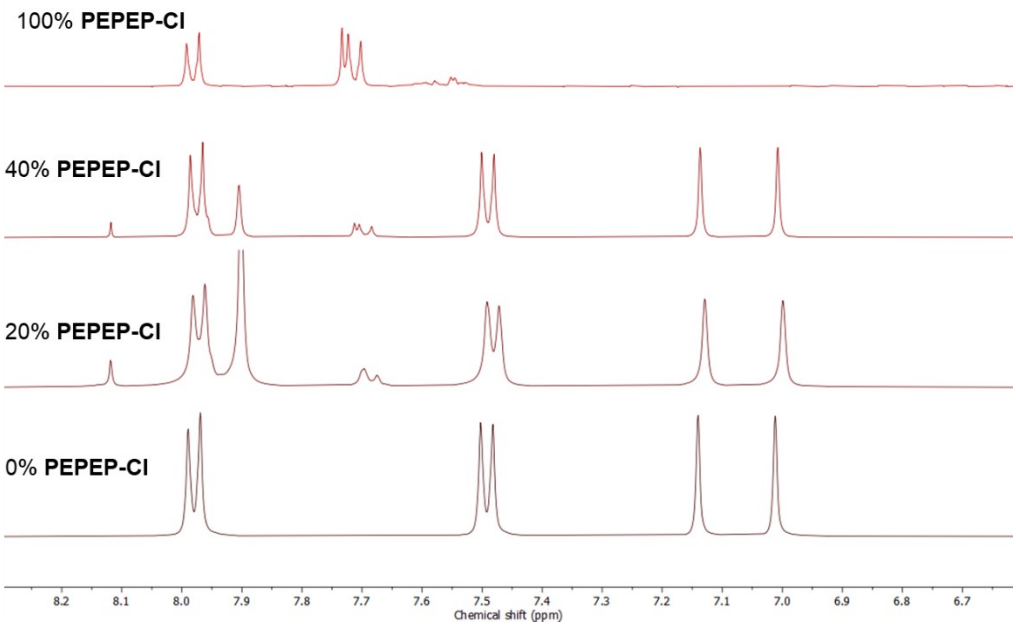

Figure S15. I/O composition plot determined by acid digested **PEPEP-Cl** samples.

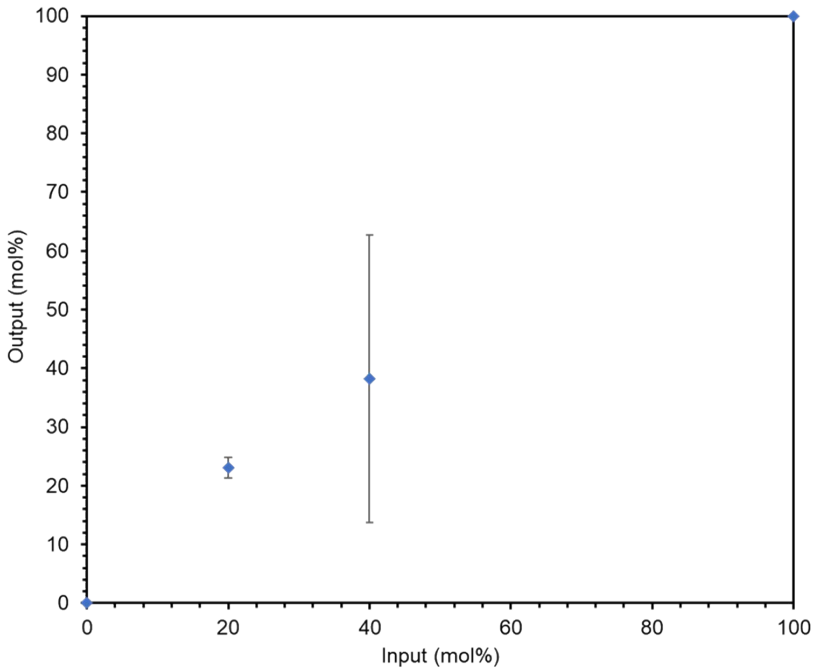

Figure S16. NMR spectra of **PEPEP-Br** (^{1}H NMR, DMSO-d_6, 25 °C). Quantification done using ratios of signals at δ = 7.68 ppm (**PEPEP-Br**) and δ = 7.46 ppm (**QPDC-Me**).

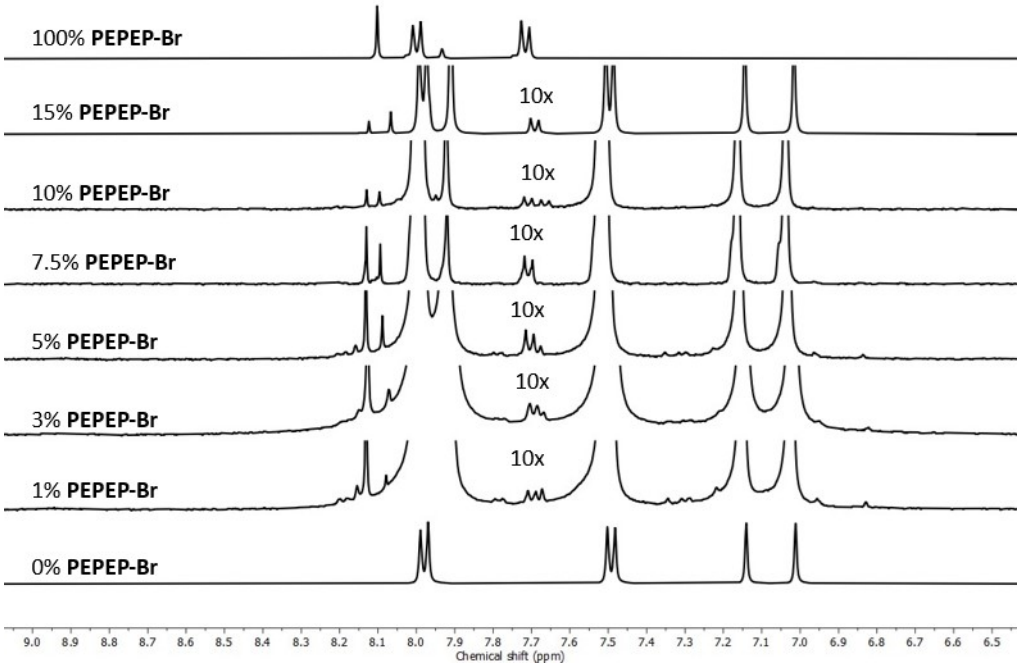

Figure S17. I/O composition plot determined by acid digested **PEPEP-Br** samples with linear fitting.

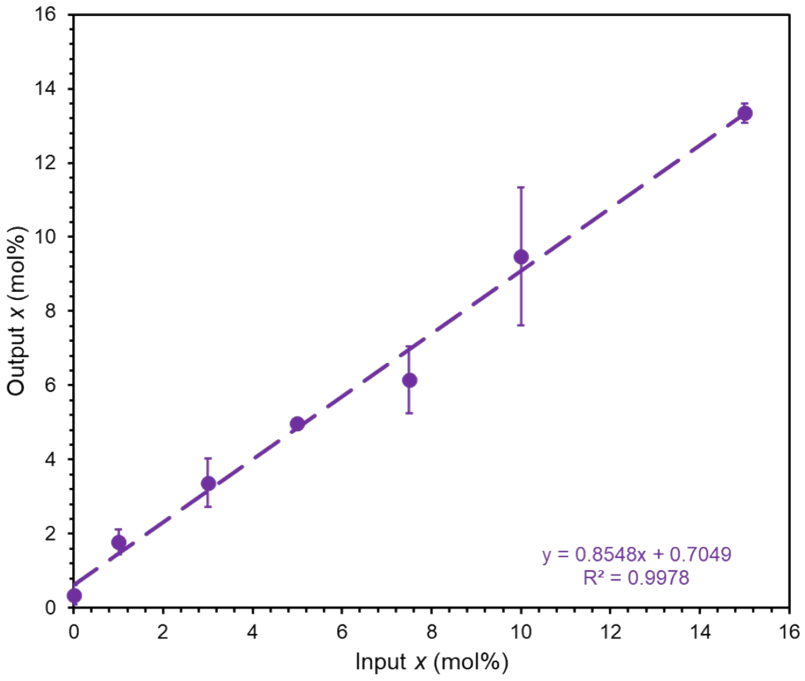

Section S5. **Powder X-ray diffraction and powder crystallography.**

Indexing of the patterns was done using *GSAS-II*.[S11] The background was first fitted with a 10th order shifted Chebyshev polynomial. Peaks were manually chosen and refined using LeBail fitting (peak fit in *GSAS-II*). The asymmetry of the peaks was refined, followed by refinement of the X and Y parameters of a Thomson-Cox-Hasting modified pseudo-Voigt functions and Finger-Cox-Jephcoat asymmetry. The peaks were then indexed and used to find the lattice parameters for a cubic system using the autoindexing function in *GSAS-II*.[s12]

Crystal models were created using *Materials Studio*. Starting from the published CIF of PIZOF-2, CIFs were loaded and modified to include heteroatoms in the position in the **PEPEP** linker. The models were then geometry optimized using the *Forcite* module and the crystal was relaxed (lattice parameters and atom positions) using the Universal Force Field (UFF).[S13]

Rietveld refinements were performed in *GSAS-II* using the models obtained from *Materials Studio.* Refinements of the PIZOF-2(F) were performed using Thomson-Cox-Hasting modified pseudo-Voigt functions and Finger-Cox-Jephcoat asymmetry. First, the patterns were indexed using the same method as above. Then, the crystallographic information file (CIF) of crystal models were loaded, using the purely rotational space group $F4_132$. First, refined the scale factor, then added the unit cell, and refined until no changes were observed. Then, refined the scale factor versus the zero shift and sample displacement. The unit cell was refined again. Then refined versus *X*, versus *Y*, and then versus *X* and *Y*. The *W*, *V*, and *U* were then refined separately and then together. Then, *W*, *V*, *U*, *X*, and *Y* were all refined together. Everything was then unchecked and only refined the scale factor versus the size and strain. The unit cell parameter was then added followed by the sample displacement. A preferred orientation was then added to the refinements using a 2nd order spherical harmonic function. Fraction, position, and Isotropic atomic displacement (U_{iso}) were then refined for the solvent oxygen atoms. Oxygen atoms with negative occupancies were removed. The scale factor and unit cell parameter were then refined again. Then U_{iso} for zirconium atoms and solvent oxygens were refined. Followed by adding in the oxygen and carbon atoms that form the cluster. Then, U_{iso} was refined for all atoms. The scale factor and the unit cell parameter were then added back in. Followed by strain, particle size, and harmonic order. Refined multiple times and then added in the *X* and *Y* parameters. Then, only refined U_{iso} for atoms. Followed by refining the instrument parameters (*X*, *Y*, *W*, *V*, and *U*) with the scale factor again. Refined U_{iso} for carbon, zirconium, fluorine, and oxygen in the MOF again. Followed by refining only the scale factor and unit cell again. Then, refined the scale factor and the background. Then, added in the zero shift and asymmetry. Final refinements

included all parameters, which were refined iteratively until convergent refinements were obtained. F_{obs} were extracted bond distances and angles were calculated, and the CIF was generated. Oxygen atoms were used to represent solvents inside the pores.

Figure S18. Stacked PXRD of (Cu kα) of *x*% **PEPEP-Me**/**QPDC-Me**.

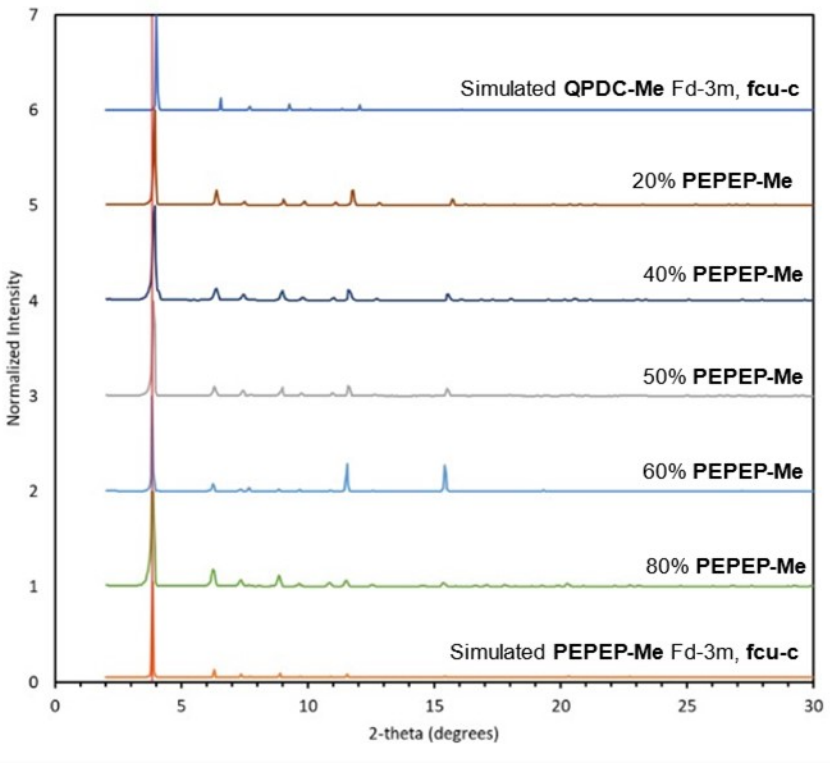

Figure S19. Stacked PXRD of (Cu kα) of *x*% **PEPEP-Me**/**QPDC-Me** zoomed.

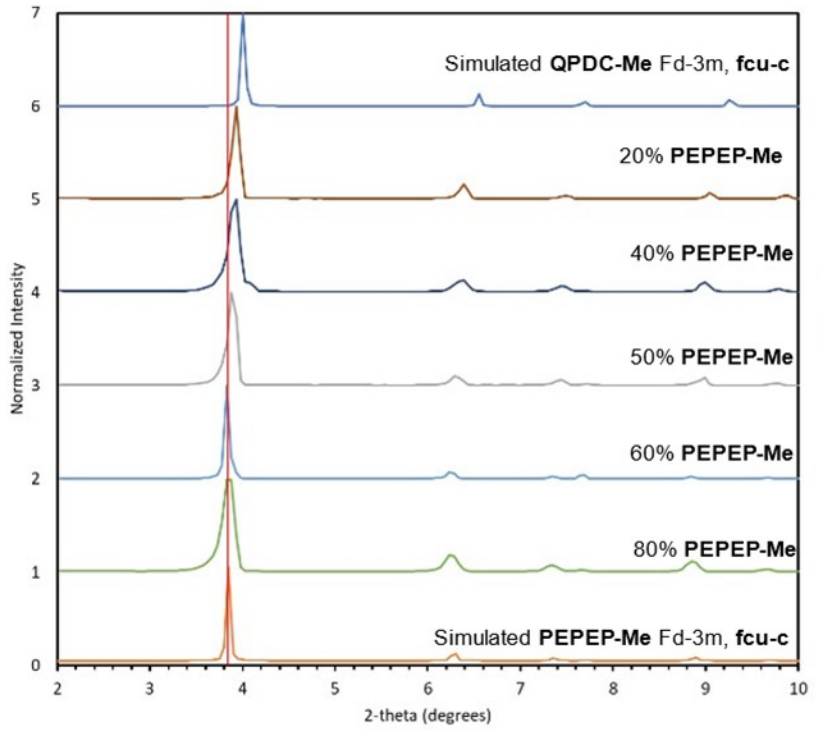

Figure S20. Stacked PXRD of (Cu kα) of *x*% **PEPEP-TMS**/**QPDC-Me**.

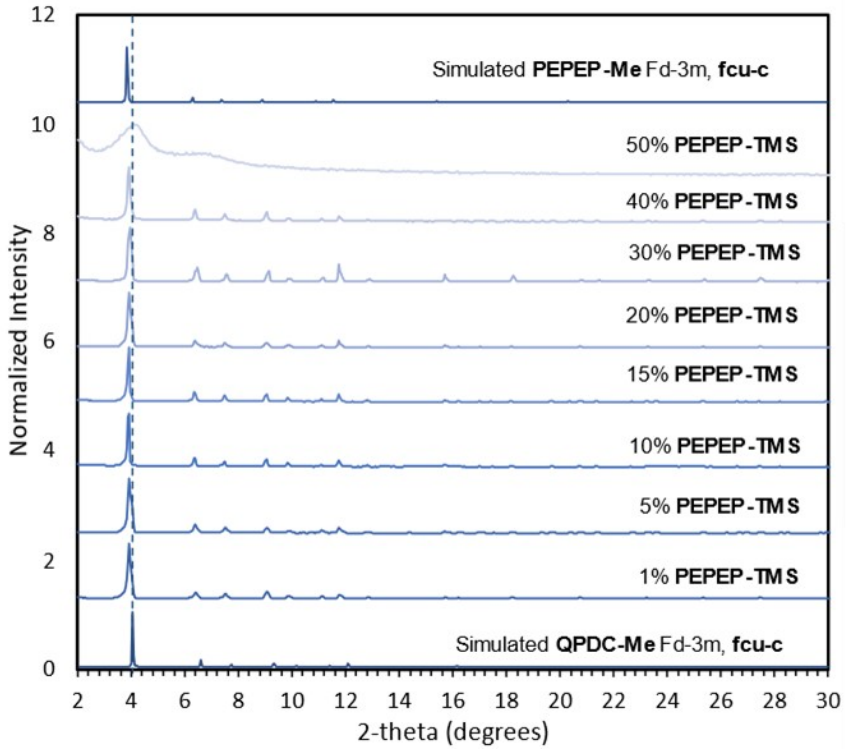

Figure S21. Stacked PXRD of (Cu kα) of *x*% **PEPEP-TMS**/**QPDC-Me** zoomed.

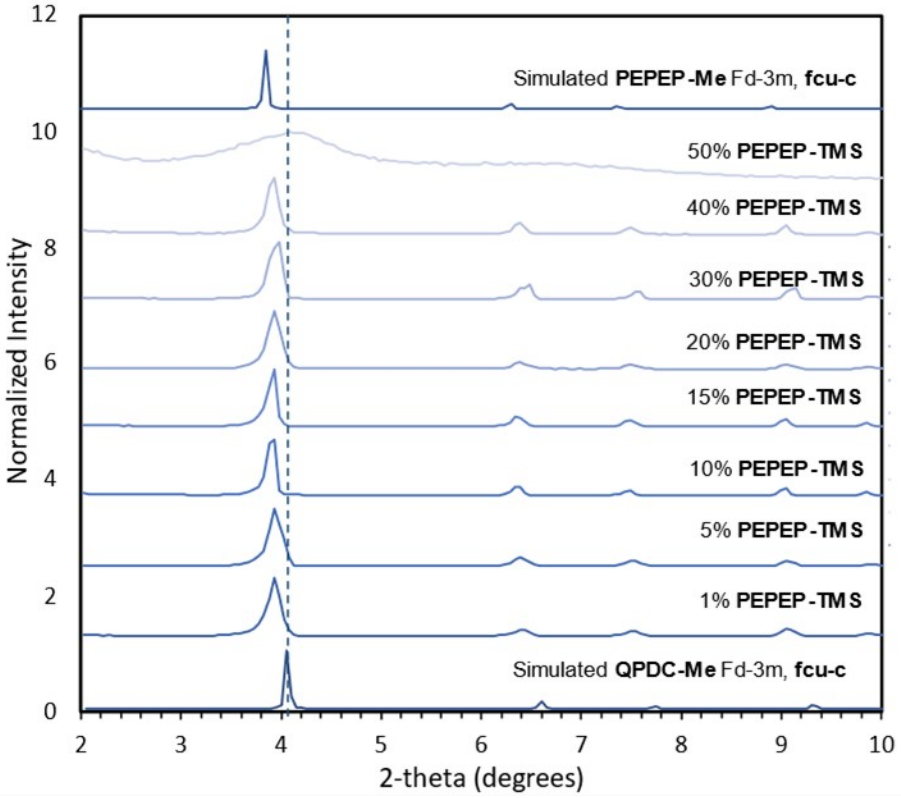

Figure S22. Stacked PXRD of (Cu kα) of *x*% **PEPEP-Cl**/**QPDC-Me**.

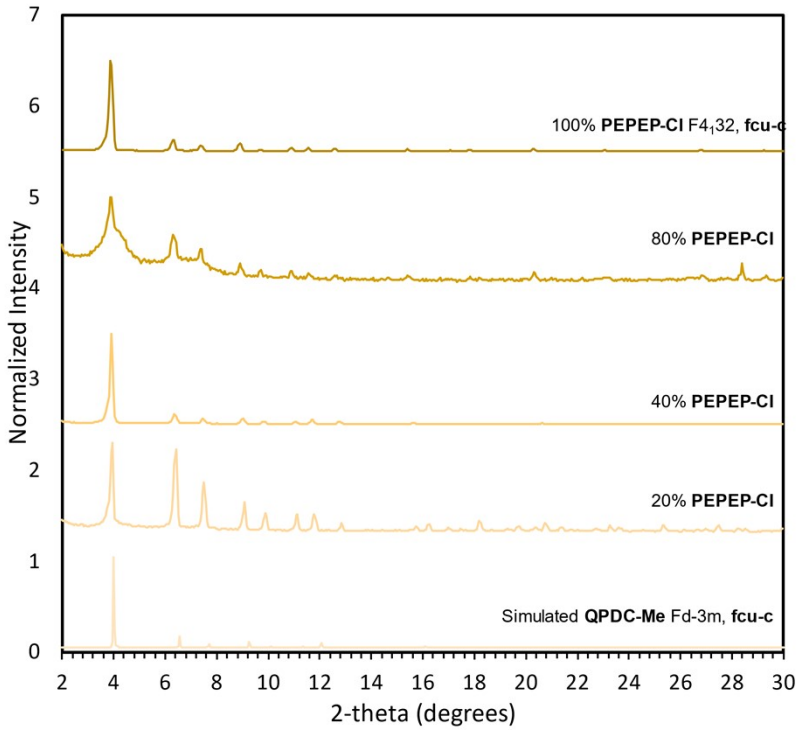

Figure S23. Stacked plot of *x*% **PEPEP-CI**/**QPDC-Me** zoomed.

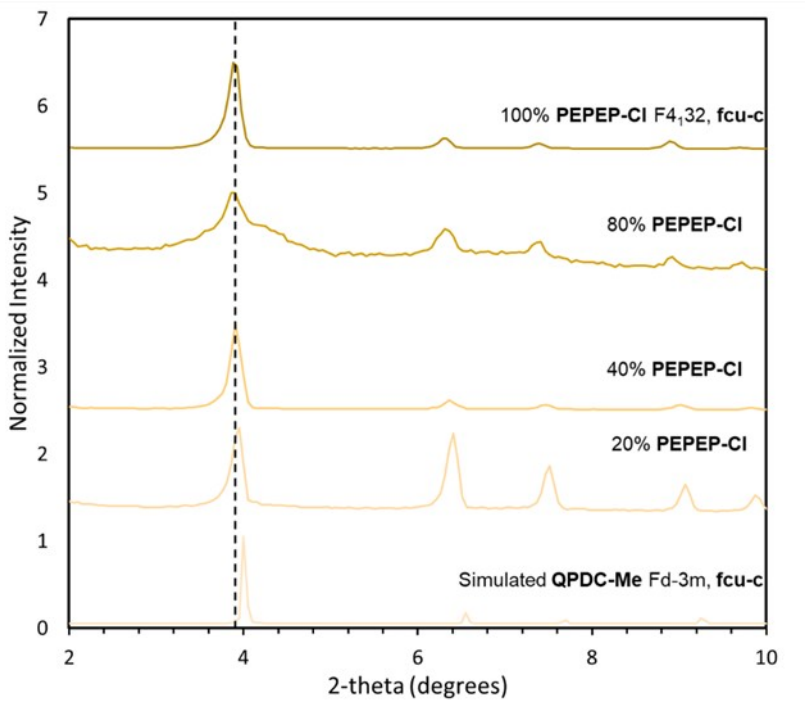

Figure S24. Stacked PXRD of (Cu kα) of *x*% **PPP-Me**/**QPDC-Me** demonstrating lack of MTV formation.

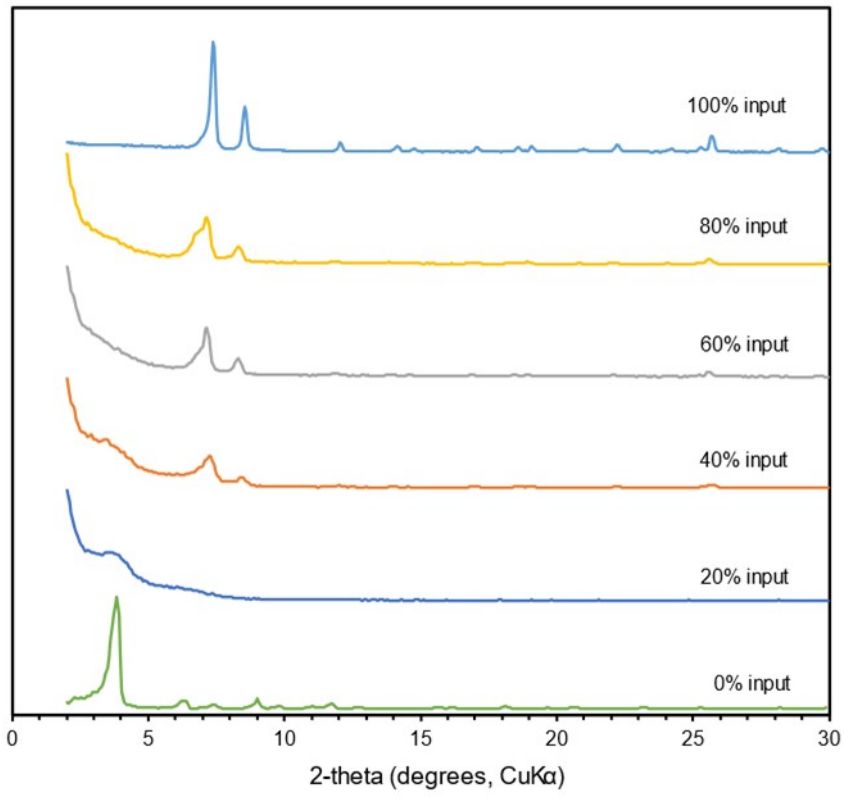

Table S8. Lattice parameter and volumes for **PEPEP-Me**/**QPDC-Me** System

mol%	Sample	a (Å)	V (Å^3)	M20
10	a	38.92057	58957.285	23.43
	b	38.94385	59063.155	36.94
	c	38.91014	58909.917	24.37
	average	38.9249(04)	58977(78)	
20	a	38.95804	59127.74	22.12
	b	38.99728	59285.57	29.66
	c	39.01102	59369.30	21.33
	average	38.989(27)	59260(122)	
30	a	39.16938	60095.24	24.44
	b	39.12972	59912.88	20.89
	c	39.18743	60178.36	43.61
	average	39.1662(03)	60062(136)	
40	a	39.33191	60846.42	33.55
	b	39.29484	60879.83	30.77
	c	39.29673	60683.29	20.13
	average	39.3088(21)	60803(105)	
50	b	39.46472	61464.91	34.71
	c	39.3306	60840.35	24.61
	d	39.47341	61505.48	20.46
	average	39.423(80)	61270(373)	
60	a	39.59662	62083.23	38.79
	b	39.58223	62015.56	35.48
	c	39.49649	61613.45	29.81
	average	39.558(54)	61904(254)	
80	a	39.86389	63348.88	40.92
	b	39.79078	63000.99	24.23
	c	39.86499	63354.16	36.72
	average	39.840(43)	63235(202)	

Table S9. Lattice parameter and volumes for **PEPEP-Me**/**QPDC-Me** System collected from single crystal X-ray diffraction

mol% **PEPEP-Me**	Lattice parameter (Å)	Standard deviation of lattice parameters(Å)	Crystal System	Cell Volume(Å^3)	Cell Volume ESD(Å^3)
20%	39.015	.005	Cubic F	59389	7
40%	39.325	.002	Cubic F	60305	3
60%	39.465	.002	Cubic F	61464	3
80%	39.867	.004	Cubic F	62533	5

Table S10. Data collection conditions for **PEPEP-Me**/**QPDC-Me** System collected from single crystal X-ray diffraction

mol% **PEPEP-Me**	2θ	T (K)	Exposure Time/frame	Scans	Frames/scan
20%	-10	90(1) K	6	5	360
40%	-10	Room Temp (298K)	2	5	360
60%	-10	Room Temp	2	5	360
80%	-10	90(1) K	20	5	360

Figure S25. LeBail plot of 10% **PEPEP-Me**/**QPDC-Me**

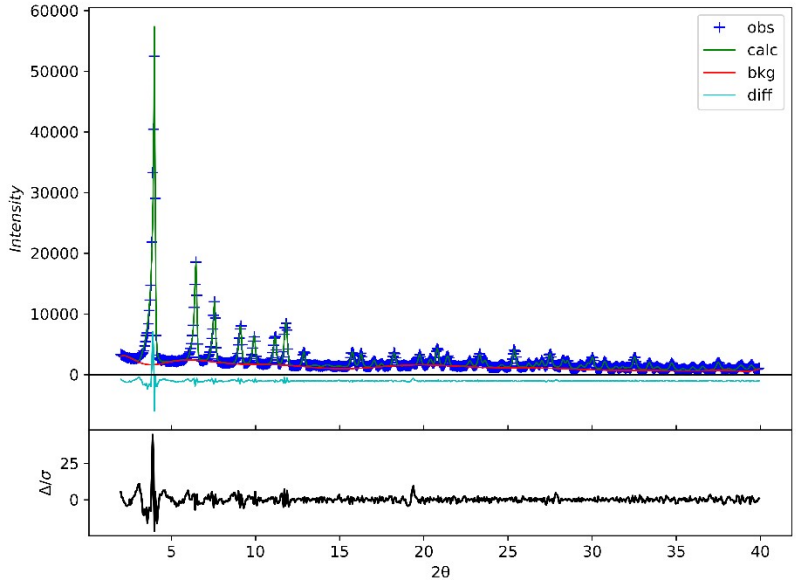

Figure 26#. LeBail plot of 20% **PEPEP-Me**/**QPDC-Me**

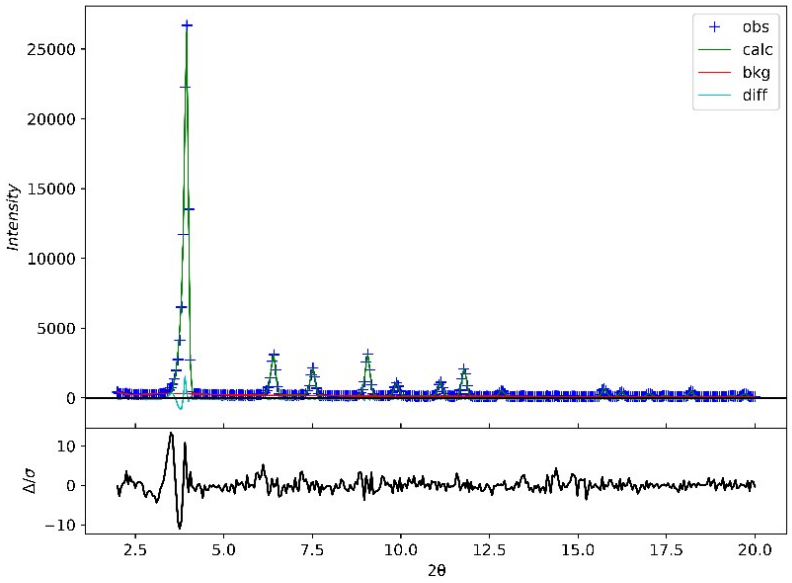

Figure S27. LeBail plot of 30% **PEPEP-Me**/**QPDC-Me**

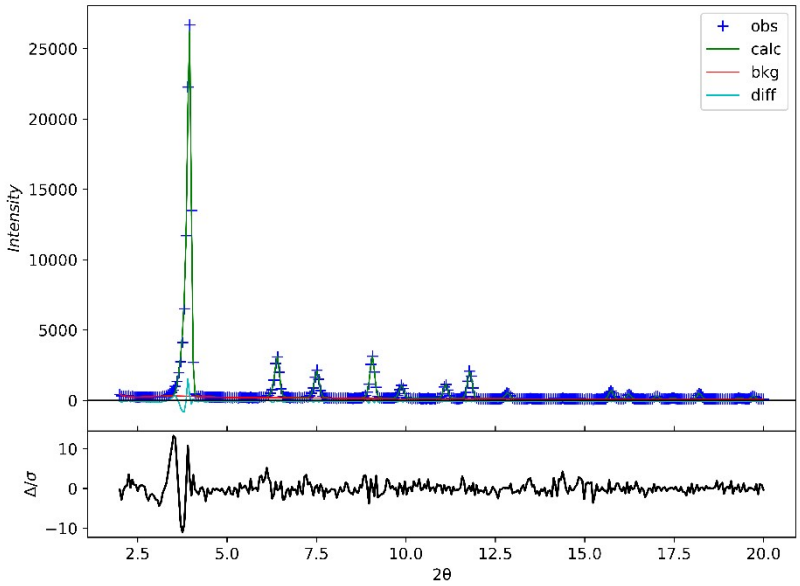

Figure S28. LeBail plot of 40% **PEPEP-Me**/**QPDC-Me**

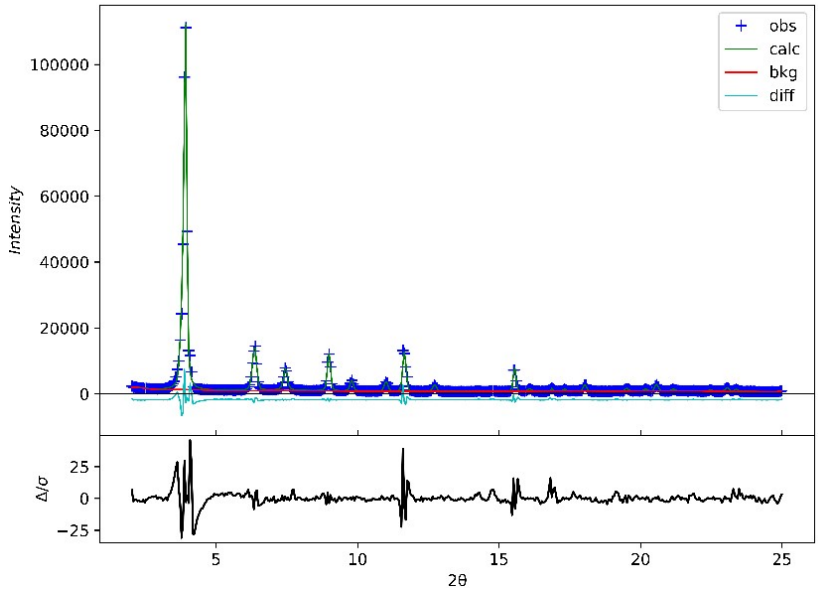

Figure S29. LeBail plot of 50% **PEPEP-Me**/**QPDC-Me**

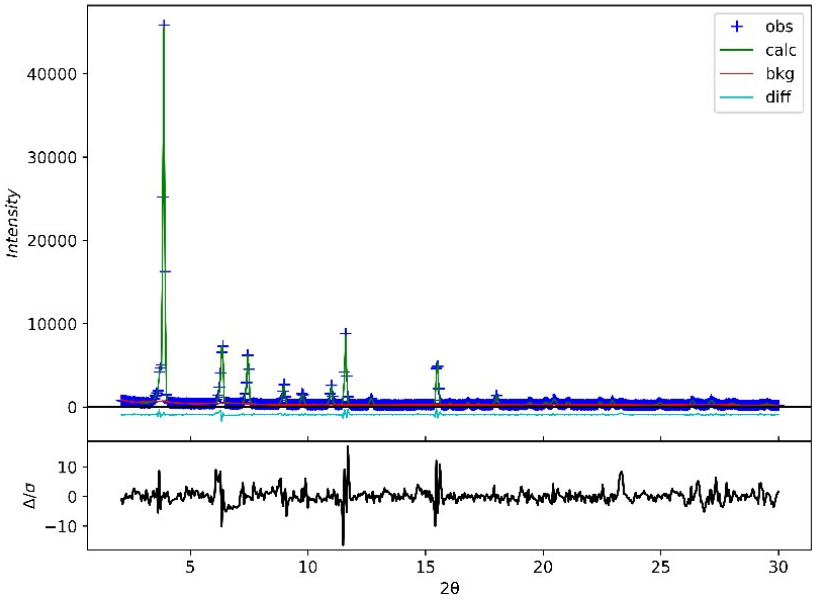

Figure S30. LeBail plot of 60% **PEPEP-Me**/**QPDC-Me**

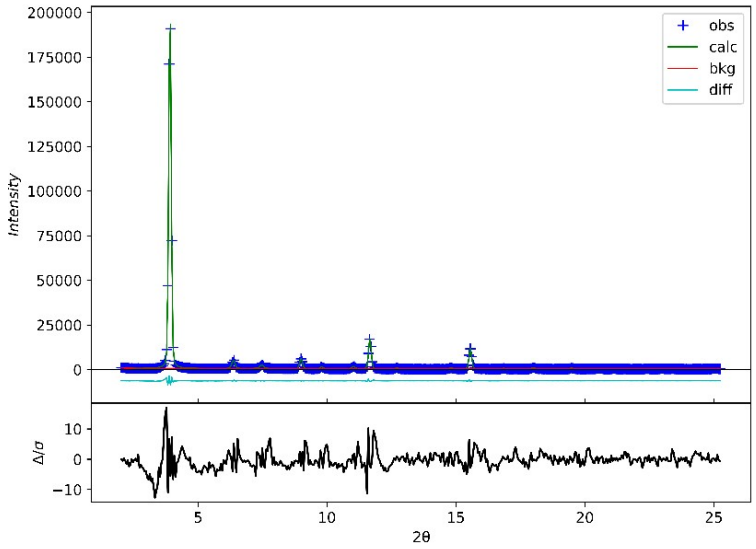

Figure S31. LeBail plot of 80% **PEPEP-Me**/**QPDC-Me**

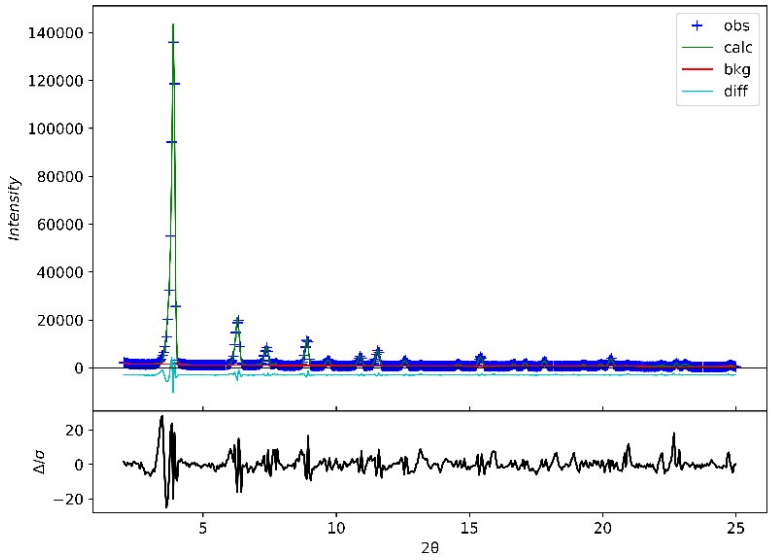

Table S11. Lattice parameter and volumes for **PEPEP-OMe**/**QPDC-Me** System

mol%	Sample	a (Å)	V (Å^3)	M20
20	a	39.05959	59591.31	24.2
	b	39.28084	60609.72	24.85
	c	39.29499	60675.23	16.57
	average	39.288(01)	60642(46)	
40	a	39.48931	61579.85	20.87
	b	39.39359	61133.13	20.23
	c	39.46654	61473.39	23.35
	average	39.450(05)	61395(233)	
60	b	39.8084	63084.74	31.31
	c	39.7915	63004.4	30.72
	d	39.78168	62957.47	20.12
	average	39.794(014)	63016(64)	
80	a	39.94655	63743.77	34.72
	b	39.94346	63728.99	19.95
	c	39.93972	63711.11	20.52
	average	39.943(003)	63728(16)	

Figure S32. Vegard's Plot for **PEPEP-OMe/QPDC-Me**

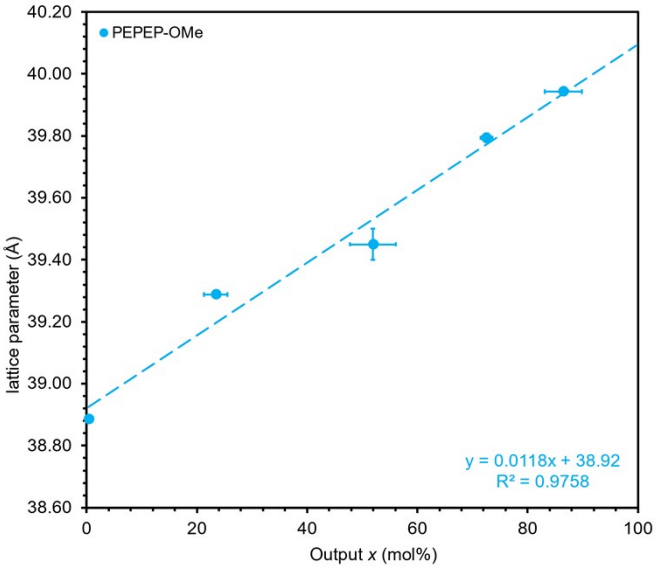

Figure S33. LeBail plot of 20% **PEPEP-OMe/QPDC-Me**

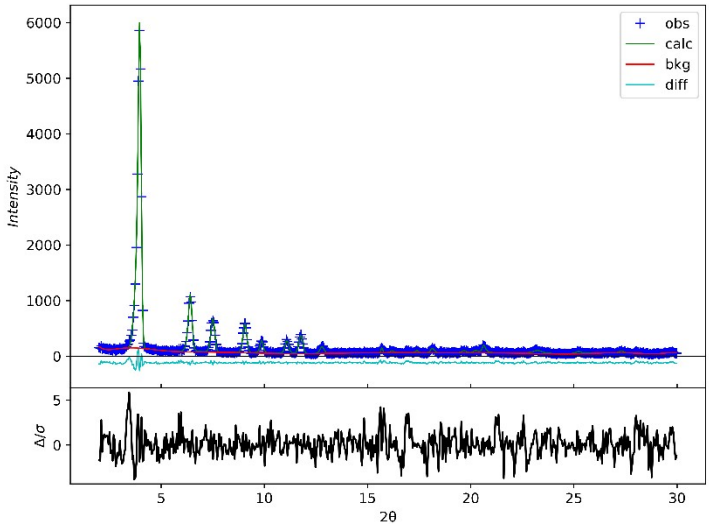

Figure S34. LeBail plot of 40% **PEPEP-OMe/QPDC-Me**

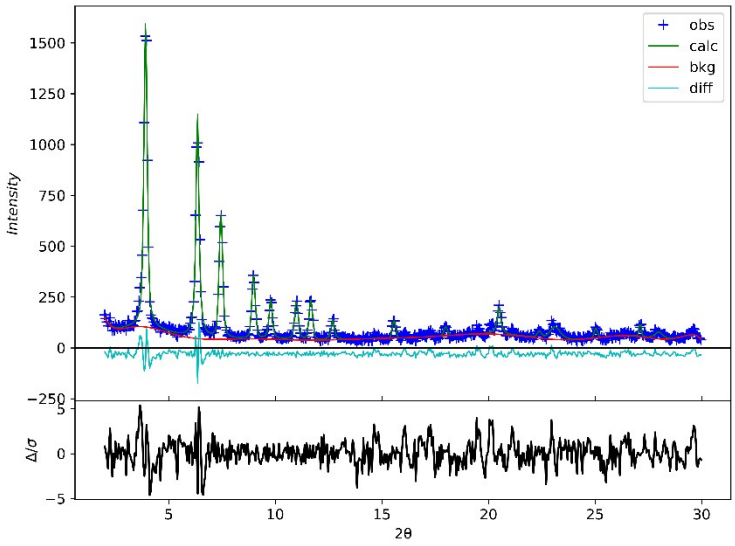

Figure S35. LeBail plot of 60% **PEPEP-OMe/QPDC-Me**

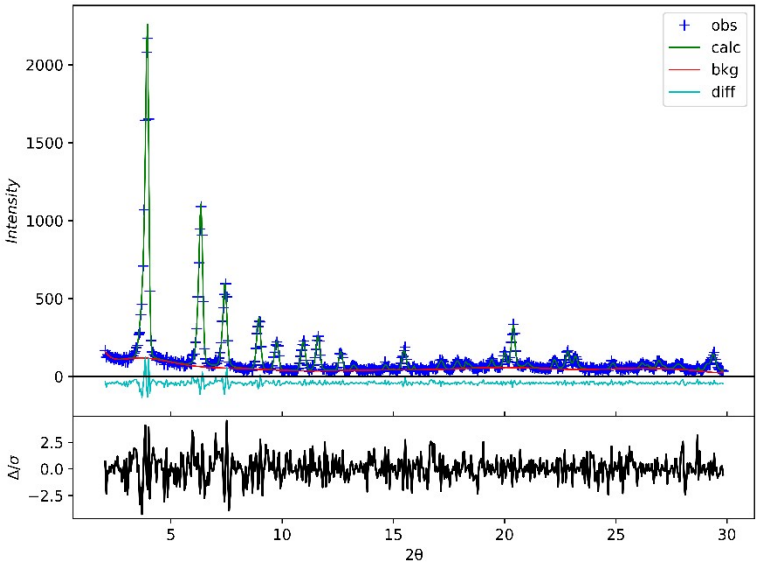

Figure S36. LeBail plot of 80% **PEPEP-OMe/QPDC-Me**

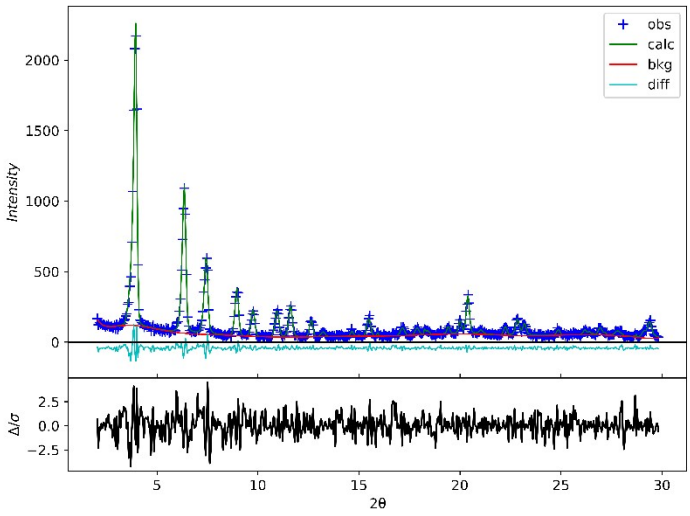

Table S12. Lattice parameter and volumes for **PEPEP-F**/**QPDC-Me** System

mol%	Sample	a (Å)	V (Å^3)	M20
1	a	38.92961	58998.392	28.97
	b	38.93054	59002.608	21.8
	c	38.92158	58961.889	20.63
	average	38.927(049)	58988(22)	
5	a	38.98332	59242.942	28.15
	b	38.94354	59061.746	33.24
	c	38.96749	59170.759	59.42
	average	38.965(02)	59158(91)	
10	a	39.01658	59394.687	60.64
	b	39.01906	59406.013	42.34
	c	39.01857	59403.76	34.31
	average	39.018(001)	59401(6)	
20	a	39.39376	61027.05	24.78
	b	39.37818	61061.44	25.22
	c	39.33398	60856.05	24.39
	average	39.369(031)	60982(110)	
40	a	39.76093	62859.304	32.22
	b	39.69175	62531.77	28.73
	c	39.76442	62875.882	22.91
	average	39.730(041)	62756(194)	
60	a	39.84135	63241.475	40.39
	b	39.83702	63220.874	24.58
	c	39.8901	63473.94	49.32
	average	39.856(03)	63312(140)	
80	a	39.90201	63530.806	74.42
	b	39.87685	63410.71	27.28
	c	39.92656	63648.14	81.49
	average	39.9018(025)	63530(119)	
100	a	39.99618	63981.68	37.15
	b	39.97706	63889.954	25.76
	c	39.99107	63957.15	25.35
	average	39.988(01)	63943(48)	

Figure S37. Vegard's Plot for **PEPEP-F/QPDC-Me**

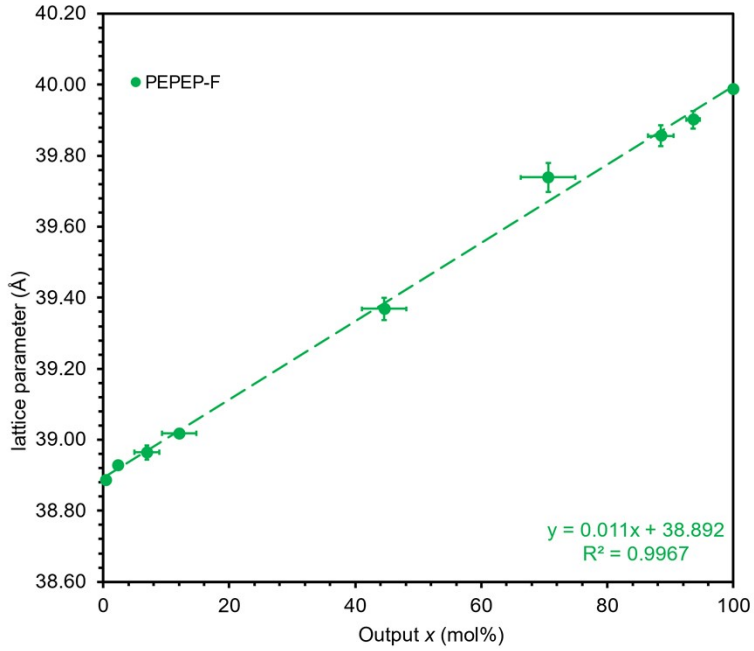

Figure S38. LeBail plot of 1% **PEPEP-F/QPDC-Me**

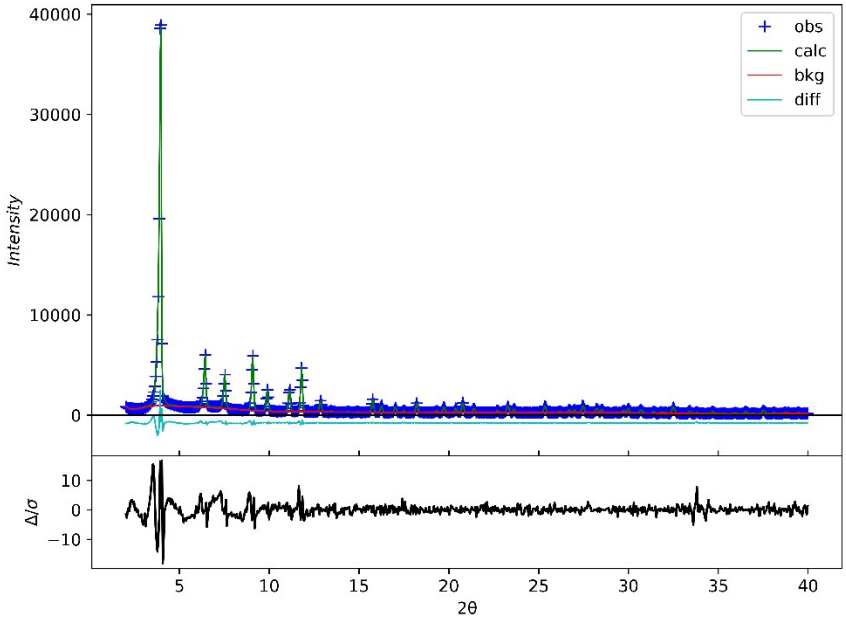

Figure S39. LeBail plot of 5% **PEPEP-F/QPDC-Me**

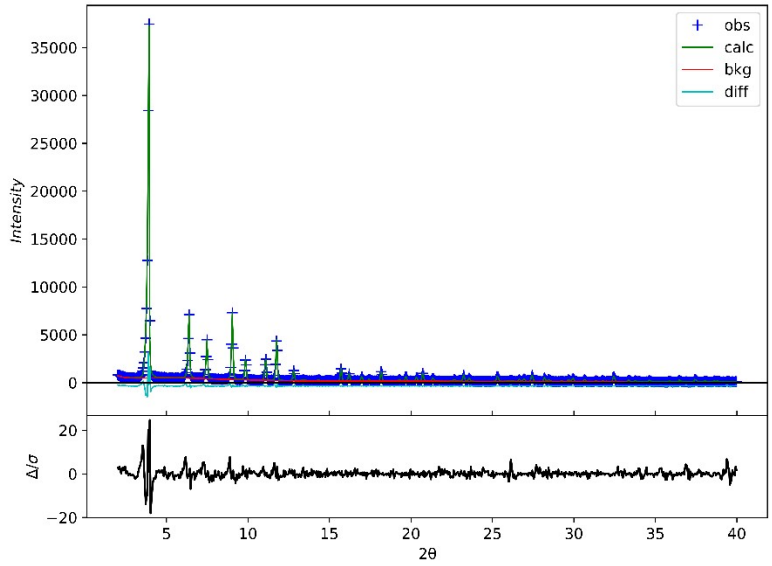

Figure S40. LeBail plot of 10% **PEPEP-F/QPDC-Me**

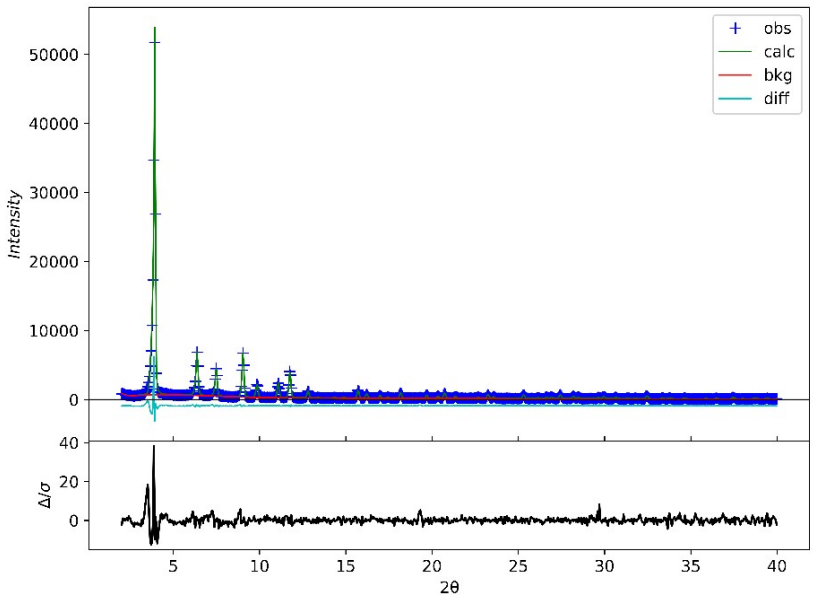

Figure S41. LeBail plot of 20% **PEPEP-F/QPDC-Me**

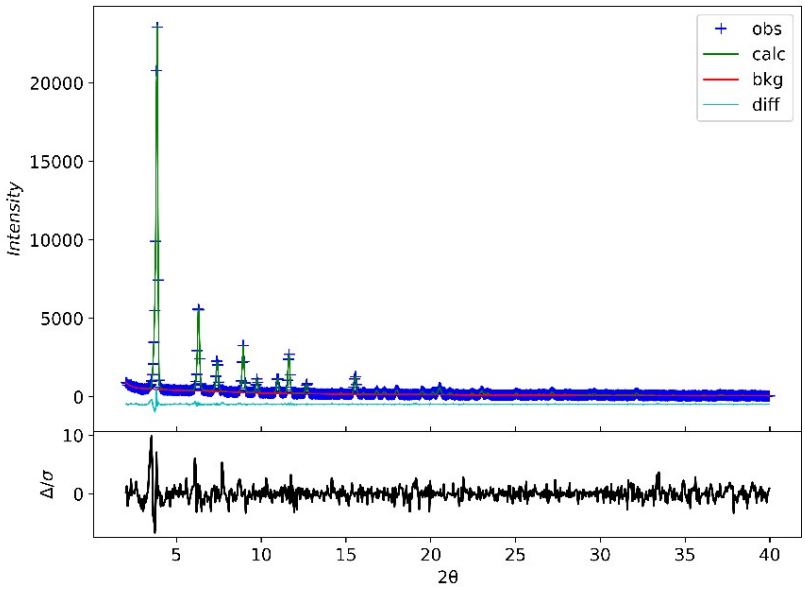

Figure S42. LeBail plot of 40% **PEPEP-F/QPDC-Me**

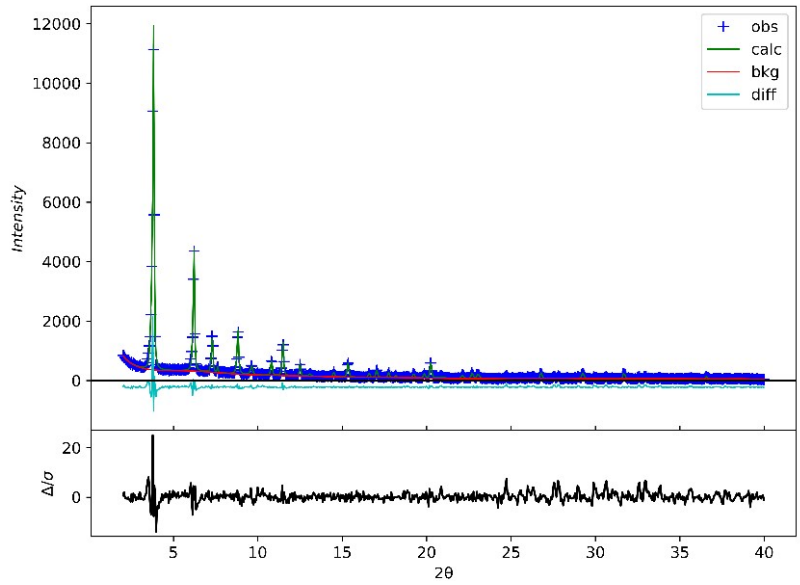

Figure S43. LeBail plot of 60% **PEPEP-F/QPDC-Me**

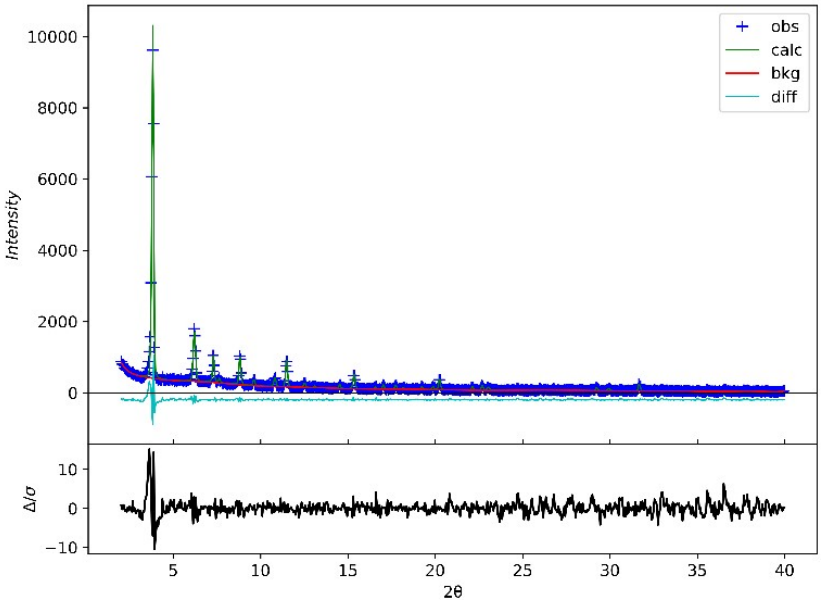

Figure S44. LeBail plot of 80% **PEPEP-F/QPDC-Me**

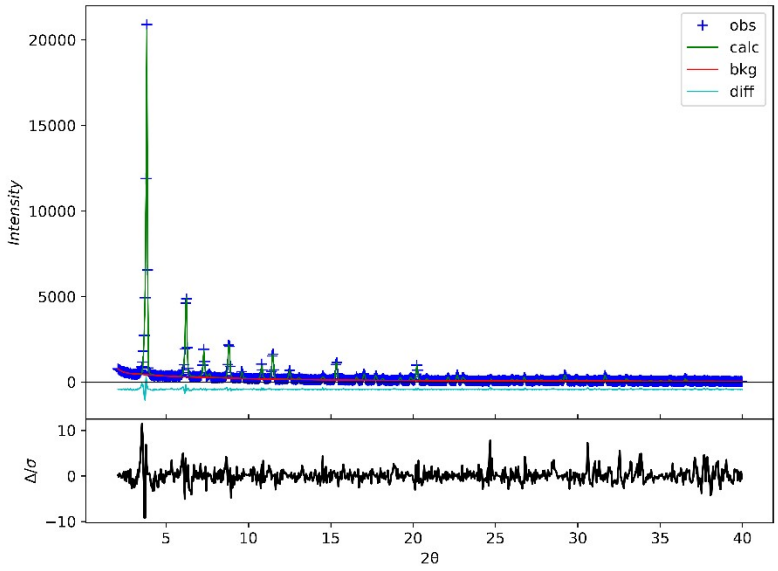

Figure S45. LeBail plot of 100% **PEPEP-F/QPDC-Me**

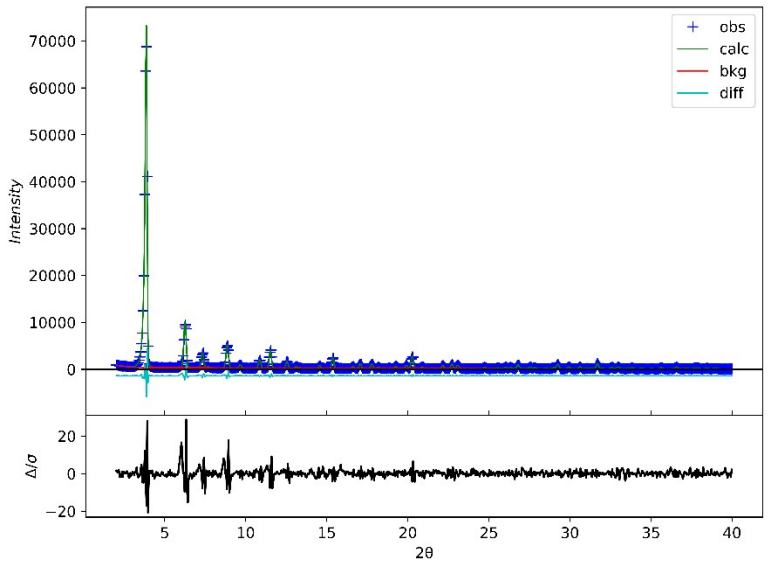

Figure S46. Rietveld refined plot of 100% **PEPEP-F/QPDC-Me**

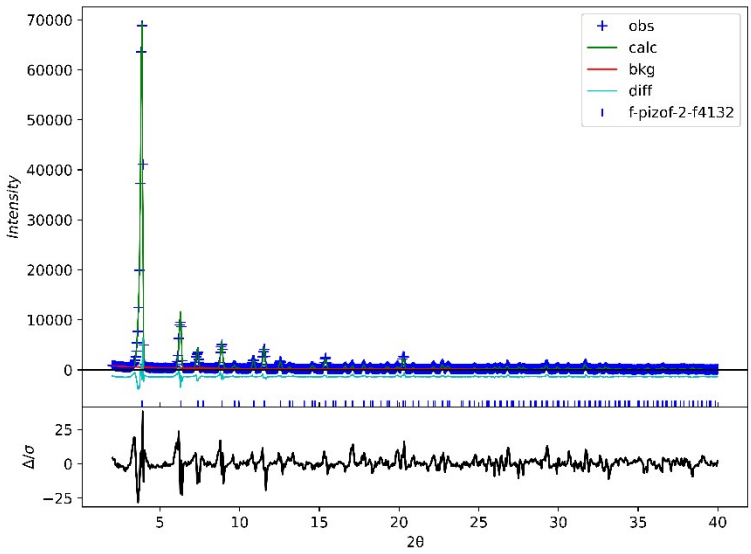

Table S13. Lattice parameter and volumes for **PEPEP-TMS**/**QPDC-Me** System

mol%	sample	a (Å)	V (Å^3)	M20
3	A	38.92051	58957.03	36.7
	B	38.92273	58967.13	36.61
	C	38.93503	59023.04	22.96
	Average	38.926(08)	58982(36)	
5	A	38.93863	59039.43	55.37
	B	38.94325	59060.42	35.35
	C	38.95195	59100.01	61.29
	Average	38.945(07)	59067(31)	
10	A	39.00624	59347.47	22.02
	B	38.98871	59267.51	41.93
	C	38.97792	59218.31	43.87
	Average	38.991(14)	59278(65)	
15	A	38.96276	59149.24	56.81
	B	38.96196	59145.59	45.85
	C	38.97138	59188.51	31.5
	Average	38.965(05)	59161(24)	
20	A	38.93696	59274.41	45.52
	B	38.93907	59041.41	15.61
	C	38.93651	29029.77	32.79
	Average	38.938(01)	59115(138)	
30	A	38.90233	58874.43	22.04
	B	38.99132	59279.41	27.13
	C	39.03460	59478.66	32.30
	Average	38.976(67)	59211(308)	
40	A	38.91427	58928.65	20.04
	B	39.10651	59806.33	20.24
	C	39.14290	59970.20	21.26
	Average	39.055(12)	59568(560)	

Figure S47. Vegard's Plot for **PEPEP-TMS/QPDC-Me** showing linearity ends after 10 mol% input of **PEPEP-TMS**

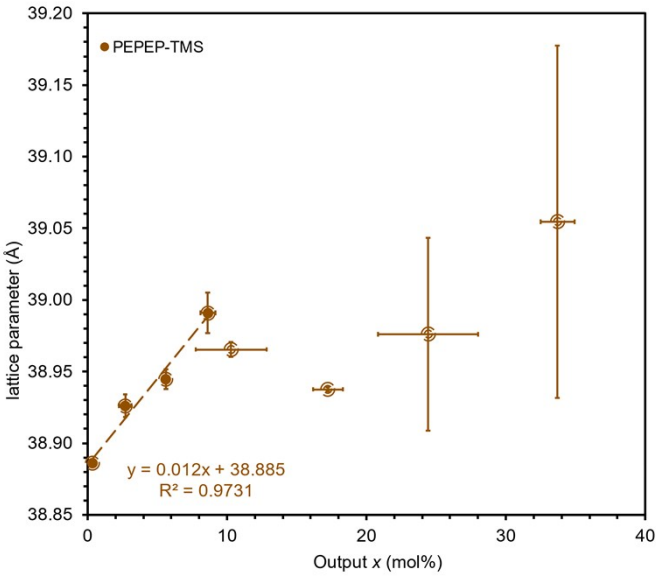

Figure S48. LeBail plot of 3% **PEPEP-TMS/QPDC-Me**

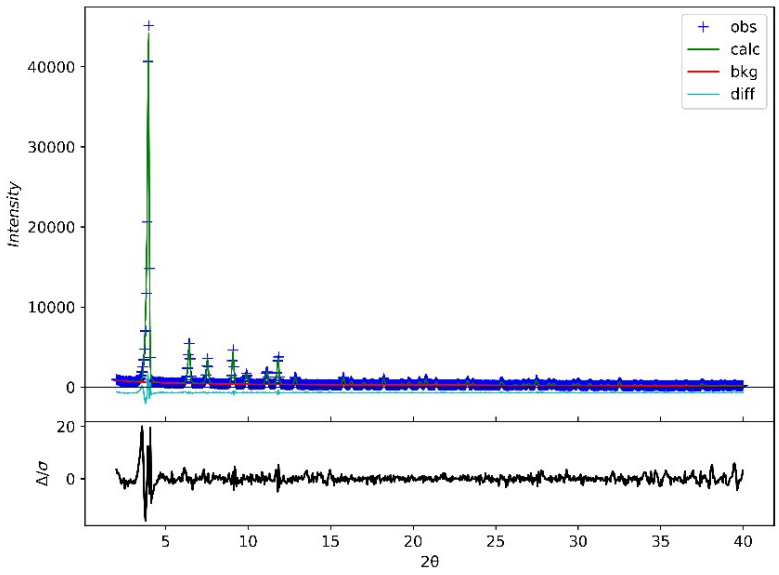

Figure S49. LeBail plot of 5% **PEPEP-TMS/QPDC-Me**

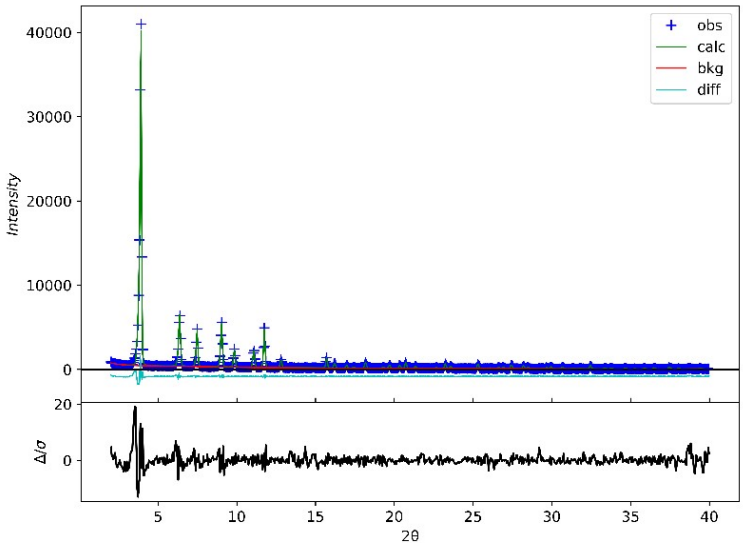

Figure S50. LeBail plot of 10% **PEPEP-TMS/QPDC-Me**

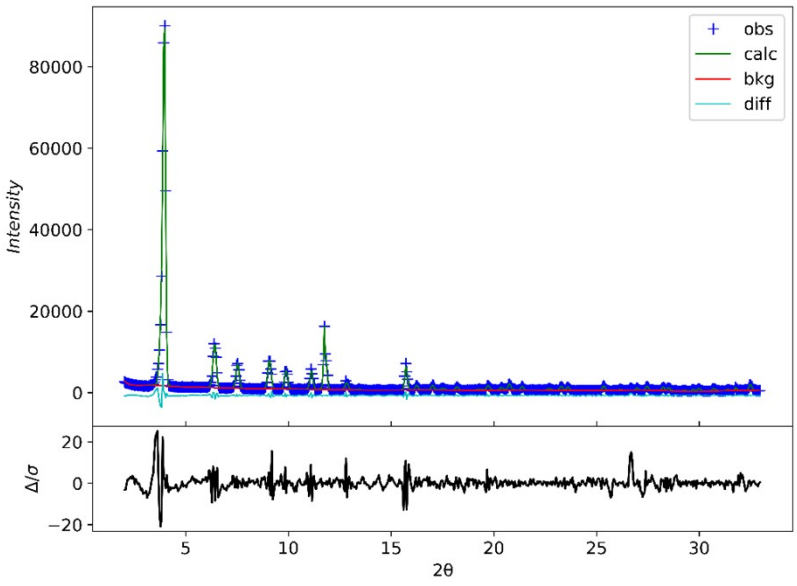

Figure S51. LeBail plot of 20% **PEPEP-TMS/QPDC-Me**

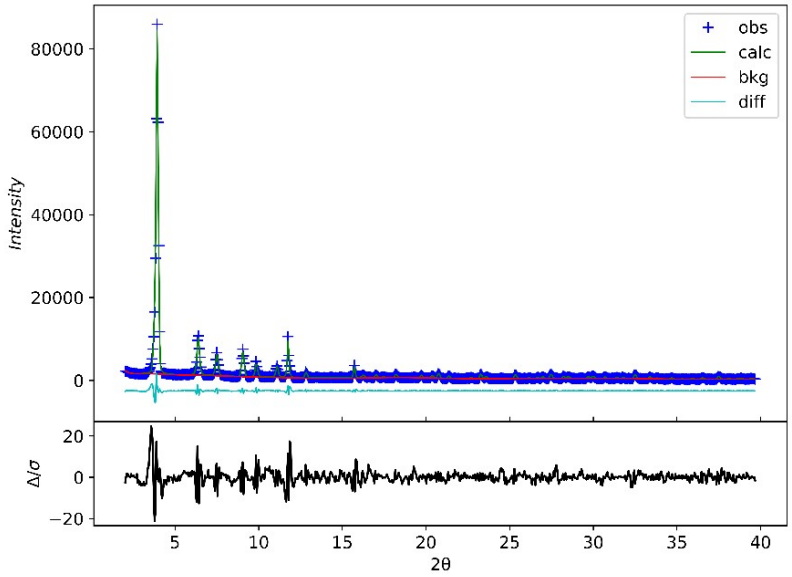

Figure S52. LeBail plot 30% **PEPEP-TMS/QPDC-Me**

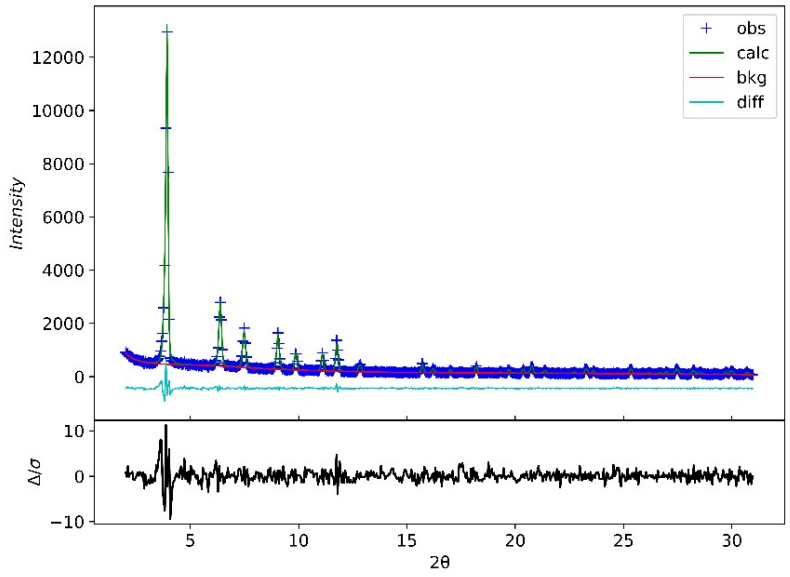

Figure S53. LeBail plot of 40% **PEPEP-TMS/QPDC-Me**

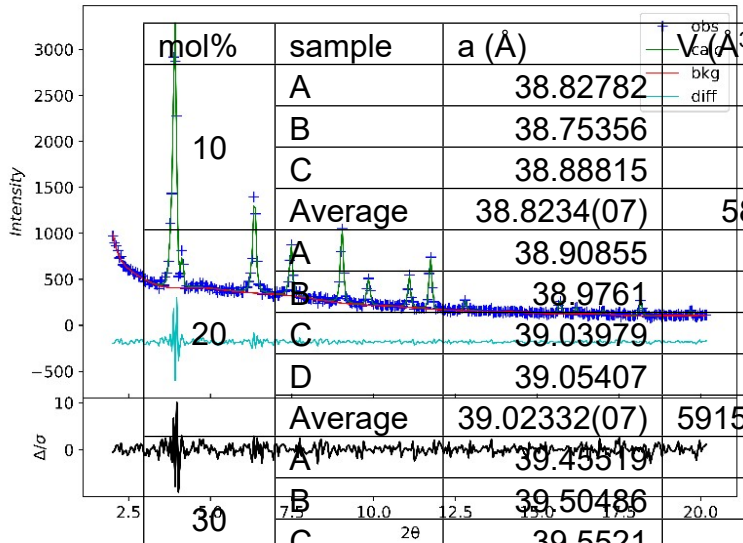

Table S14. Lattice parameter and volumes for **PEPEP-Fc/QPDC-Me** System

mol%	sample	a (Å)	V (Å^3)	M20
10	A	38.82782	58536.82	30.42
	B	38.75356	58201.58	20.6
	C	38.88815	58812.38	40.43
	Average	38.8234(07)	58517(306)	30.48
20	A	38.90855	58902.67	33.45
	B	38.9761	58985.82	18.04
	C	39.03979	59500.75	18.09
	D	39.05407	58985.82	11.43
	Average	39.02332(07)	59157.46(297)	20.25
30	A	39.45519	61874.49	20.02
	B	39.50486	61652.61	26.51
	C	39.5521	61874.11	21.22
	Average	39.50405(05)	61800.4(128)	22.58
40	A	39.65739	62869.51	30.35
	B	39.66107	62386.87	30
	Average	38.659(03)	62628(341)	
60	A	39.86884	63372.51	36.43
	B	39.92173	63625.04	26.63
	Average	38.895(04)	63498(178)	31.53
80	A	39.95047	58874.43	25.29
	B	39.87584	59279.41	21.02
	Average	39.91316(05)	59211(252)	23.16

Figure S54. Vegard's Plot for **PEPEP-Fc/QPDC-Me**

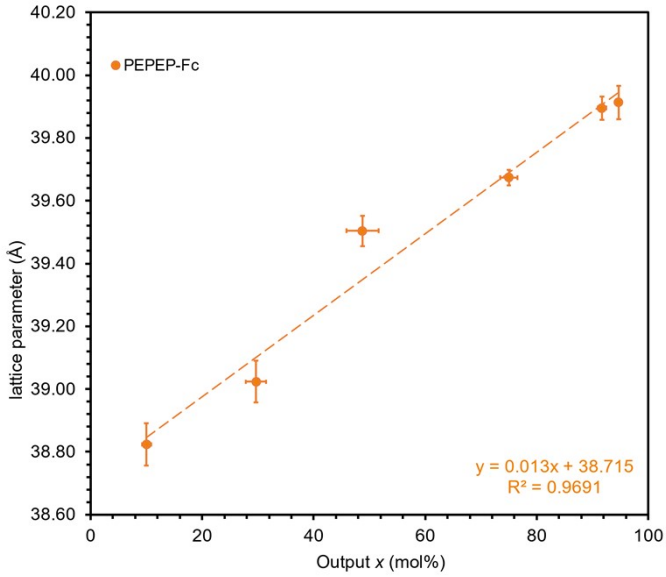

Figure S55. LeBail plot of 10% **PEPEP-Fc/QPDC-Me**

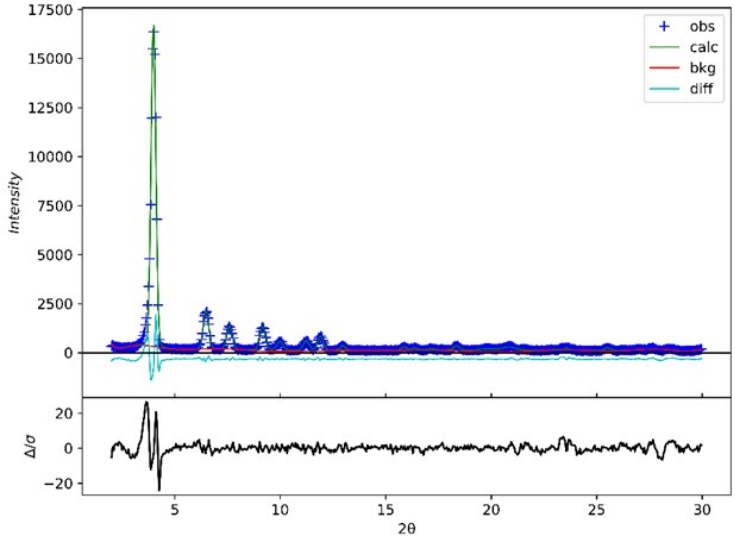

Figure S56. LeBail plot of 20% **PEPEP-Fc/QPDC-Me**

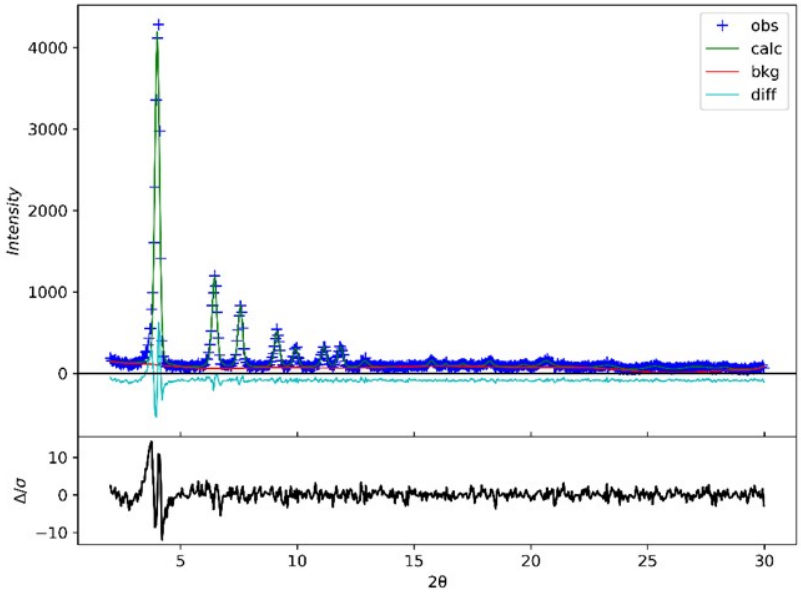

Figure S57. LeBail plot of 30% **PEPEP-Fc/QPDC-Me**

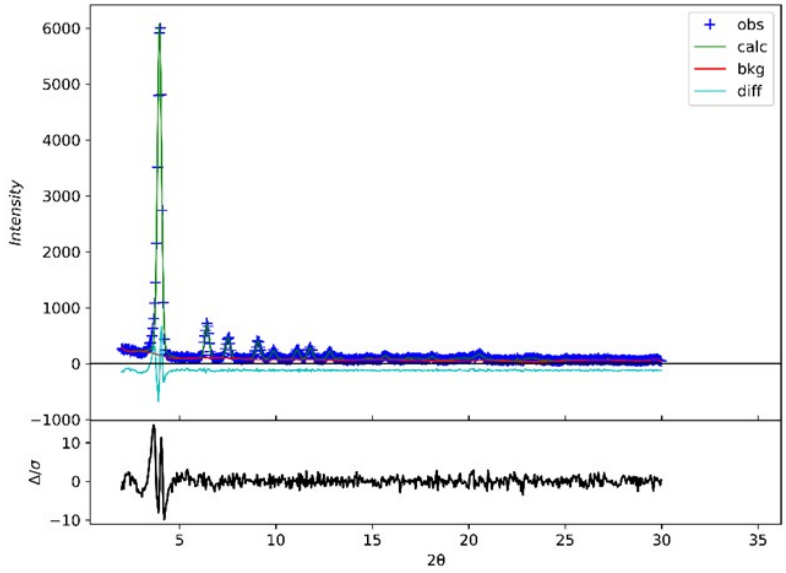

Figure S58. LeBail plot of 40% **PEPEP-Fc/QPDC-Me**

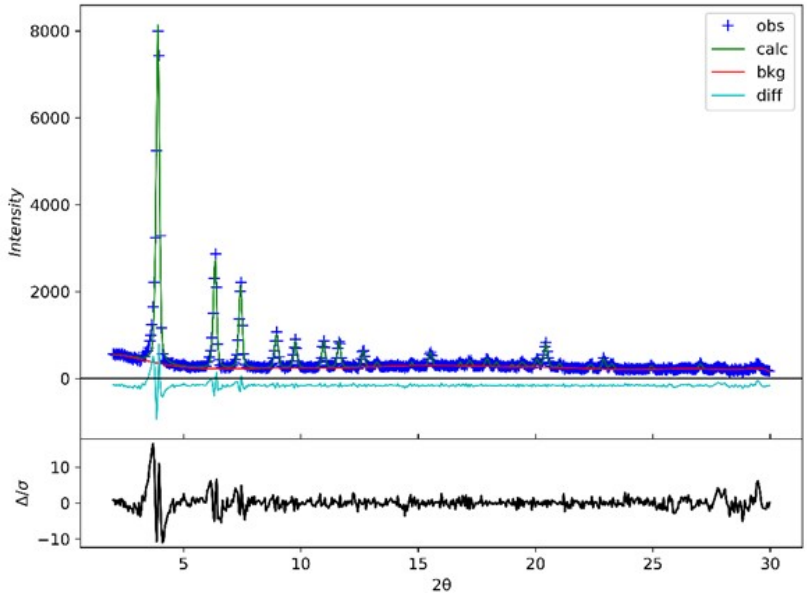

Figure S59. LeBail plot of 60% **PEPEP-Fc/QPDC-Me**

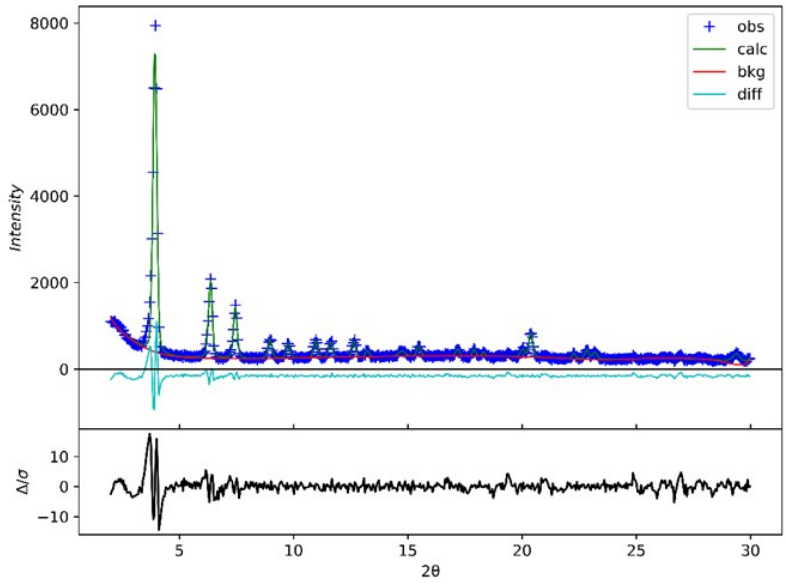

Figure S60. LeBail plot of 80% **PEPEP-Fc/QPDC-Me**

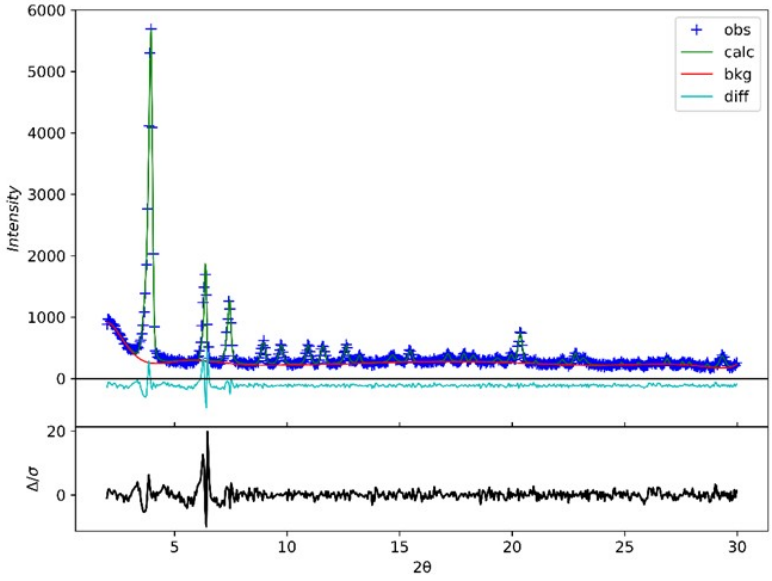

Table S15. Lattice parameter and volumes for **PEPEP-Cl/QPDC-Me** System

mol%	sample	a (Å)	V (Å^3)	M20
20	A	38.93694	59031.722	42.67
	B	38.96964	59180.590	55.52
	C	38.99949	59316.673	11.88
	Average	38.9689(03)	59176(143)	
40	A	39.24812	60458.390	21.51
	C	39.14993	60005.764	18.51
	Average	38.945(07)	60232(320)	
100	A	40.00519	64024.915	42.71

Figure S61. Vegard's Plot for **PEPEP-Cl**

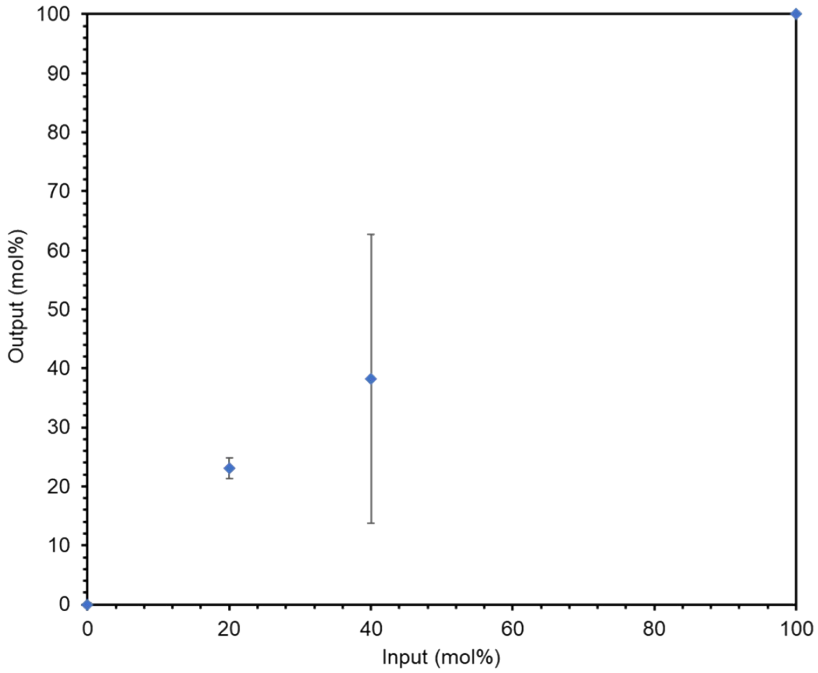

Figure S62. LeBail plot of 20% **PEPEP-Cl/QPDC-Me**

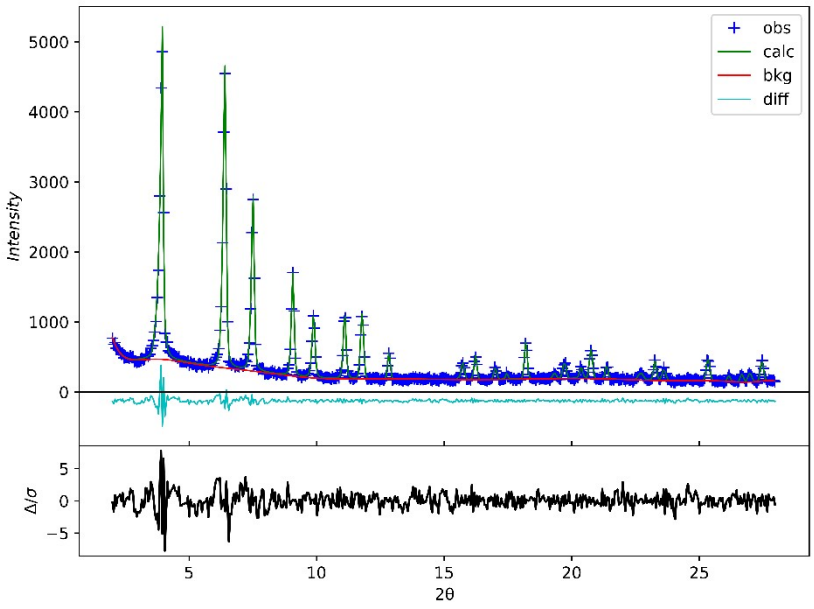

Figure S63. LeBail plot of 20% **PEPEP-CI/QPDC-Me**

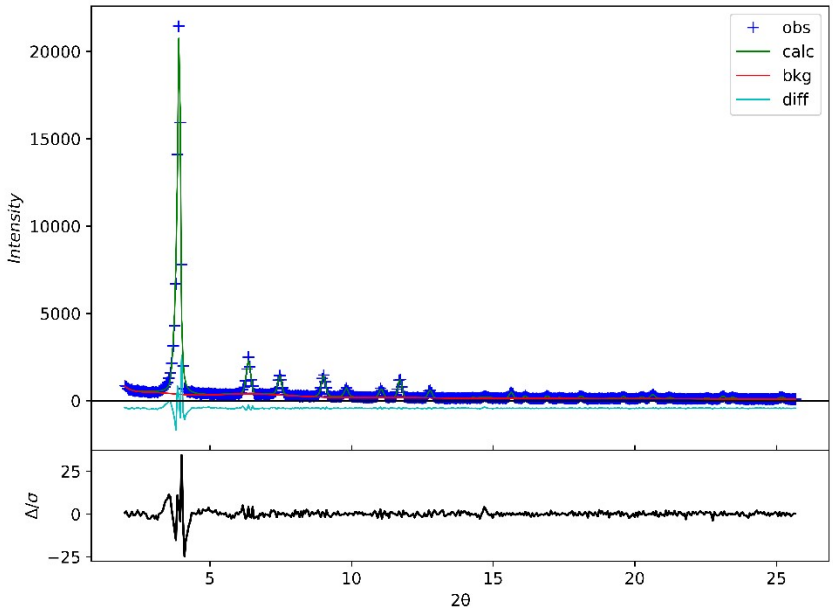

Figure S64. Rietveld plot of 100% **PEPEP-CI**

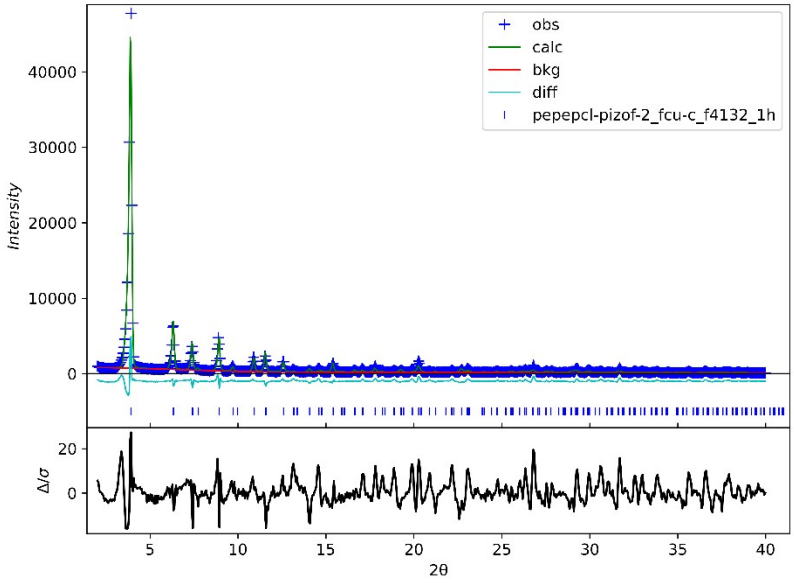

Table S16. Lattice parameter and volumes for **PEPEP-Br**/**QPDC-Me** System

mol%	Sample	a (Å)	V (Å^3)	M20
1	a	38.89964	58862.235	27.01
	b	38.91462	58930.263	20.24
	c	38.90771	58898.876	22.08
	average	38.9073(07)	58897(34)	
3	a	38.91515	58932.68	22.74
	b	38.92761	58989.293	7.04
	c	38.92603	58982.115	8.84
	average	38.9229(067)	58968(31)	
5	a	38.93723	59033.028	78.92
	b	38.93316	59014.53	31.55
	c	38.935	59022.899	23.87
	average	38.9351(02)	59023(09)	
7.5	a	38.96711	59169	21.01
	b	38.94981	59090	25.32
	c	38.94222	59055	21.56
	average	38.9460(5)	59105(58)	
10	a	38.95766	59126.016	27.13
	b	38.91492	58931.626	25.13
	c	38.88731	58806	14.09
	average	38.920(3)	58955(161)	
15	a	38.90113	58869.017	24.67
	b	38.95328	59106.072	49.66
	c	38.99178	59282	48.54
	average	38.9487(455)	59086(207)	

Figure S65. Vegard's Plot for **PEPEP-Br/QPDC-Me** showing linearity ends after 7.5 mol% input of **PEPEP-Br**

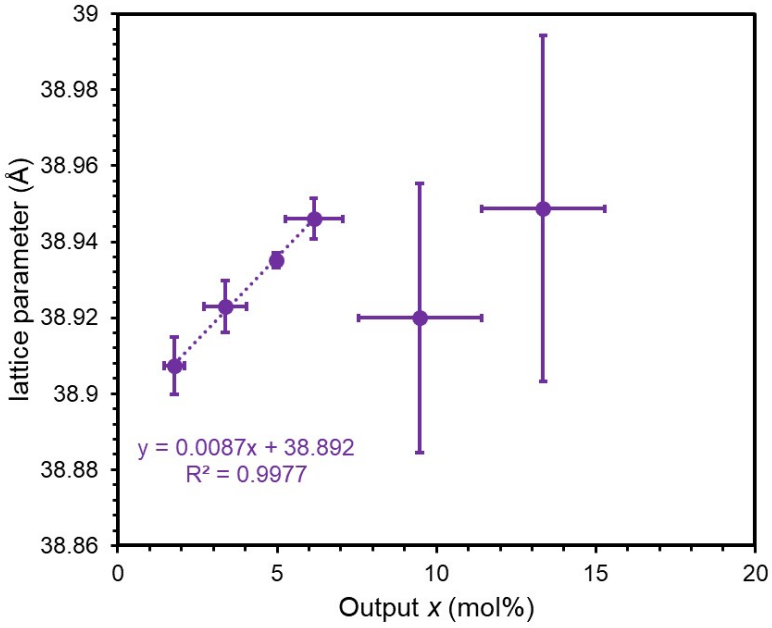

Figure S66. LeBail plot of 1% **PEPEP-Br/QPDC-Me**

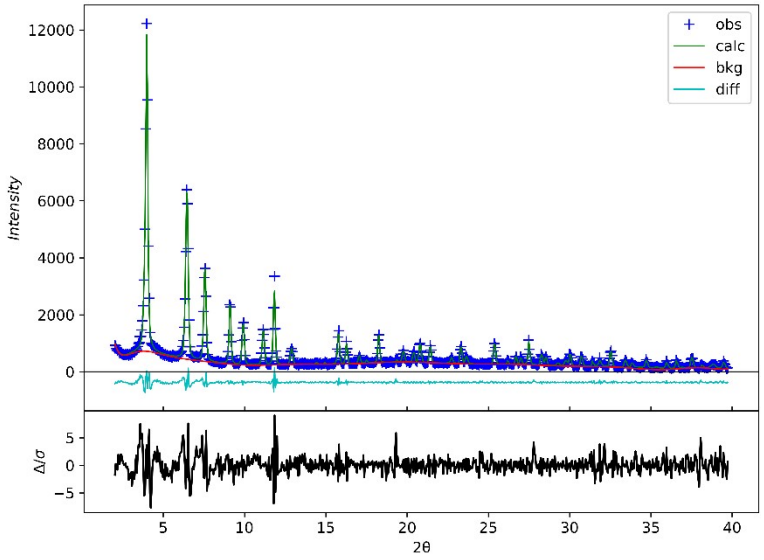

Figure S67. LeBail plot of 3% **PEPEP-Br/QPDC-Me**

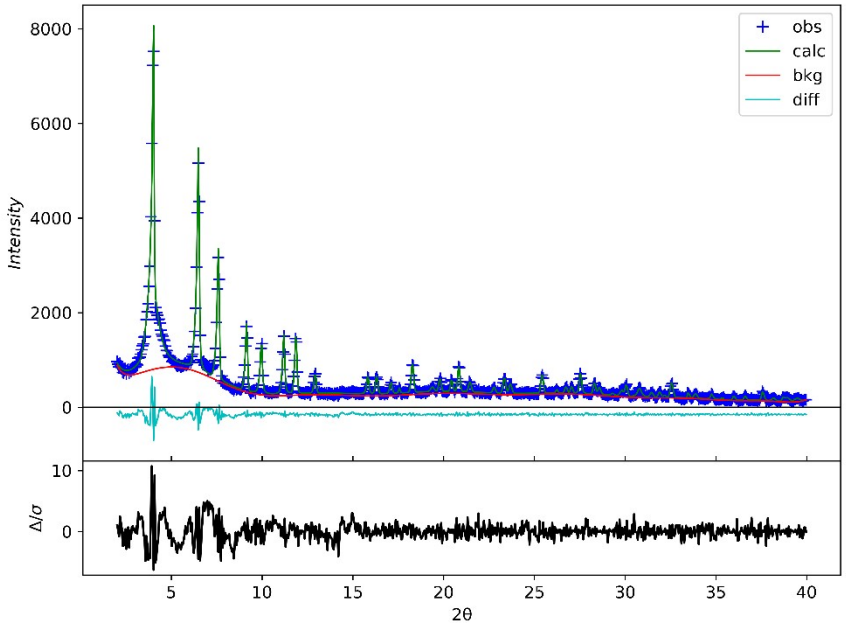

Figure S68. LeBail plot of 5% **PEPEP-Br/QPDC-Me**

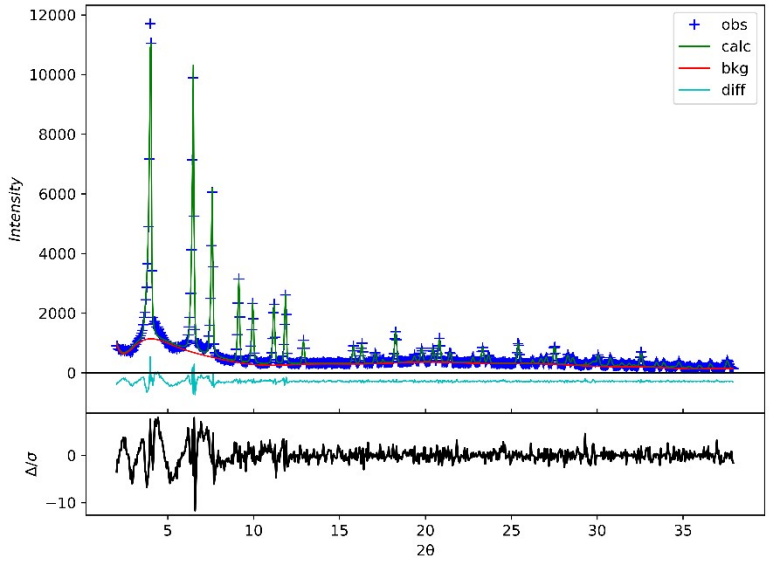

Figure S69. LeBail plot of 7.5% **PEPEP-Br/QPDC-Me**

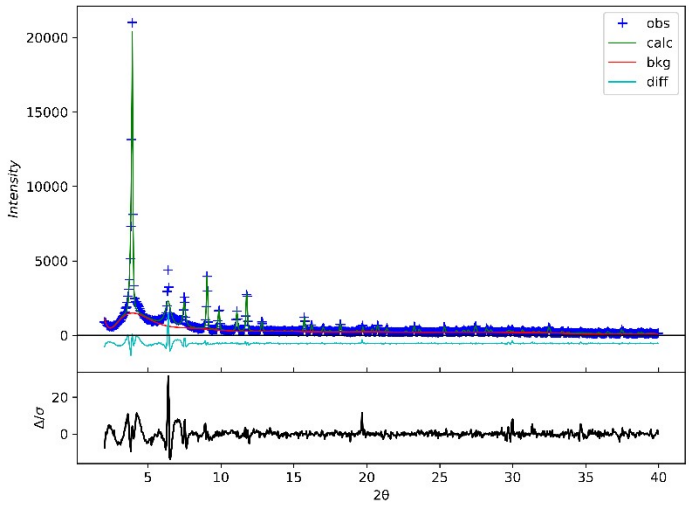

Figure S70. LeBail plot of 10% **PEPEP-Br/QPDC-Me**

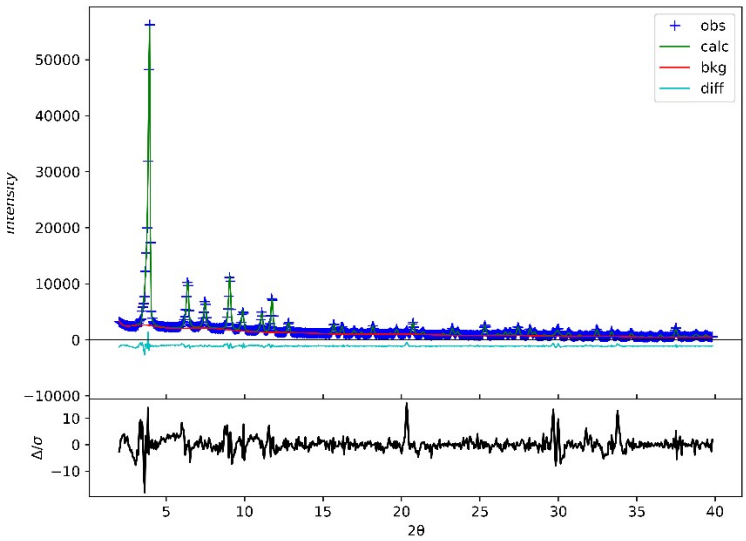

Figure S71. LeBail plot of 15% **PEPEP-Br/QPDC-Me**

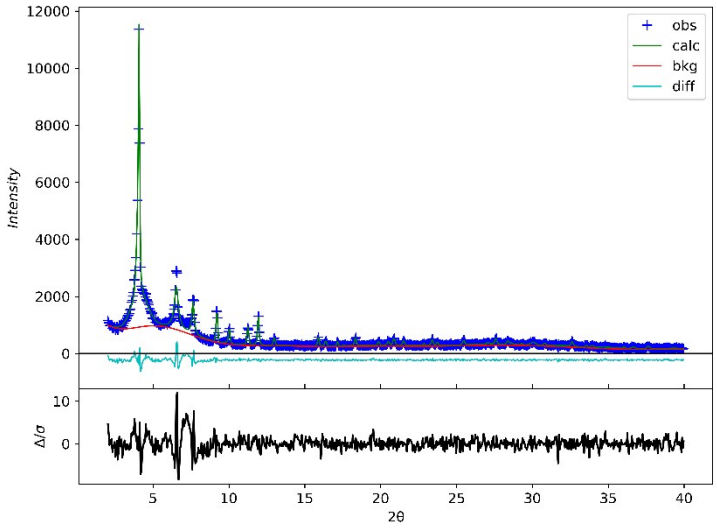

Table S17. Rietveld Refinement Results

Name	**PIZOF-PEPEP-F**	**PIZOF-PEPEP-Cl**
Formula	$C_{36}H_{15}F_3O_{18.405}Zr_{1.5}$	$C_{36}H_{15}Cl_3O_{16.696}Zr_{1.5}$
Chemical Formula (g mol^{-1})	935.79	957.82
Crystal System	Cubic	Cubic
Space group	$F4_132$	$F4_132$
a (Å)	39.999(5)	41.779(28)
V (Å$^{3)}$	63995(8)	72930(14)
Z	32	32
Wavelength (Å)	1.54051	1.54051
Temperature (K)	293.15	293.15
R_F	0.08237	0.10977
R_w	0.17600	0.17202
R_B	0.12219	0.12198
GOF	5.08	4.76

Section S6. **Scanning electron microscopy and energy dispersive X-ray analysis.**

Figure S72. Scanning electron microscopy images of 50% **QPDC-Me** 50% **PEPEP-Me** SSS MOF.

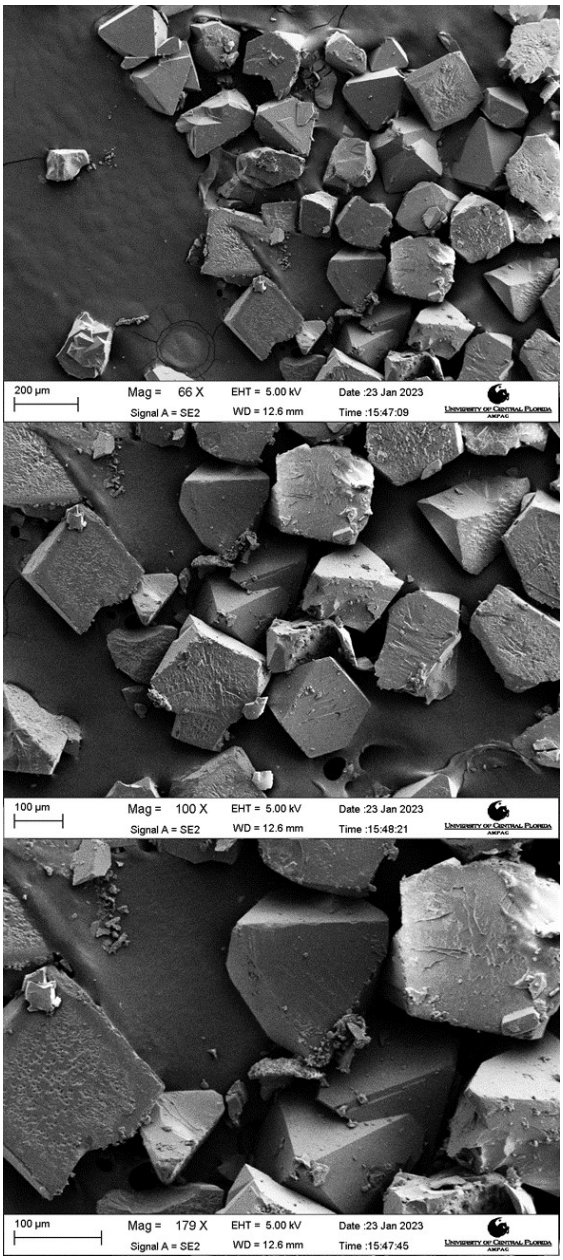

Figure S73. Scanning electron microscopy images of 40% **QPDC-Me** 60% **PEPEP-Me** SSS MOF.

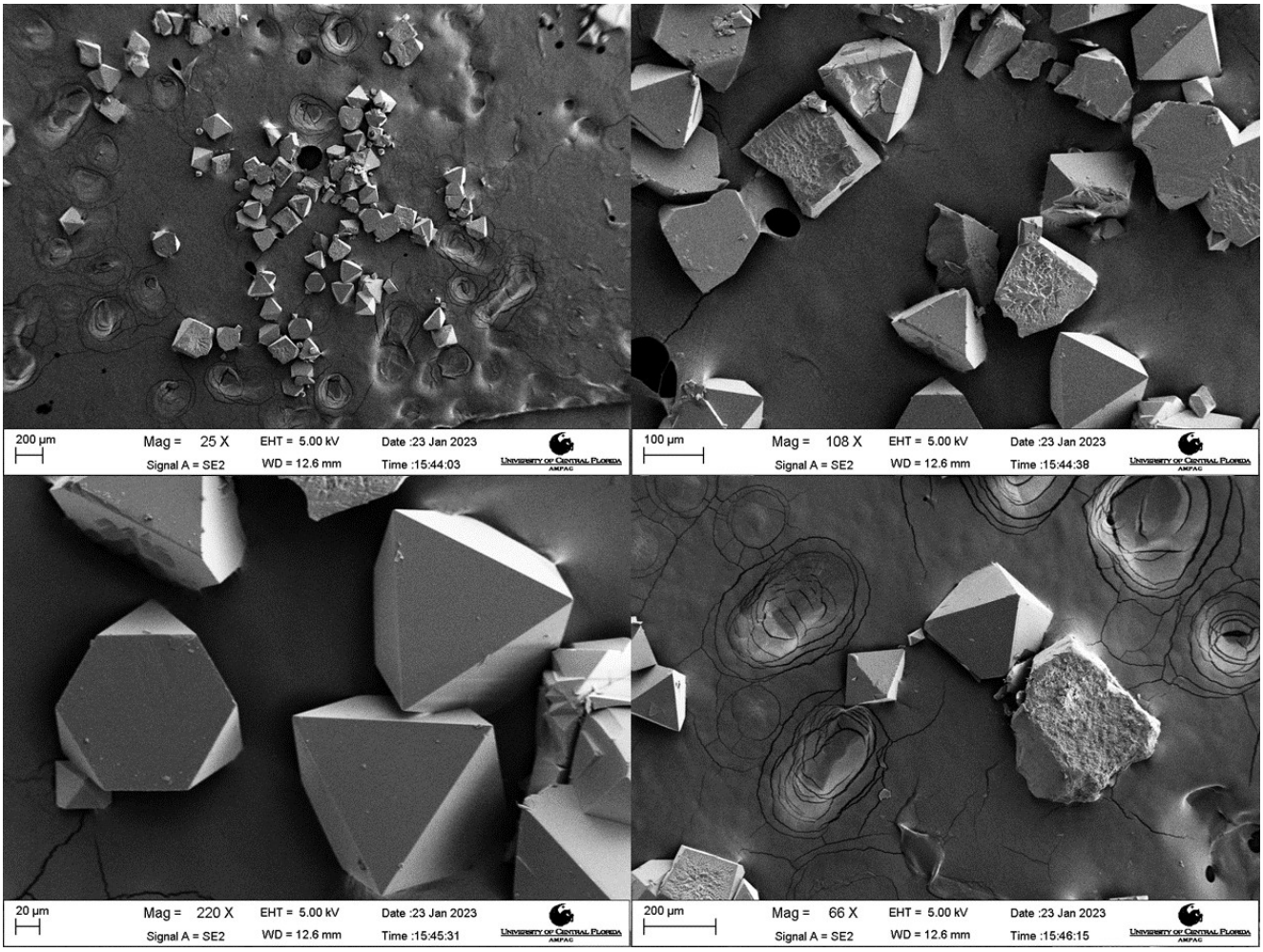

Figure S74. Scanning electron microscopy images of 20% **QPDC-Me** 80% **PEPEP-Me** SSS MOF.

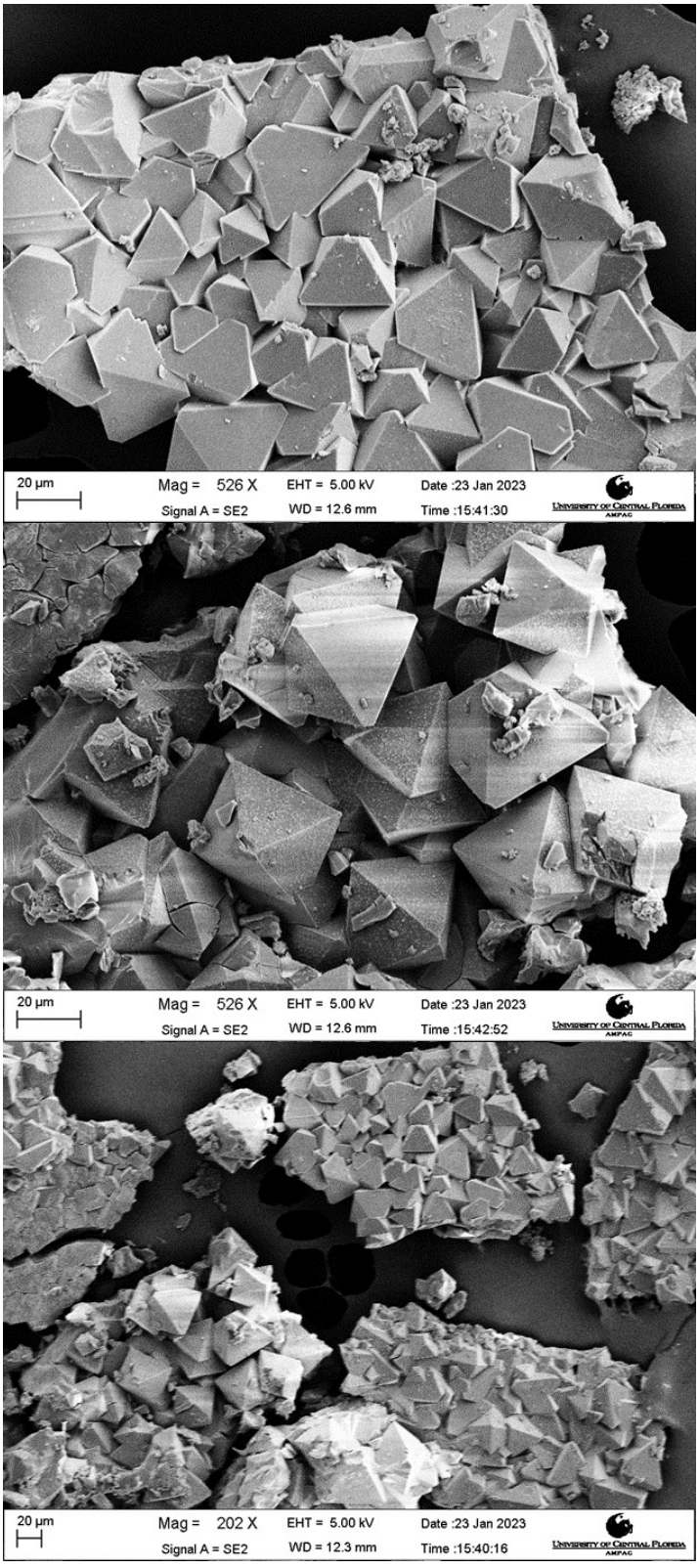

Figure S75. Scanning electron microscopy images of 60% **QPDC-Me** 40% **PEPEP-Me** SSS MOF.

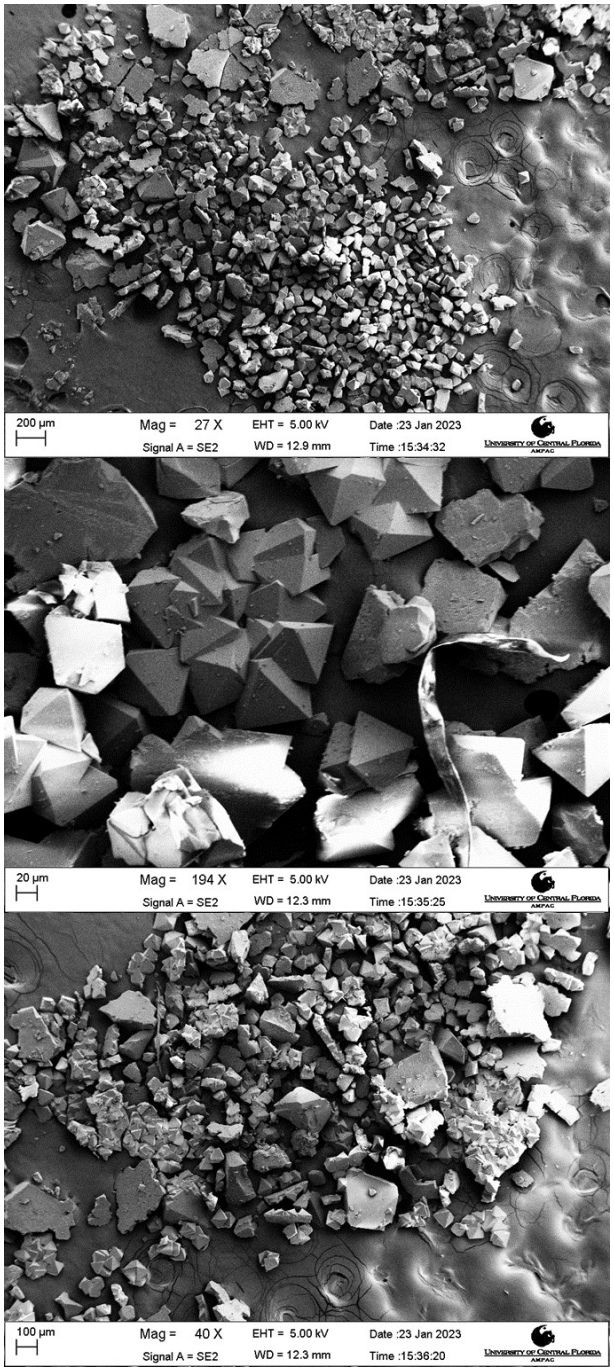

Figure S76. Scanning electron microscopy images of 80% **QPDC-Me** 20% **PEPEP-Me** SSS MOF.

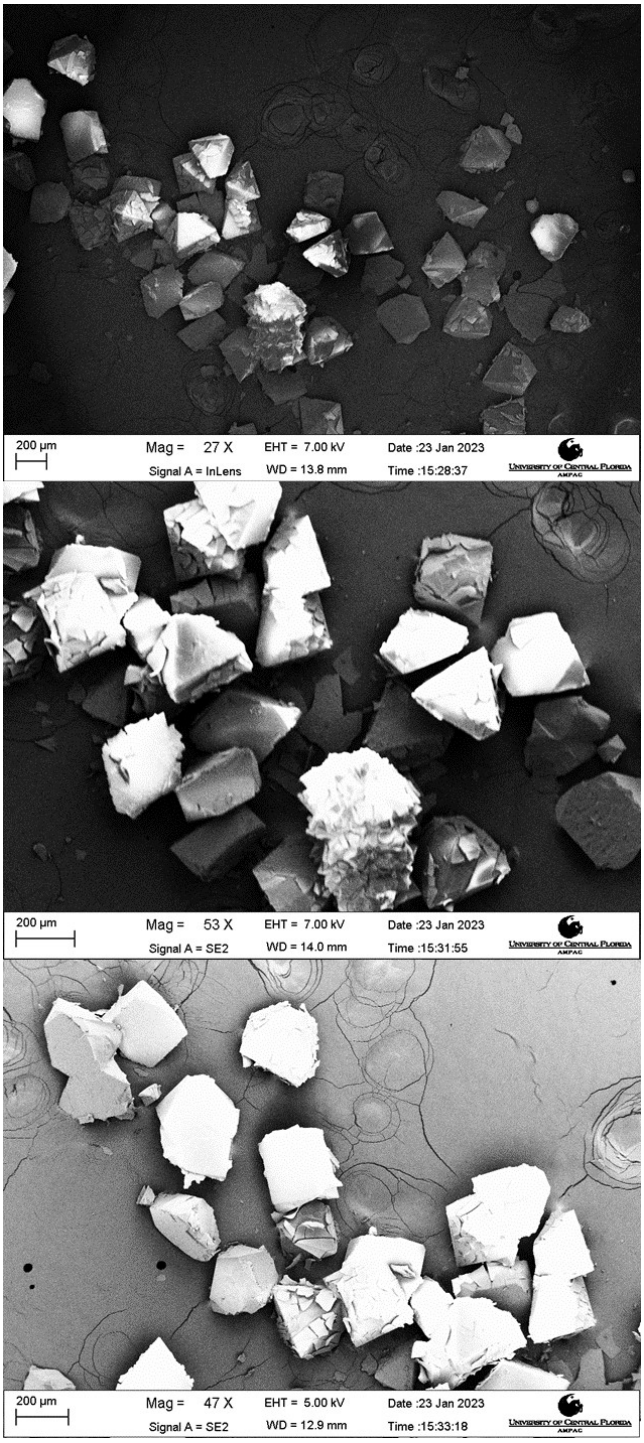

Figure S77. Scanning electron microscopy images of 80% **QPDC-Me** and 20% **PEPEP-F** SSS MOF

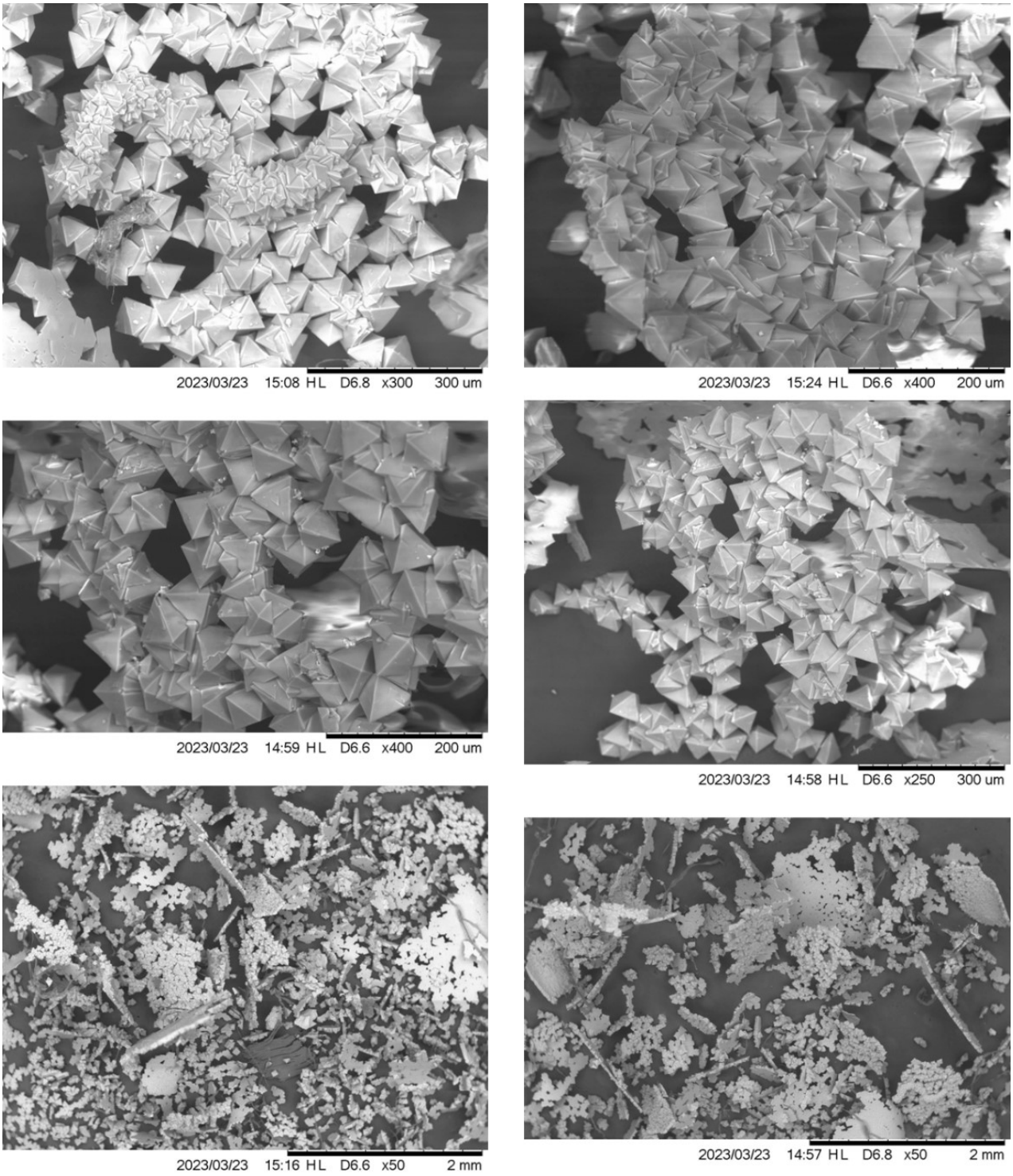

Figure S78. Scanning electron microscopy images of 60% **QPDC-Me** and 40% **PEPEP-F** SSS MOF

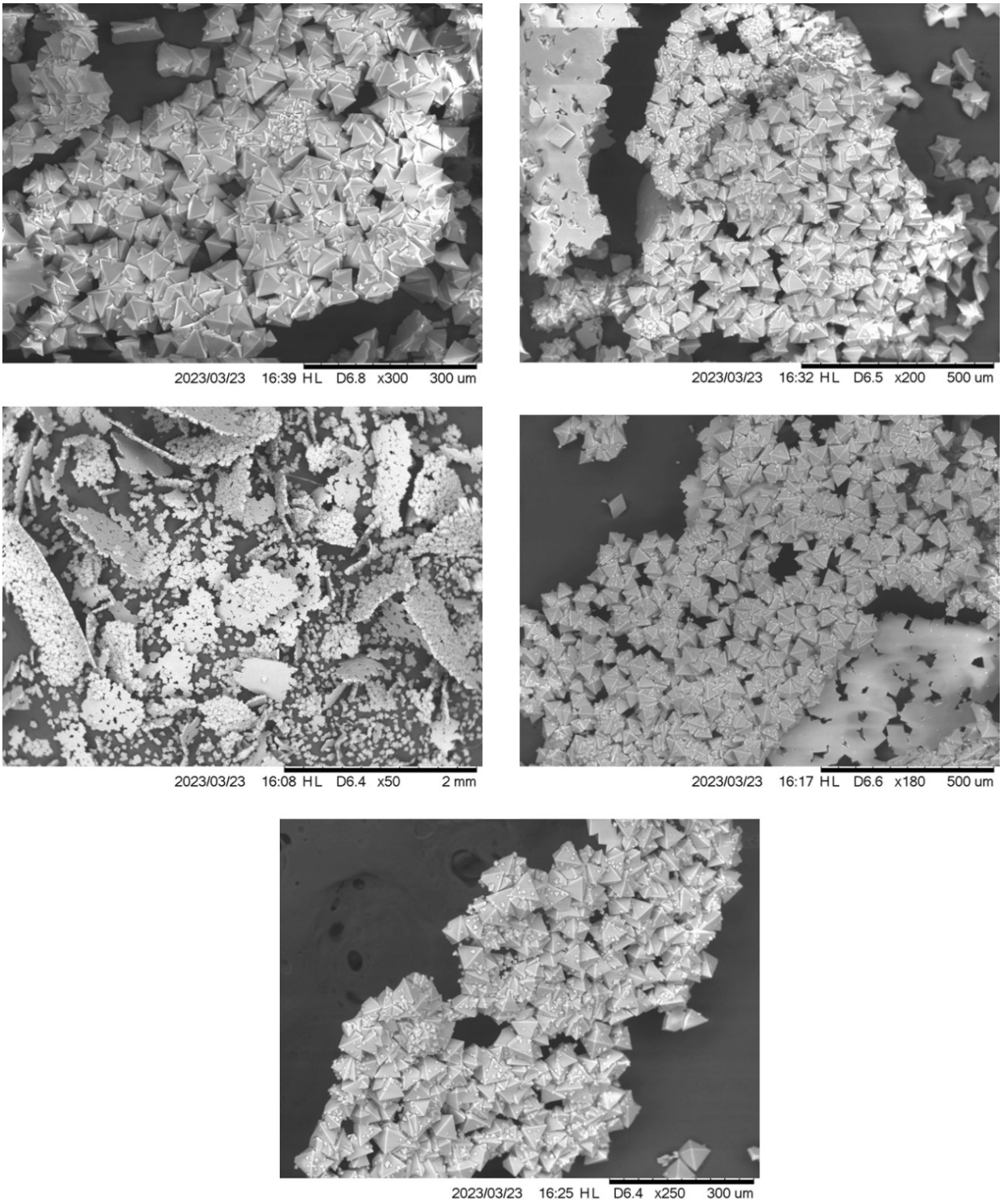

Figure S79. Scanning electron microscopy images of 40% **QPDC-Me** and 60% **PEPEP-F** SSS MOF

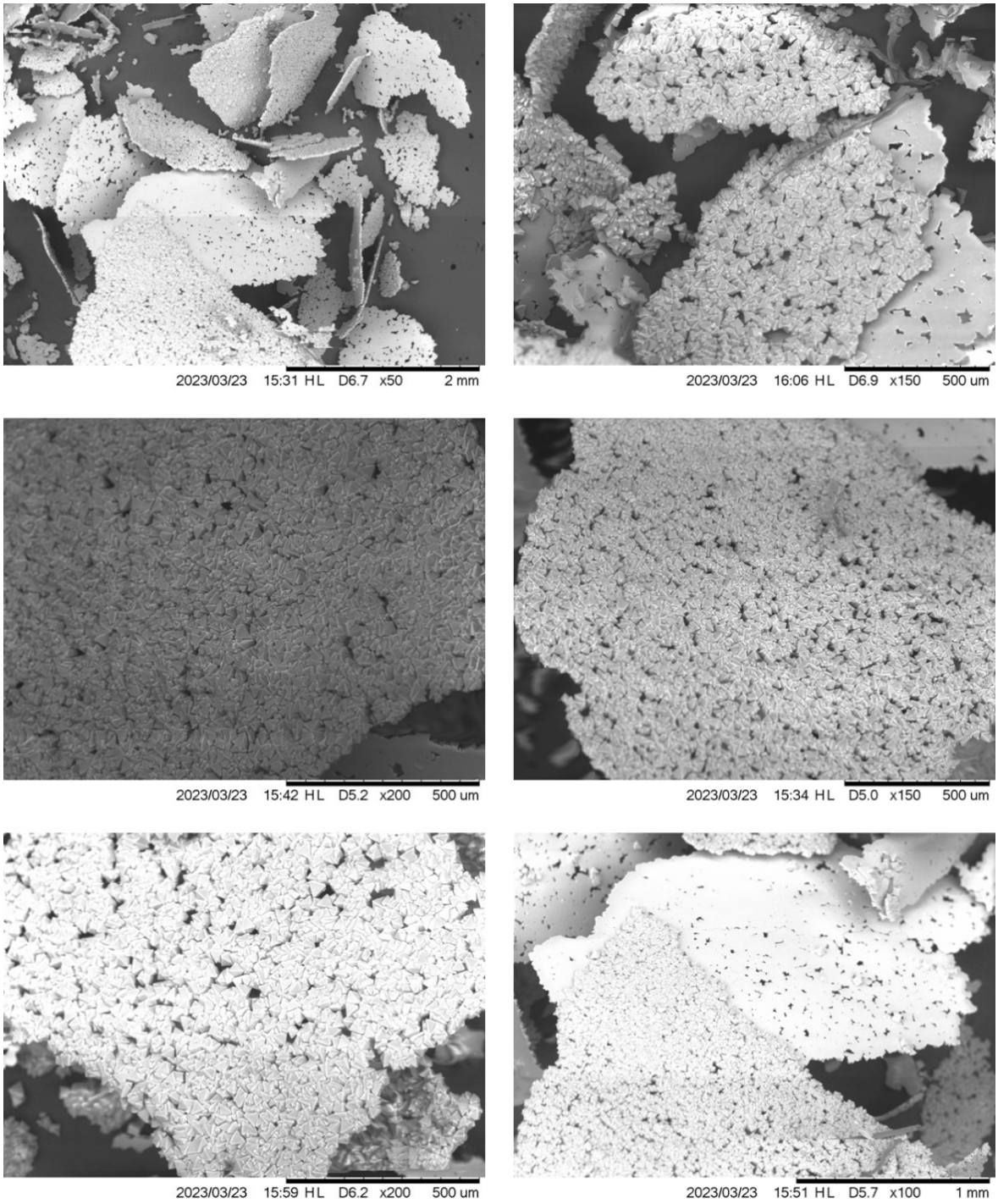

Figure S80. Scanning electron microscopy images of 20% **QPDC-Me** and 80% **PEPEP-F** SSS MOF

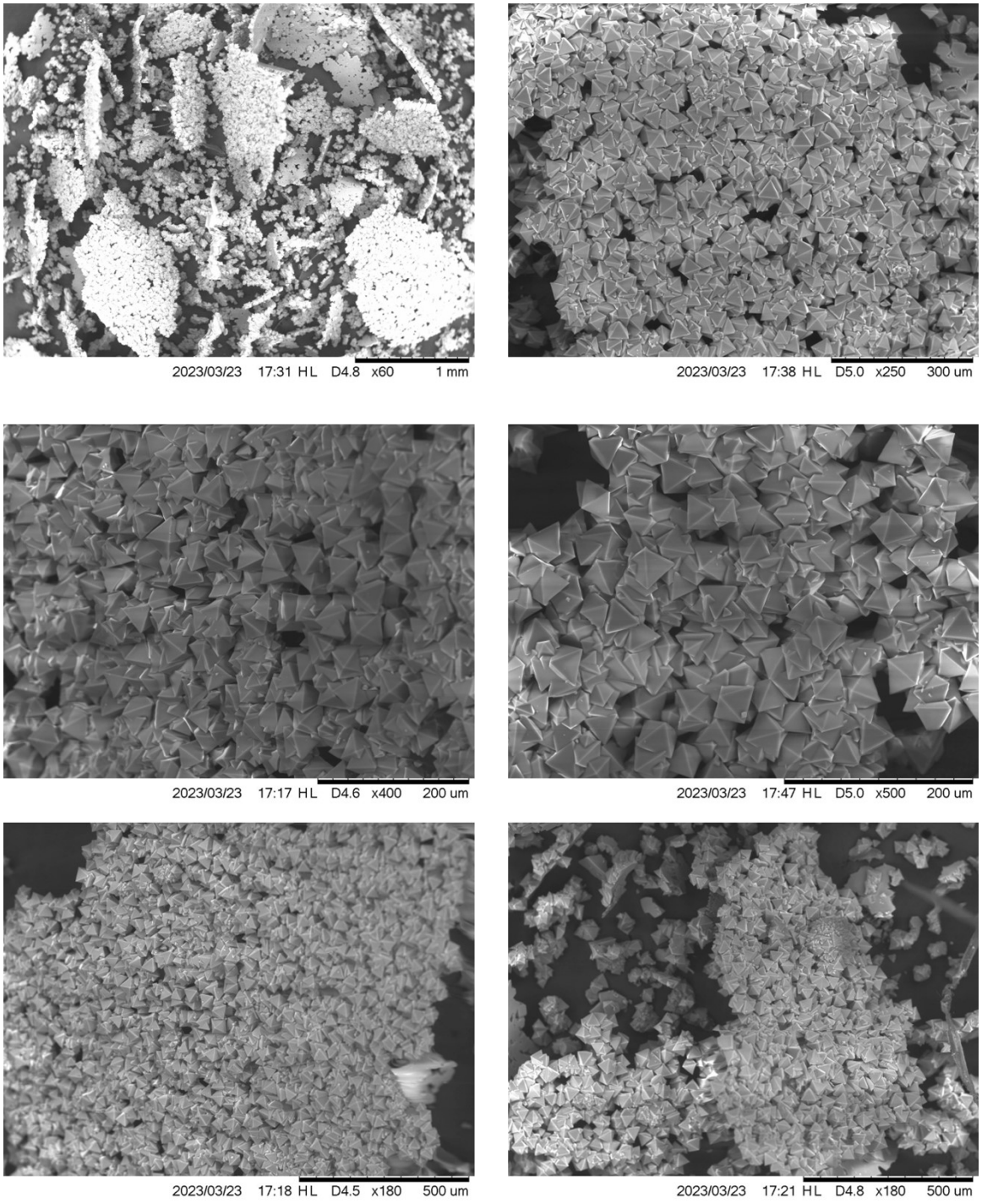

Figure S81. Scanning electron microscopy images of 100% **PEPEP-F** MOF

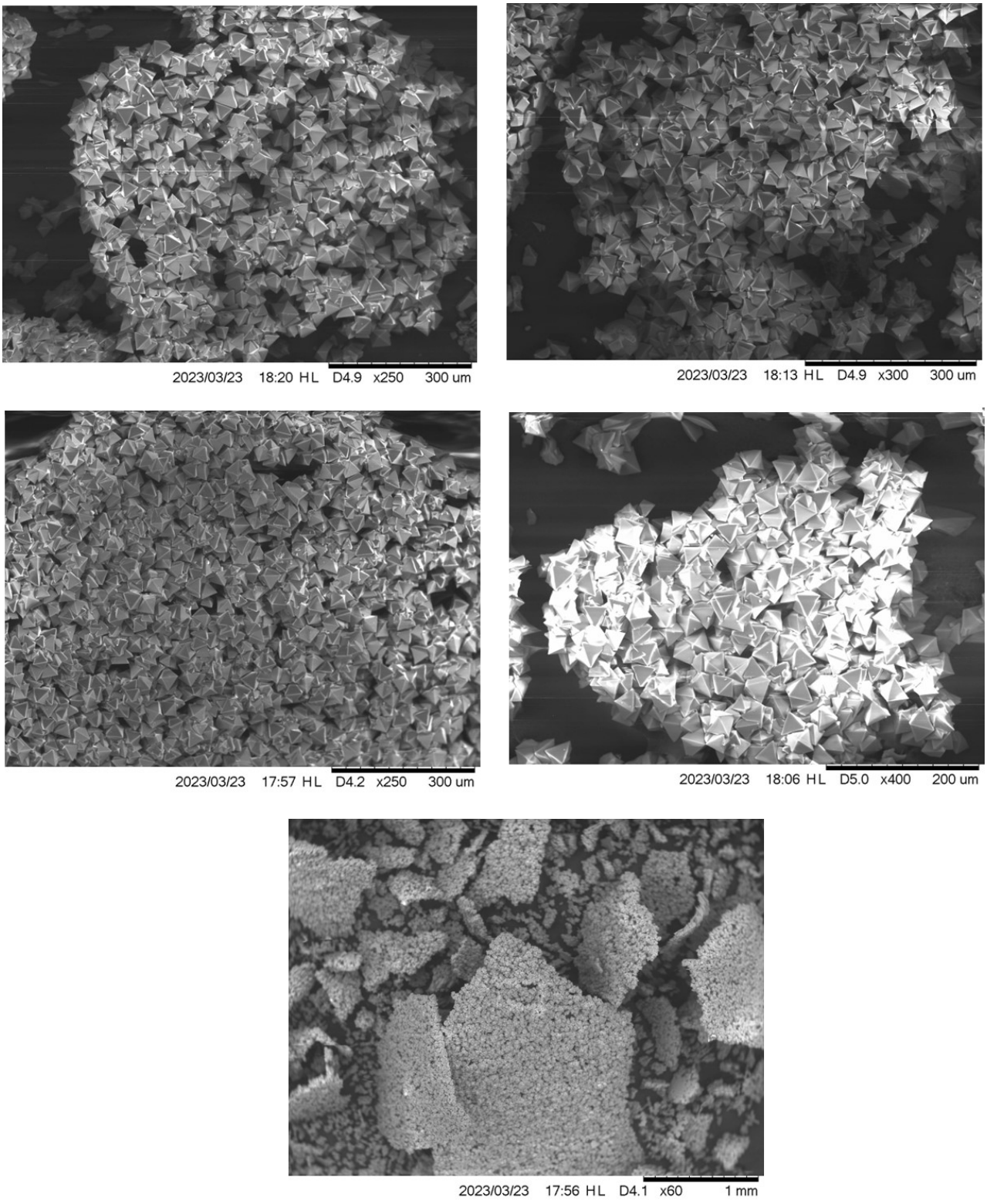

Figure S82. Scanning electron microscopy images of 90% **QPDC-Me** and 10% **PEPEP-TMS** SSS MOF

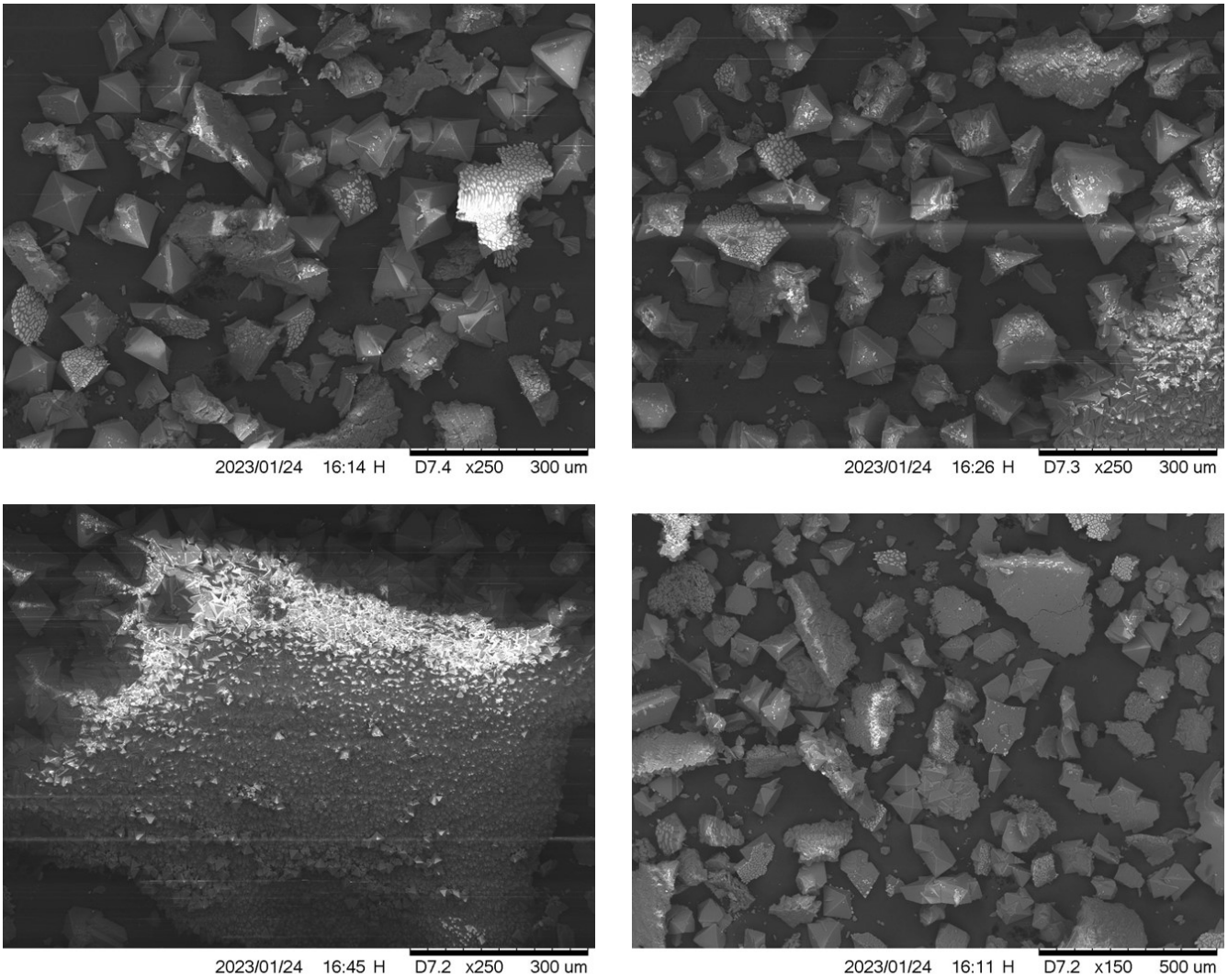

Figure S83. Scanning electron microscopy images of 80% **QPDC-Me** and 20% **PEPEP-TMS** SSS MOF

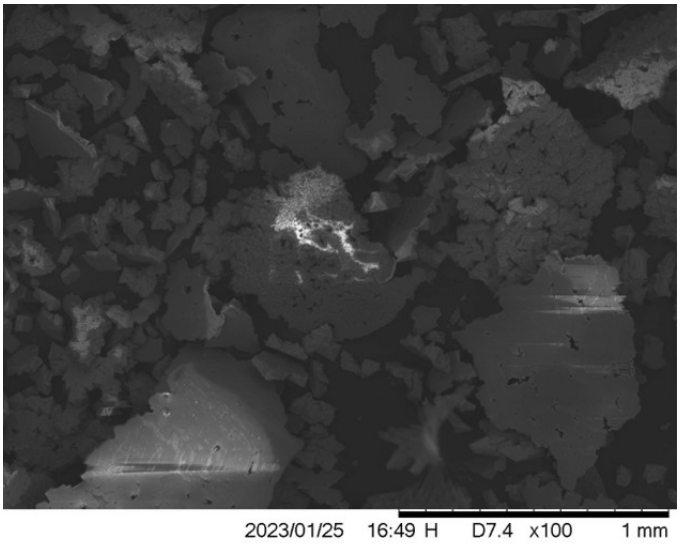

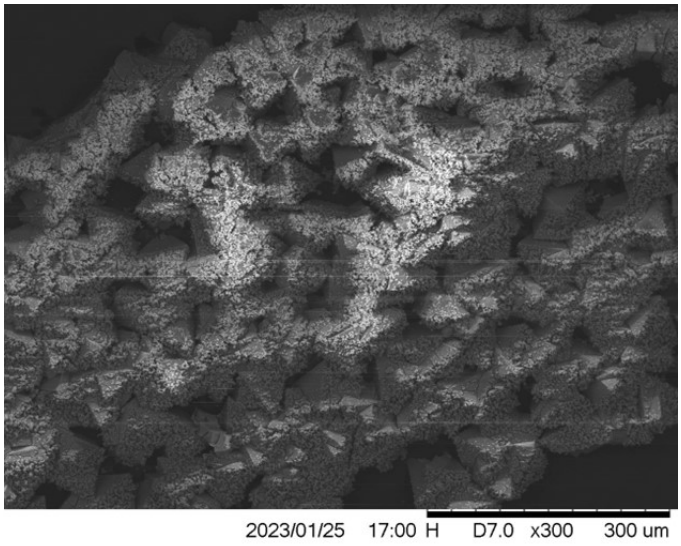

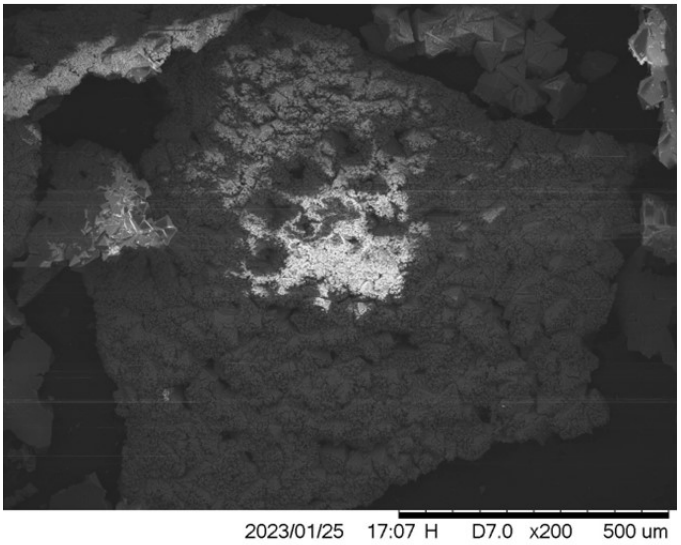

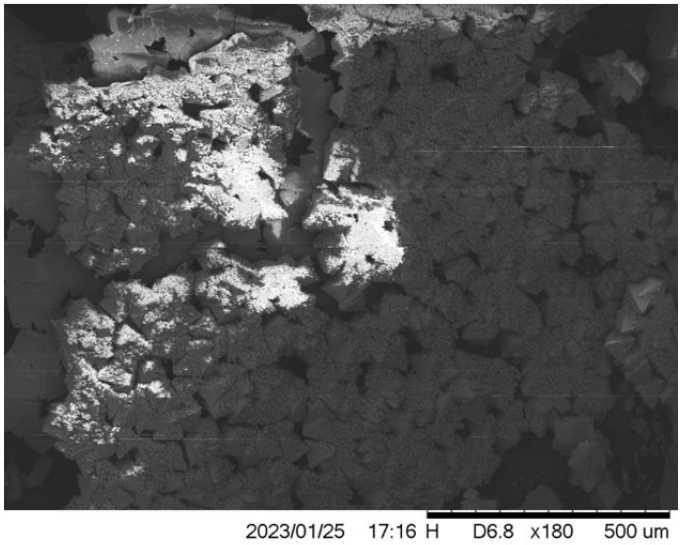

Figure S84. Scanning electron microscopy images of 70% **QPDC-Me** and 30% **PEPEP-TMS** SSS MOF

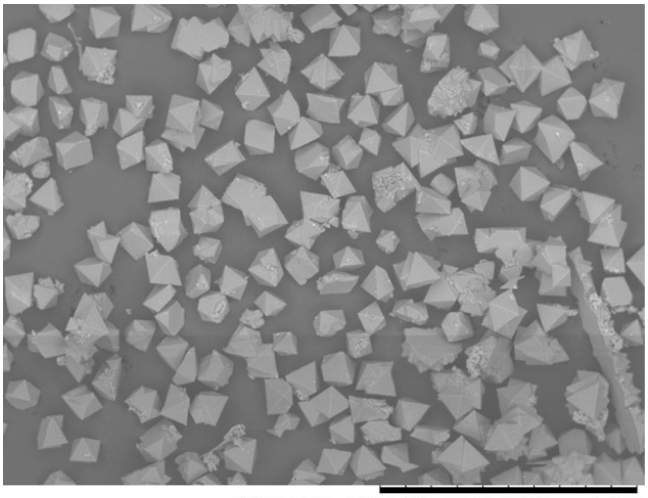

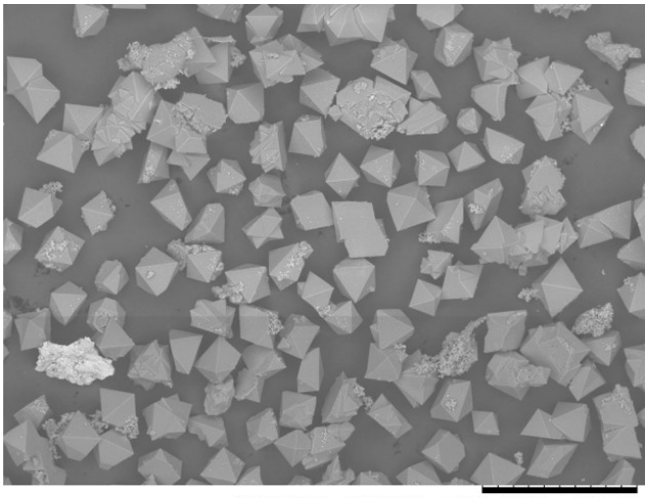

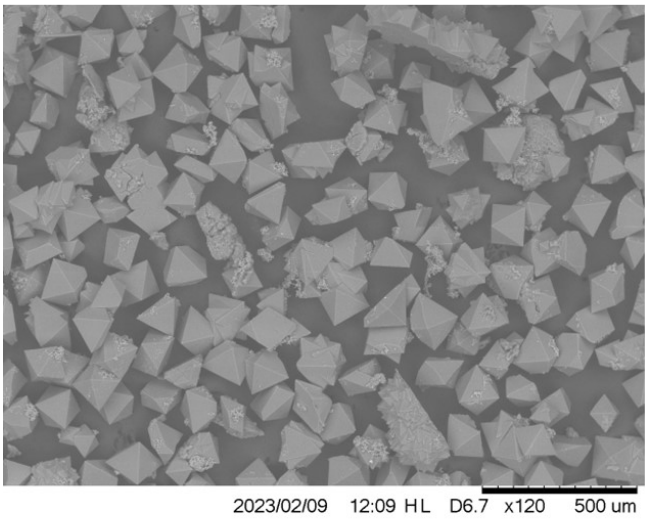

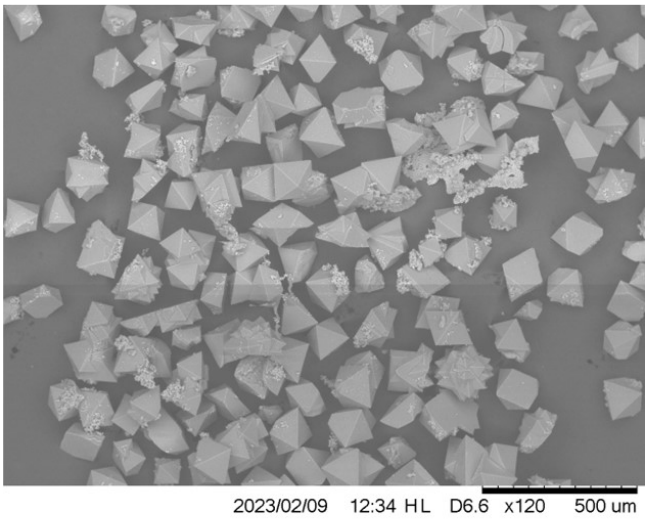

Figure S85. Scanning electron microscopy images of 60% **QPDC-Me** and 40% **PEPEP-TMS** SSS MOF

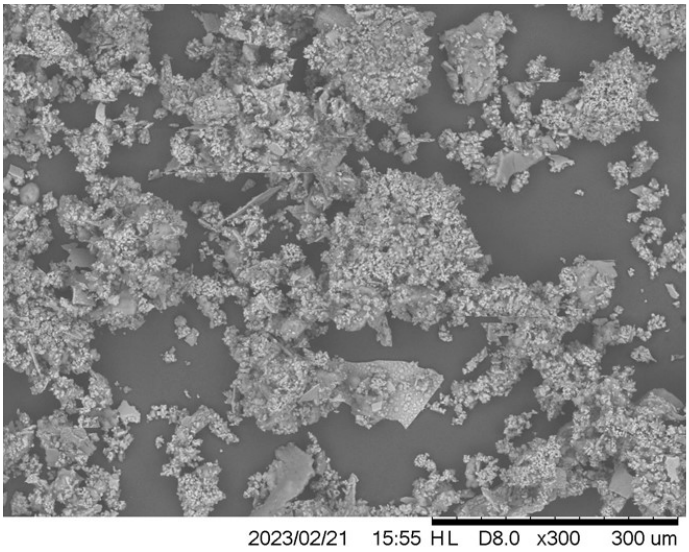

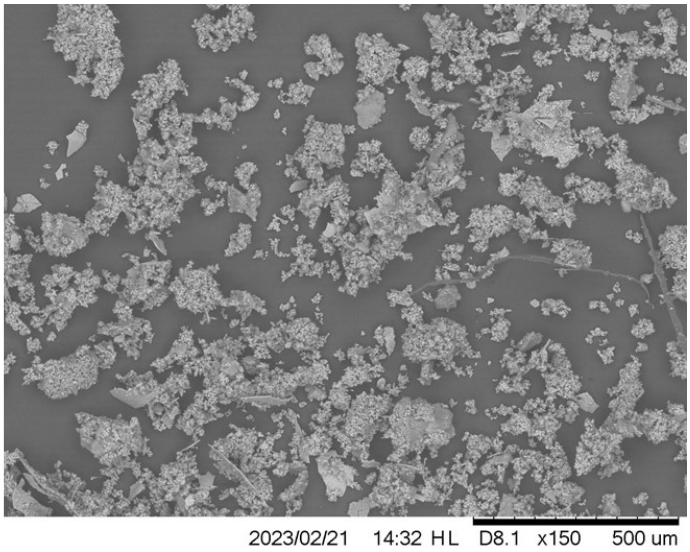

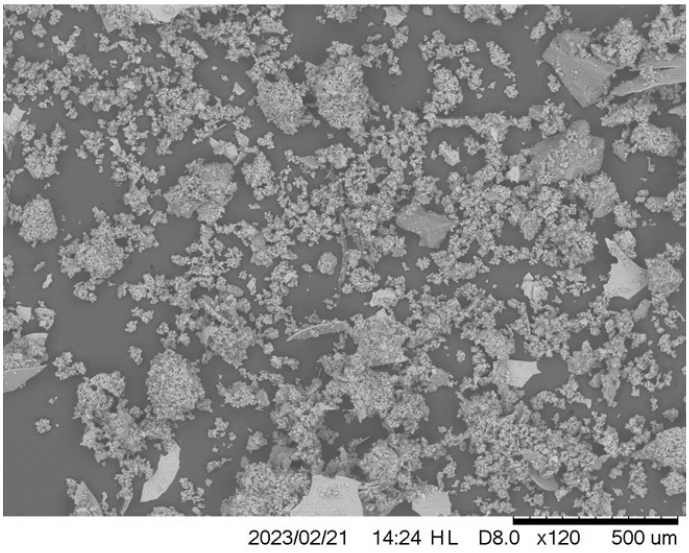

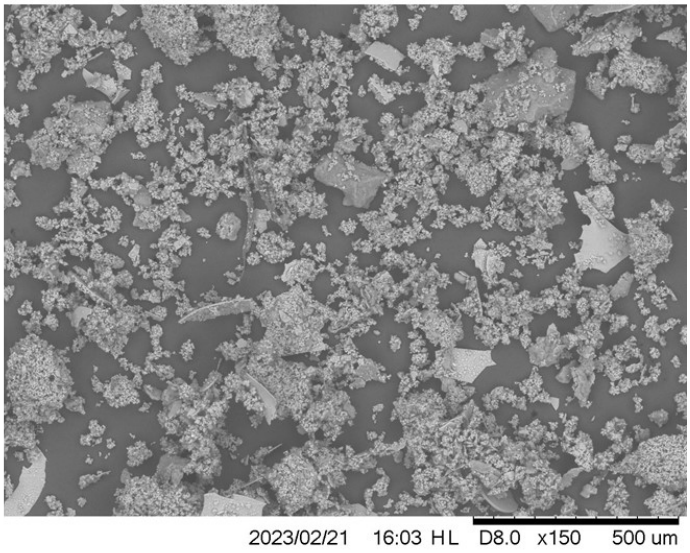

Figure S86. Energy dispersive X-ray analysis

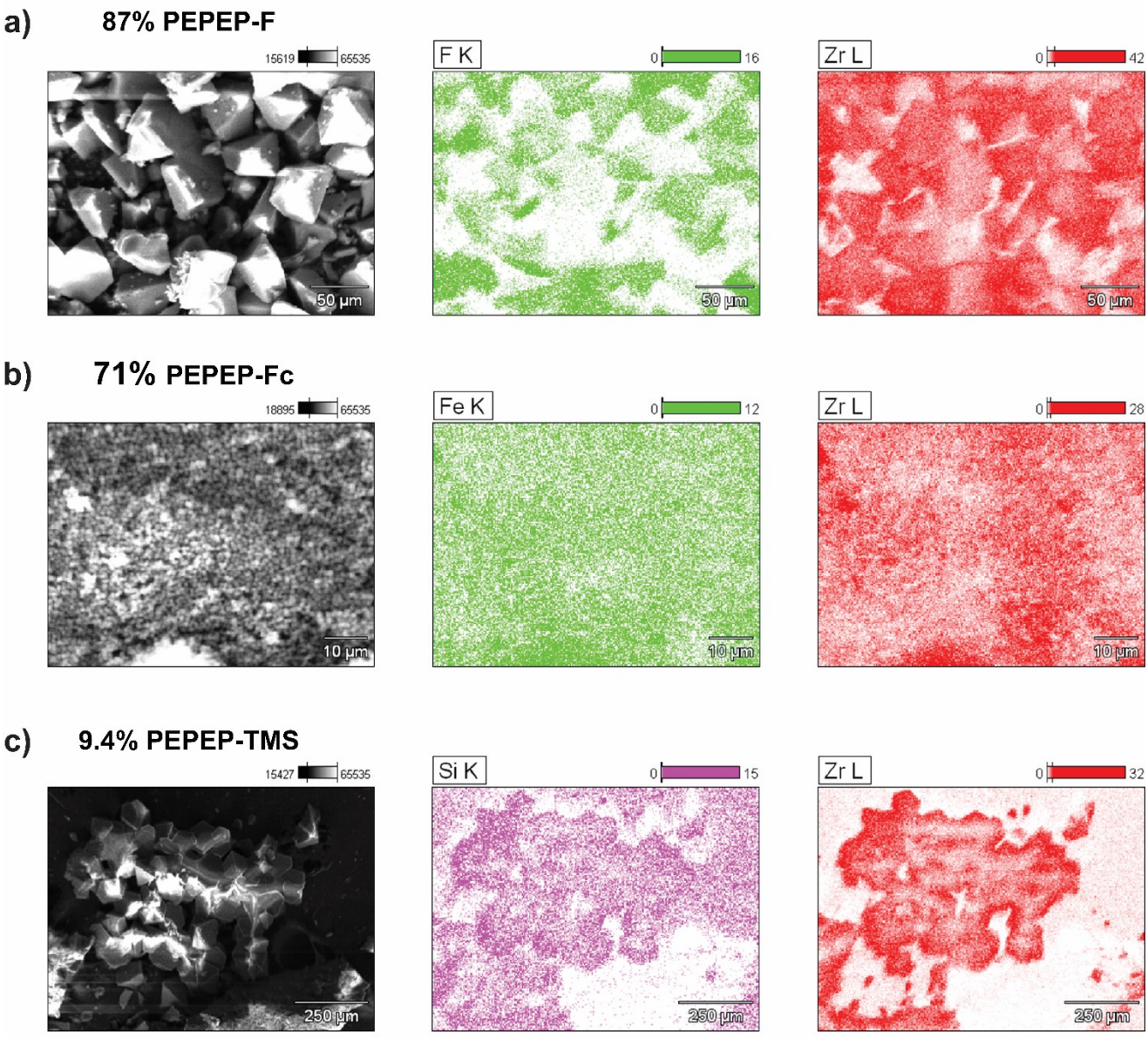

Section S7. **Vibrational spectroscopy.**

Figure S87. Fourier transform infrared spectroscopy of **PEPEP-Me/QPDC-Me**

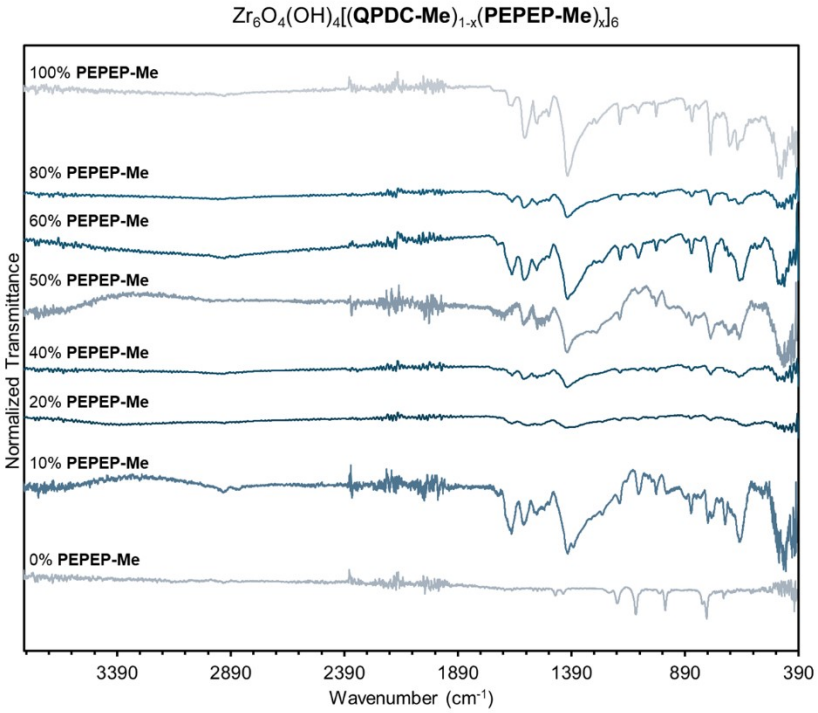

Figure S88. Fourier transform infrared spectroscopy of **PEPEP-OMe/QPDC-Me**

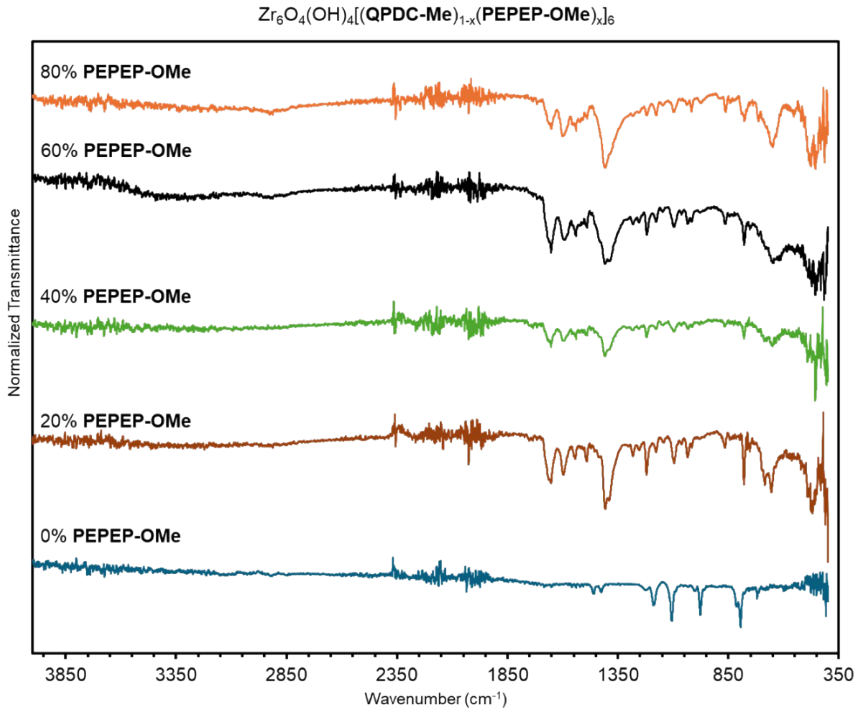

Figure S89. Fourier transform infrared spectroscopy of **PEPEP-F/QPDC-Me**

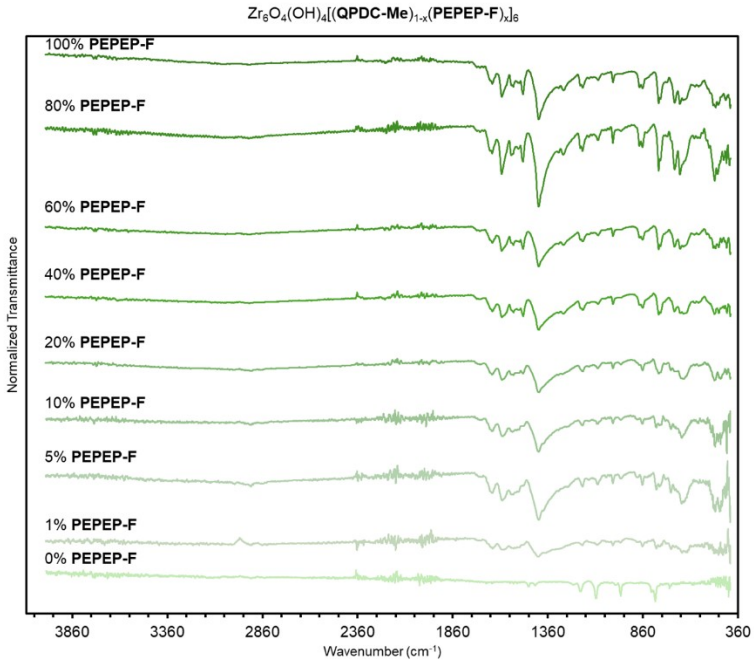

Figure S90. Fourier transform infrared spectroscopy of **PEPEP-TMS/QPDC-Me**

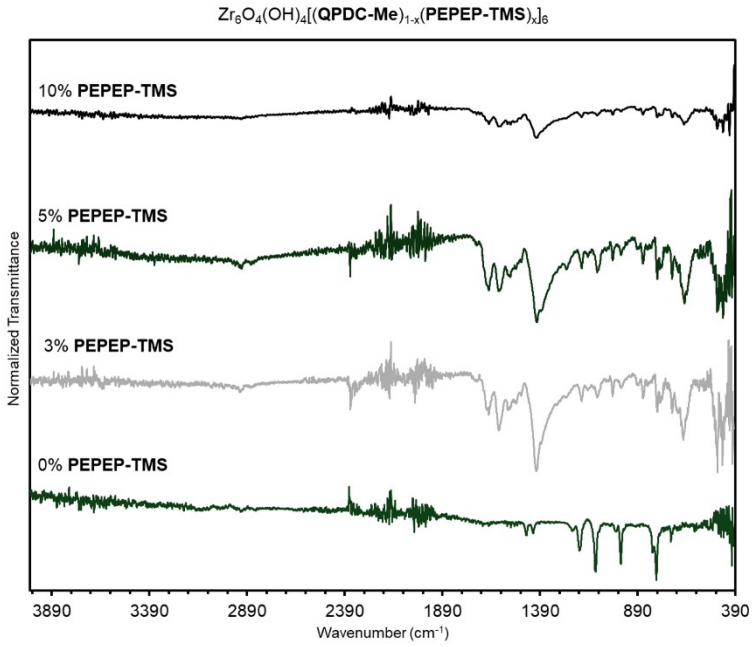

Figure S91. Fourier transform infrared spectroscopy of **PEPEP-Fc/QPDC-Me**

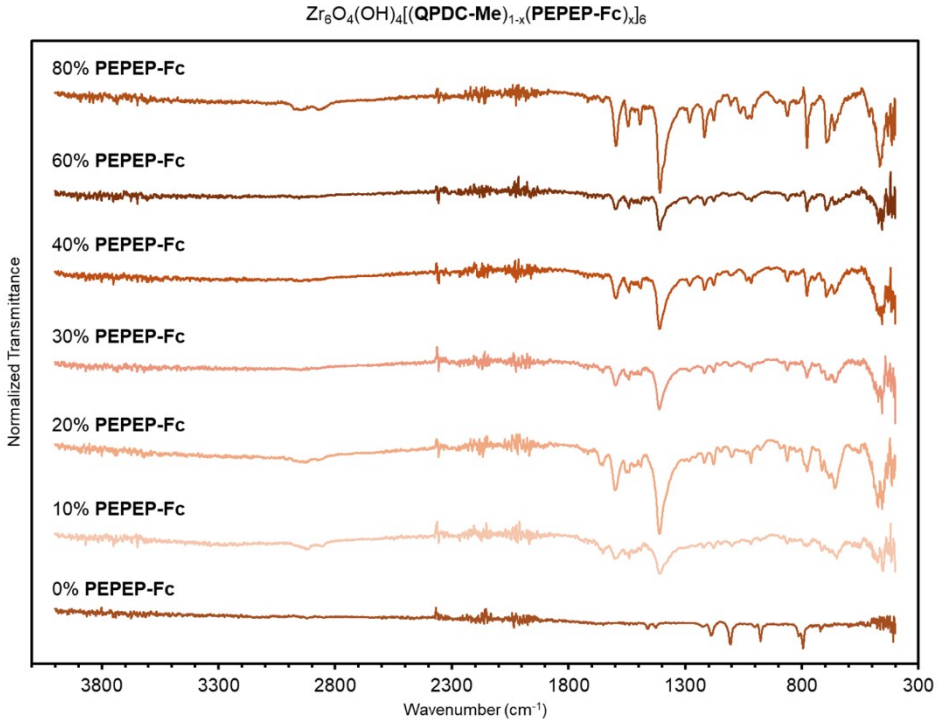

Figure S92. Fourier transform infrared spectroscopy of **PEPEP-Cl/QPDC-Me**

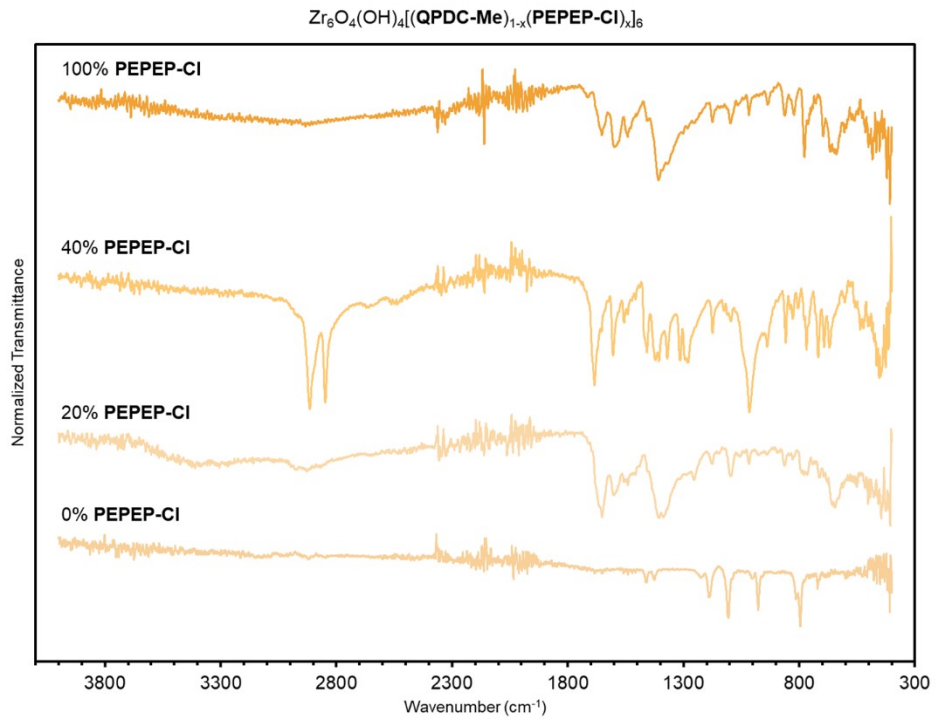

Figure S93. Fourier transform infrared spectroscopy of **PEPEP-Cl/QPDC-Me**

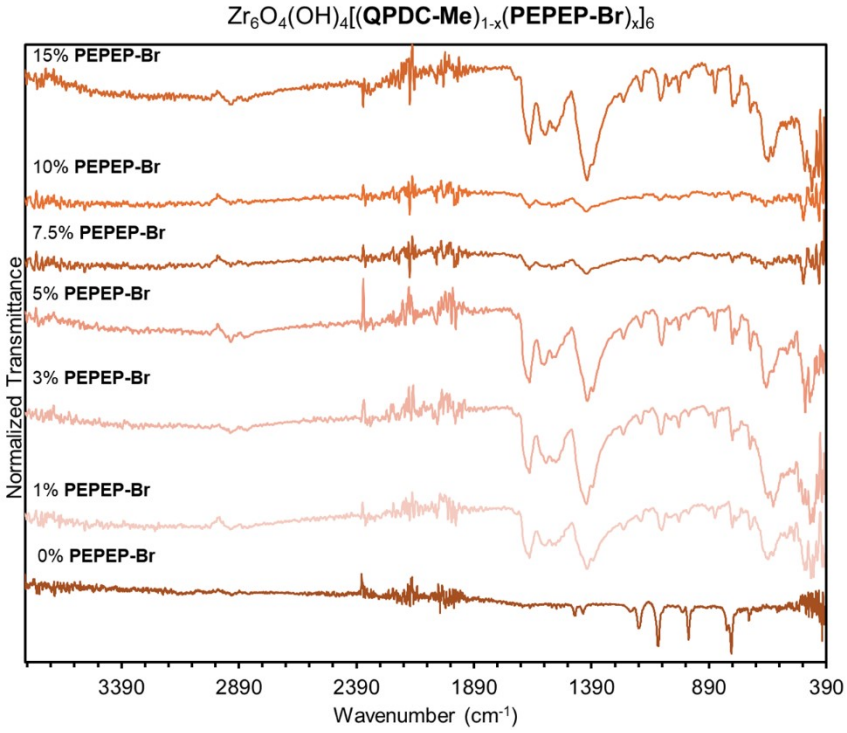

Figure S94. Fourier transform infrared spectroscopy of homeomorphic links

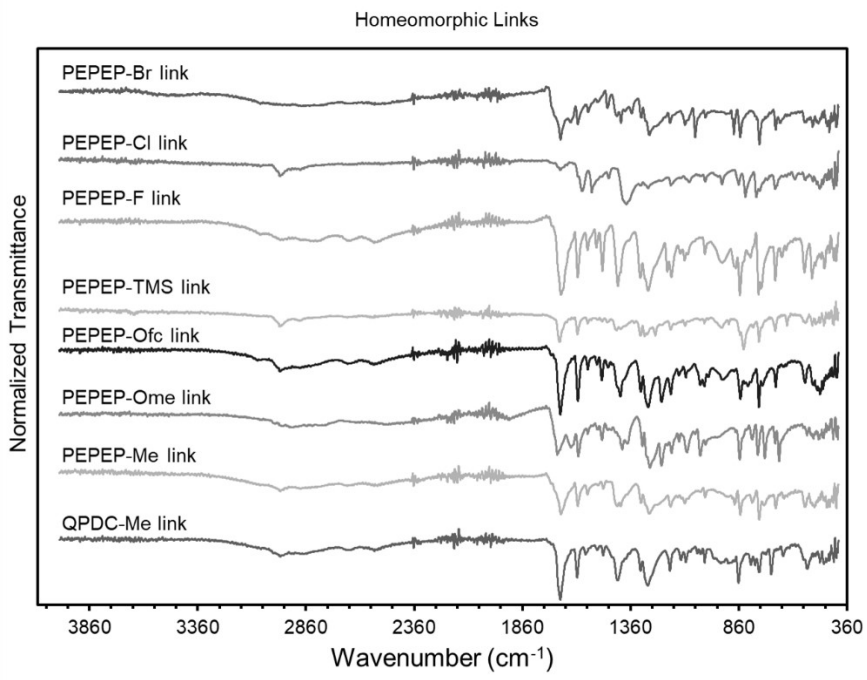

Figure S95. Raman spectra of **PEPEP-Me/QPDC-Me**

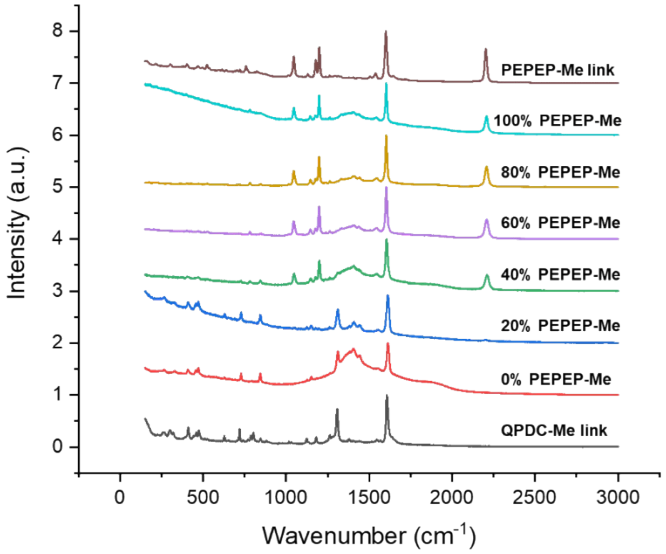

Figure S96. Raman spectra of **PEPEP-F/QPDC-Me**

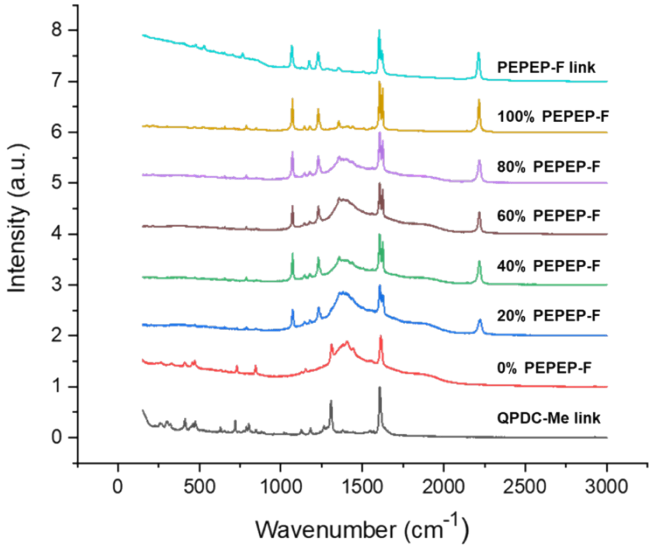

Figure S97. Raman spectra of **PEPEP-TMS/QPDC-Me**

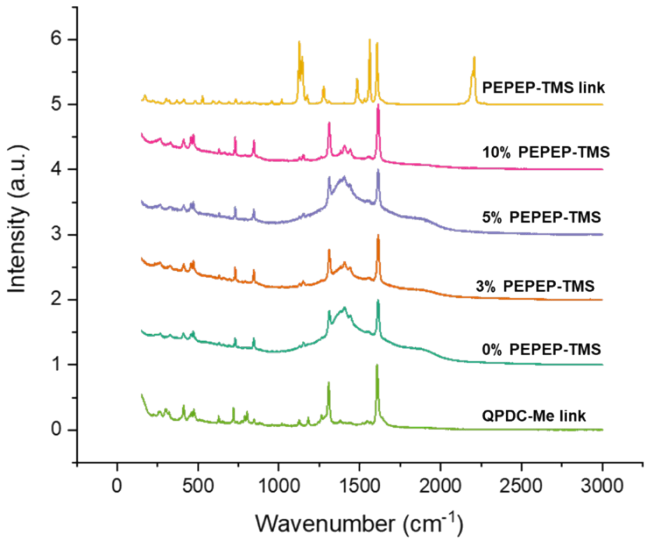

Section S8. **Gas Adsorption Isotherms:**

Figure S98. N_2 adsorption measurements (77 K) of activated (120 °C, 24 h, 2 μtorr) **PEPEP-Me**/**QPDC-Me** MTV MOFs.

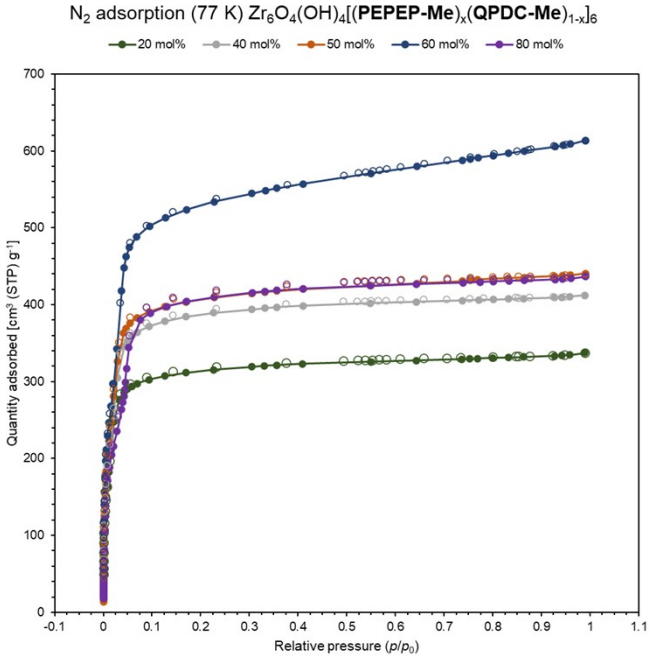

Figure S99. Semi-log adsorption isotherm (N_2, 77 K) of **PEPEP-Me**/**QPDC-Me** MTV MOFs.

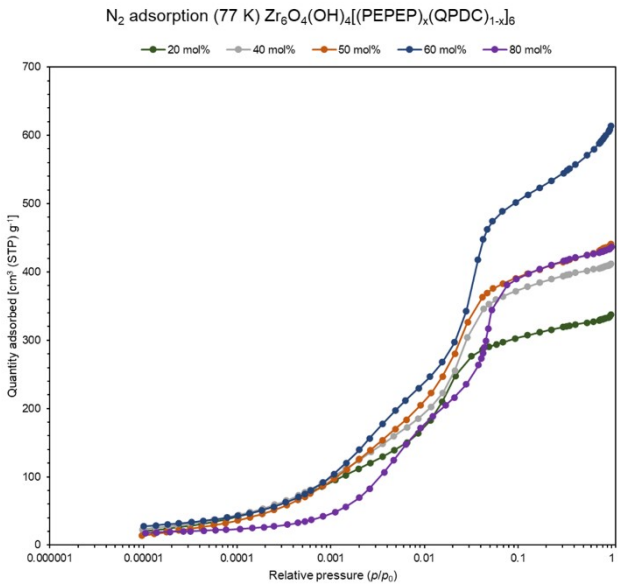

Figure S100. Cumulative pore volume from NLDFT of **PEPEP-Me**/**QPDC-Me** MTV MOFs.

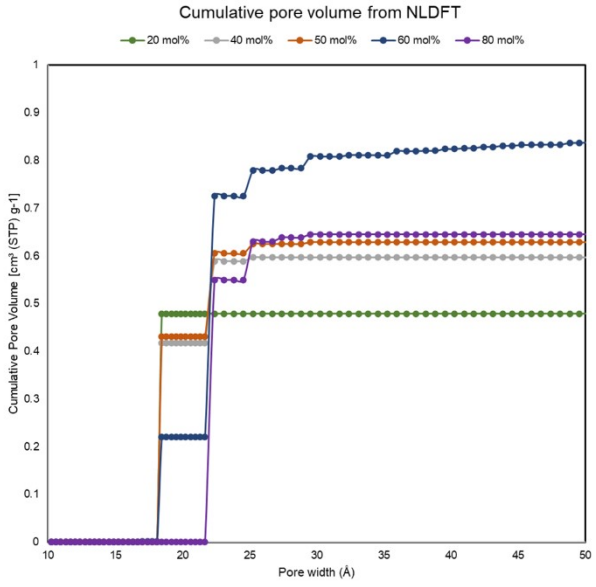

Figure S101. Differential pore volume from NLDFT of **PEPEP-Me**/**QPDC-Me** MTV MOFs.

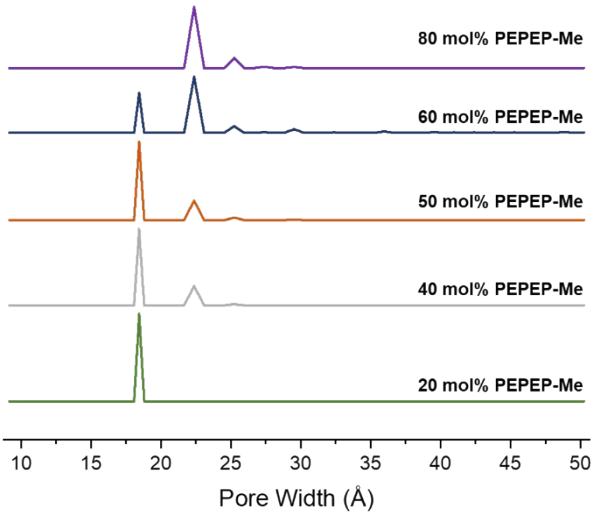

Table S18. BET surface area and total pore volume of **PEPEP-Me/QPDC-Me** MTV MOFs.

x (mol% **PEPEP-Me)**	BET surface area (m^2g^{-1})	Total pore volume (cc g^{-1})
20	629.2	0.4787
40	736.9	0.5966
50	1706.5	0.6691
60	1343.3	0.8451
80	1222.0	0.6451

Figure S102. Rouquerol plot (left) and BET plot (right) for 20% **PEPEP-Me**/**QPDC-Me.**

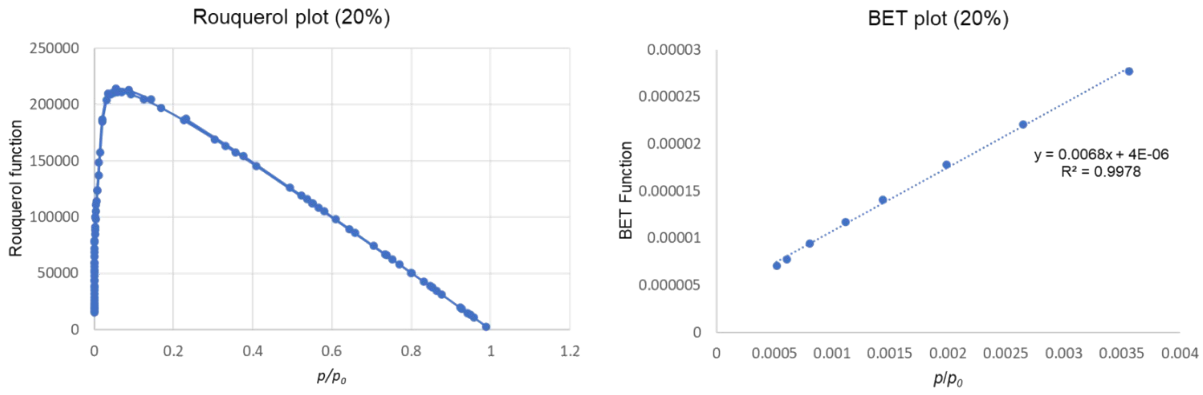

Figure S103. Rouquerol plot (left) and BET plot (right) for 40% **PEPEP-Me**/**QPDC-Me.**

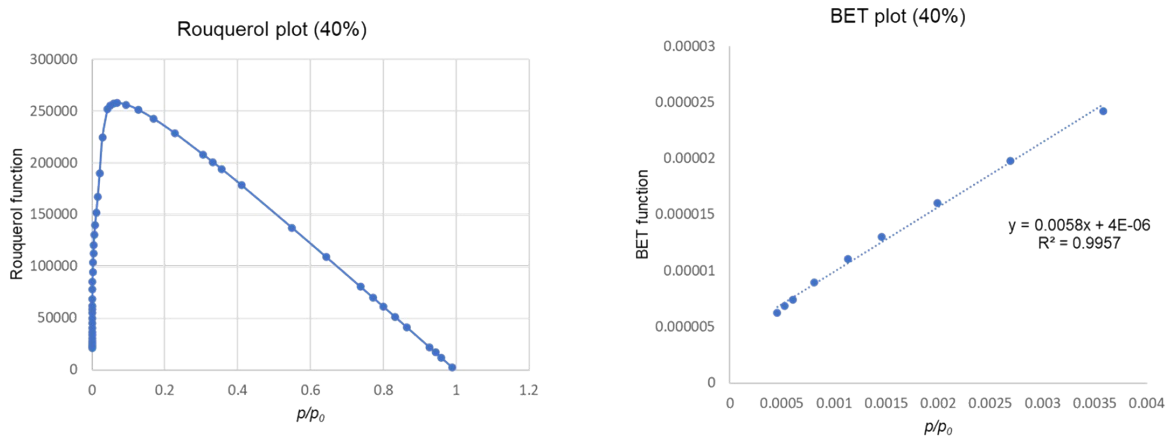

Figure S104. Rouquerol plot (left) and BET plot (right) for 50% **PEPEP-Me/QPDC-Me.**

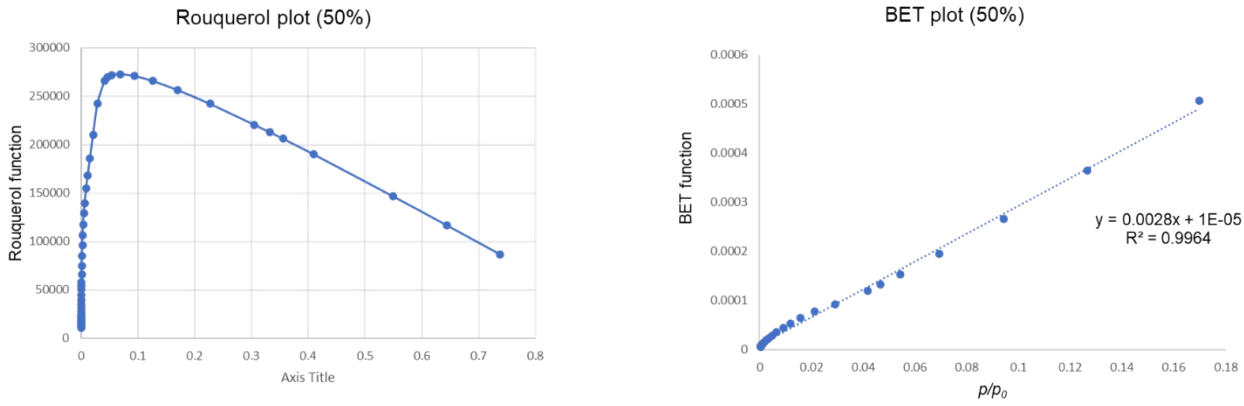

Figure S105. Rouquerol plot (left) and BET plot (right) for60% **PEPEP-Me/QPDC-Me.**

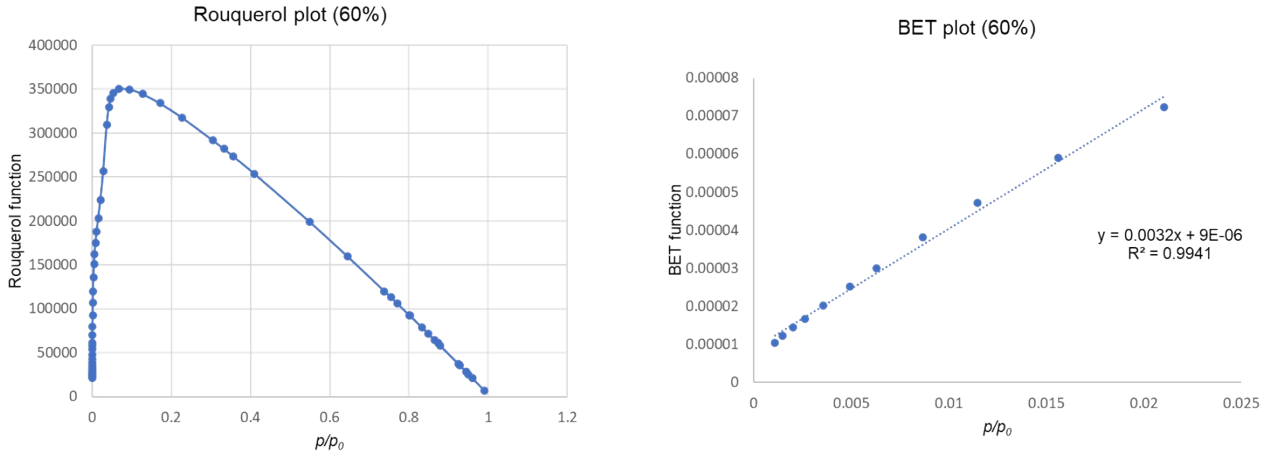

Figure S106. Rouquerol plot (left) and BET plot (right) for 60% **PEPEP-Me/QPDC-Me.**

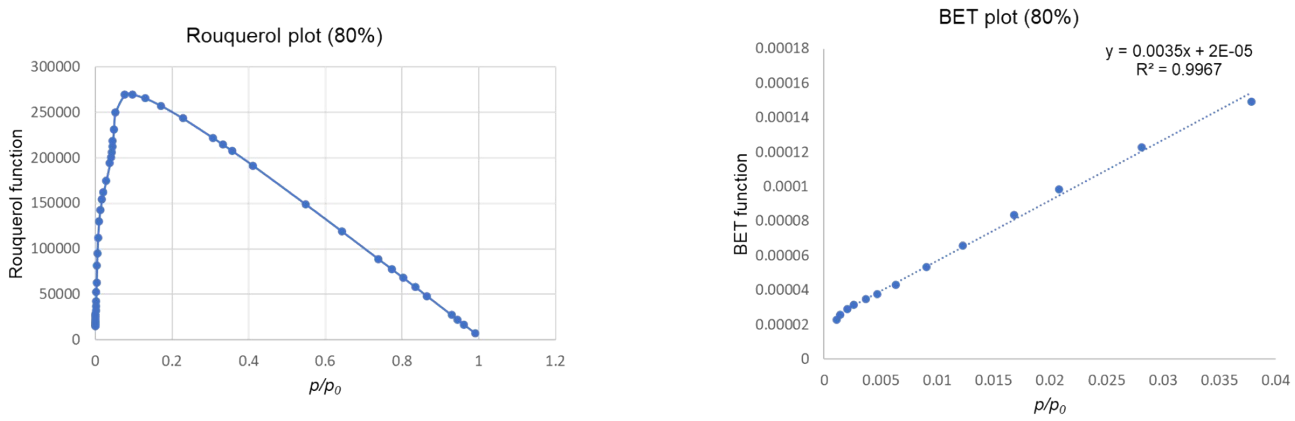

Figure S107. N_2 adsorption measurements (77 K) of activated (120 °C, 48 h, 2 μtorr) **PEPEP-CI** MOF.

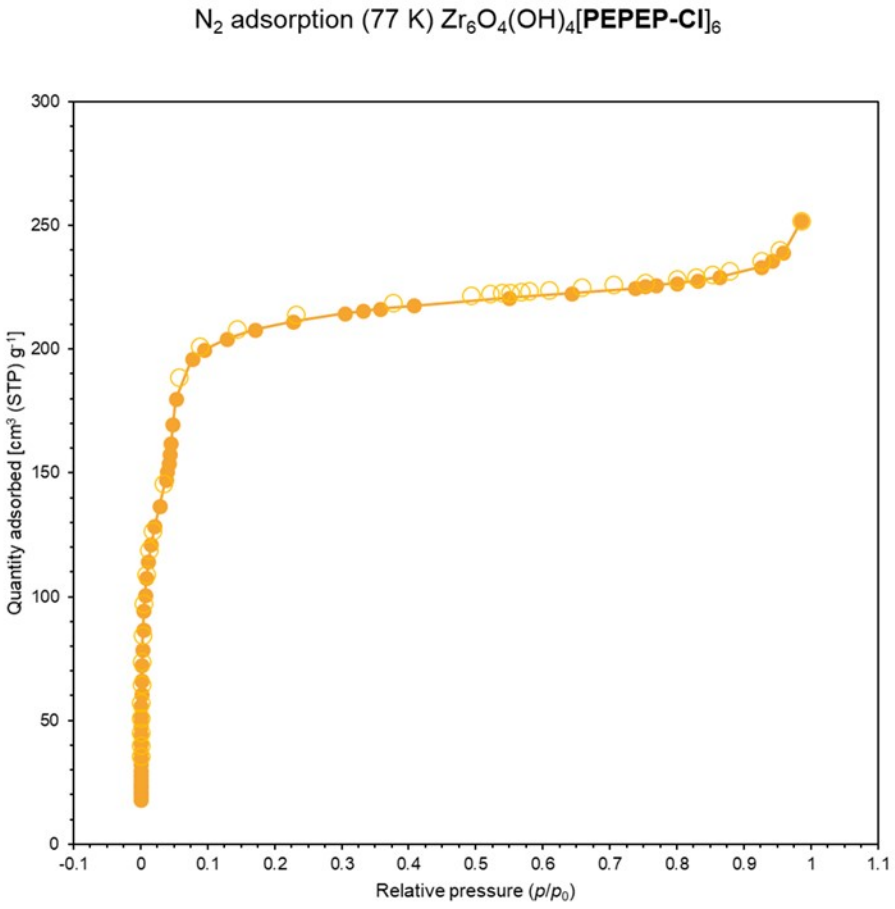

Figure S108. Rouquerol plot (left) and BET plot (right) for **PEPEP-Cl MOF.**

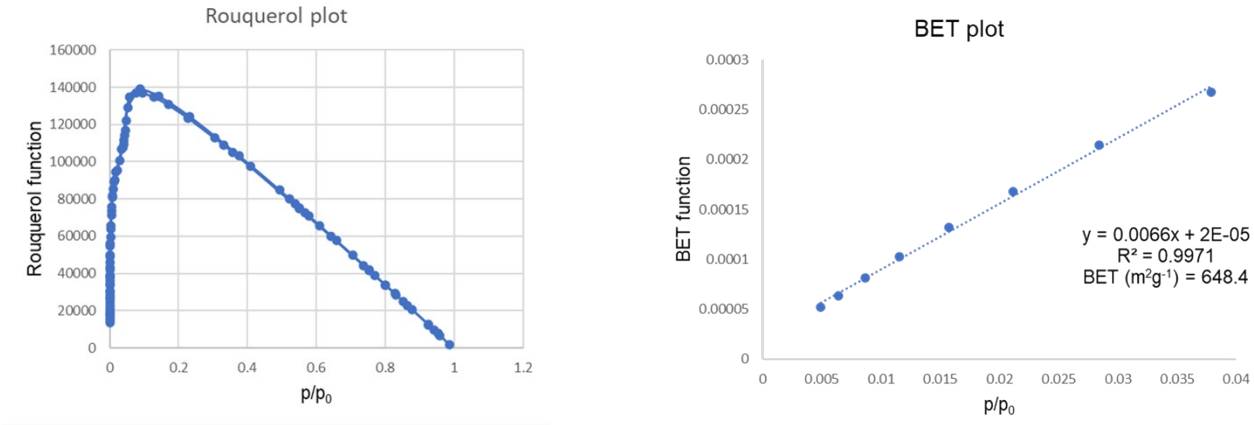

Figure S109. Cumulative pore volume from NLDFT of **PEPEP-Cl** MOF.

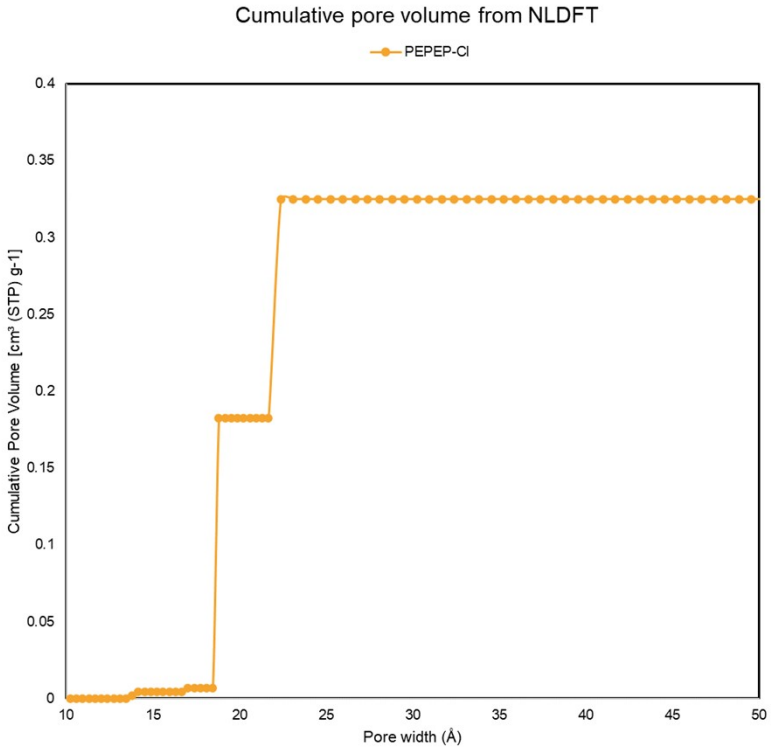

Figure S110. Differential pore volume from NLDFT of **PEPEP-CI** MOF.

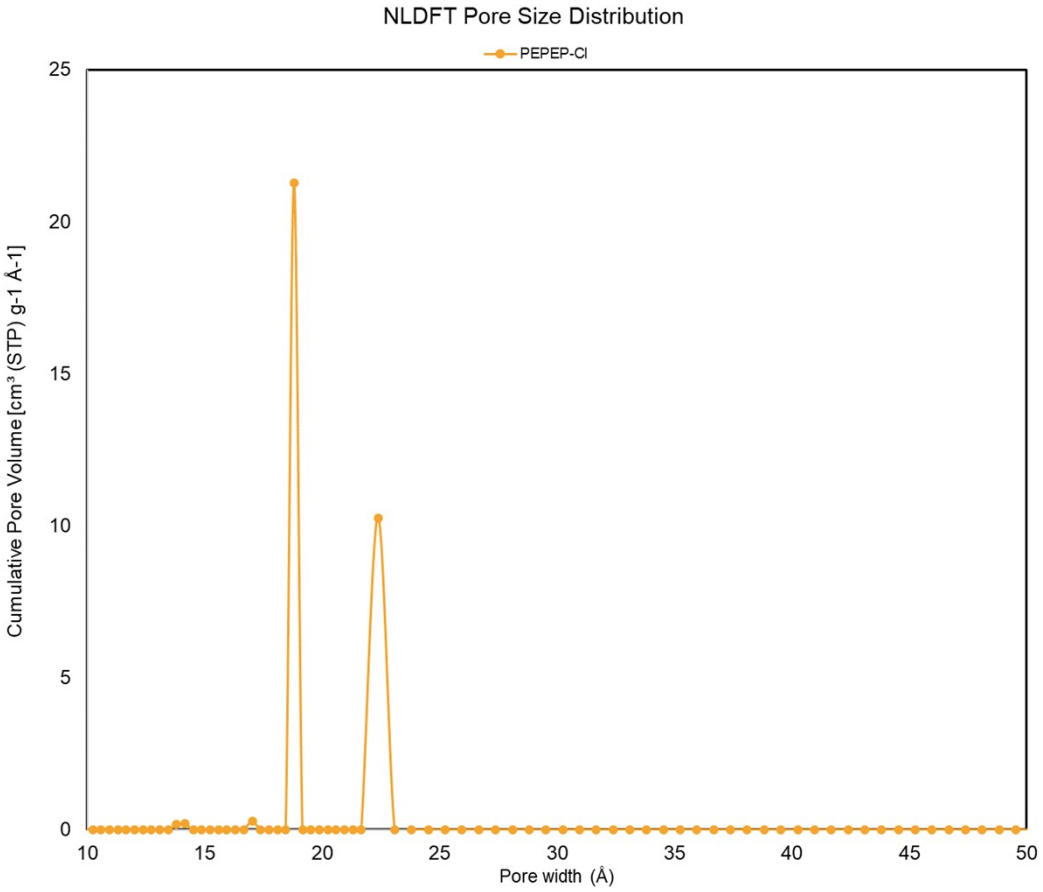

Section S9. **Thermogravimetric analysis**

Figure S111. TGA of selected MOF compositions after solvent exchange (THF).

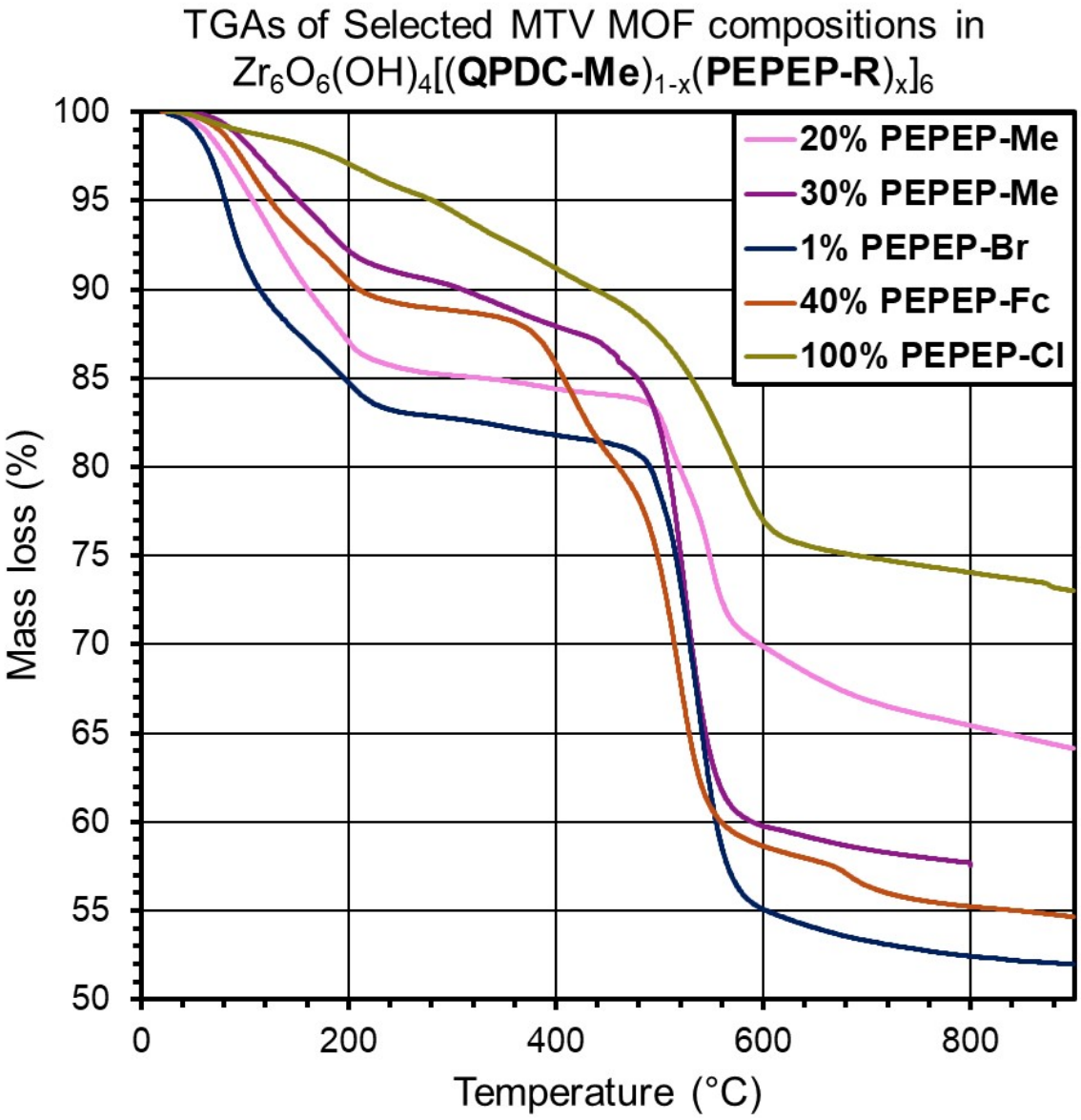

Section S10. **Solution nuclear magnetic resonance spectroscopy.**

Figure S112. ^{1}H ($CDCl_3$, 25 °C) NMR spectra of **S2**.

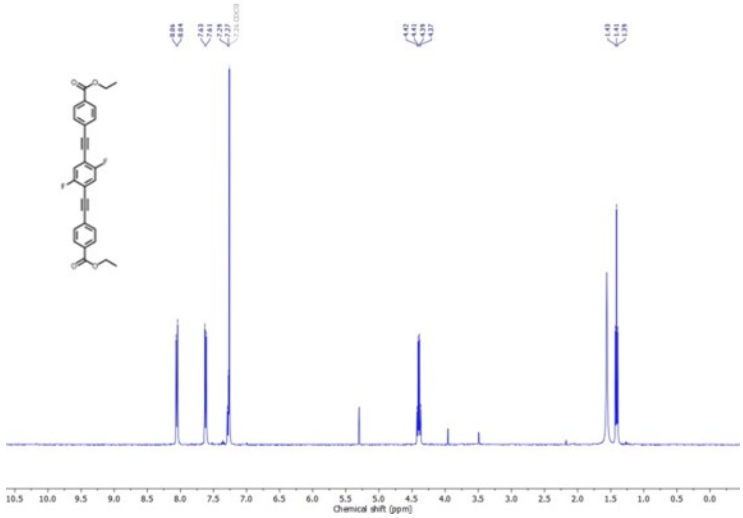

Figure S113. ^{13}C ($CDCl_3$, 25 °C) NMR spectra of **S2**.

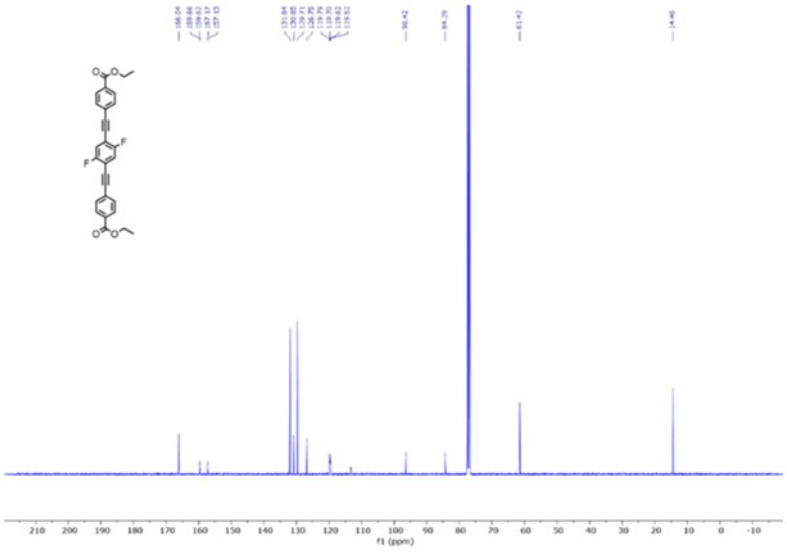

Figure S114. ^{19}F ($CDCl_3$, 25 °C) NMR spectra of **S2**.

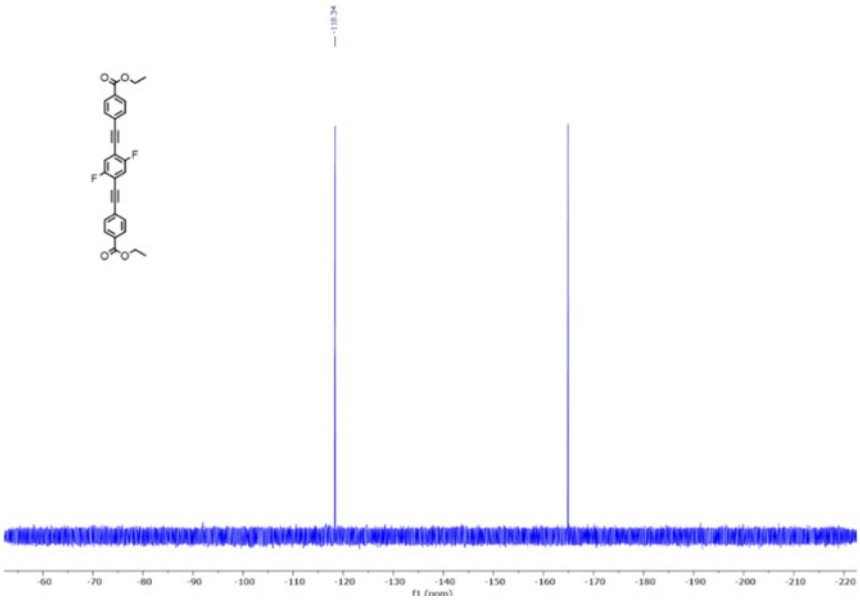

Figure S115. ^{1}H ($CDCl_3$, 25 °C) NMR spectra of **PEPEP-F**.

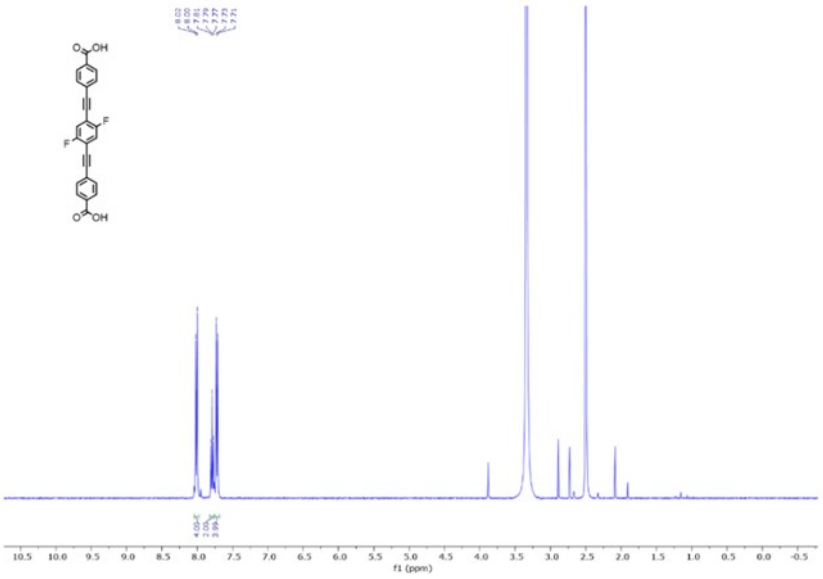

Figure S116. ^{13}C ($CDCl_3$, 25 °C) NMR spectra of **PEPEP-F**.

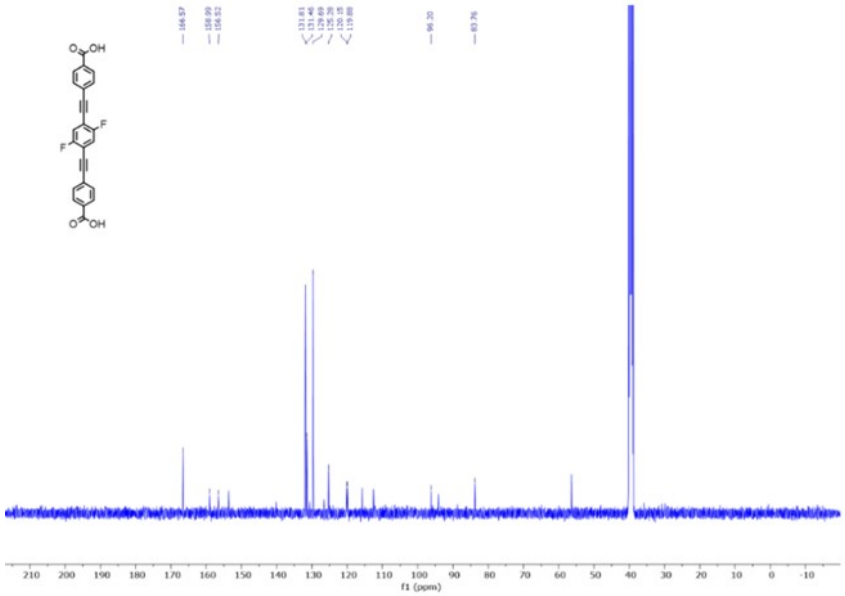

Figure S117. ^{19}F ($CDCl_3$, 25 °C) NMR spectra of **PEPEP-F**.

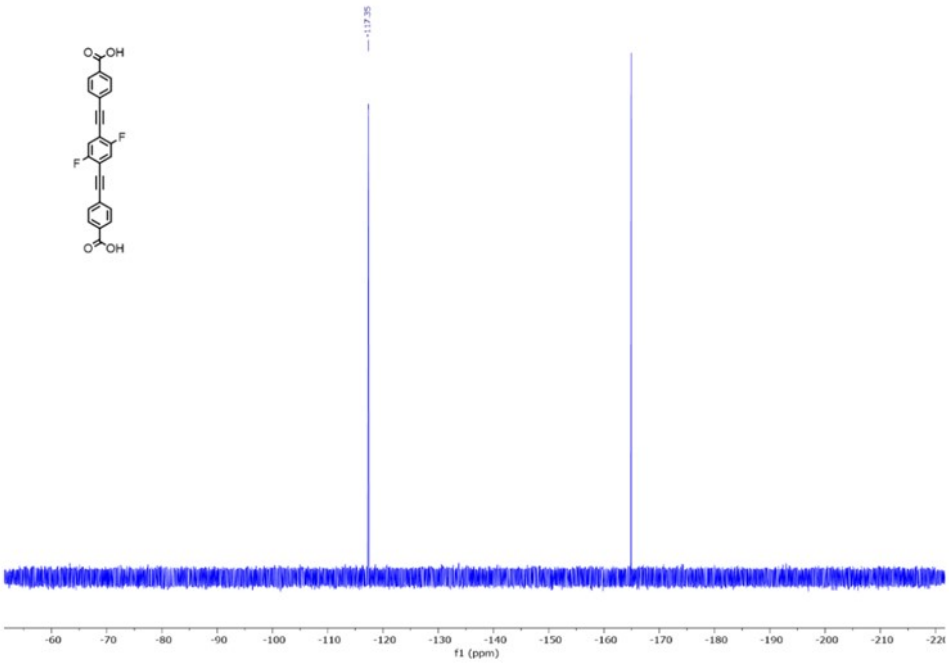

Figure S118. ^{1}H ($CDCl_3$, 25 °C) NMR spectra of **S4**.

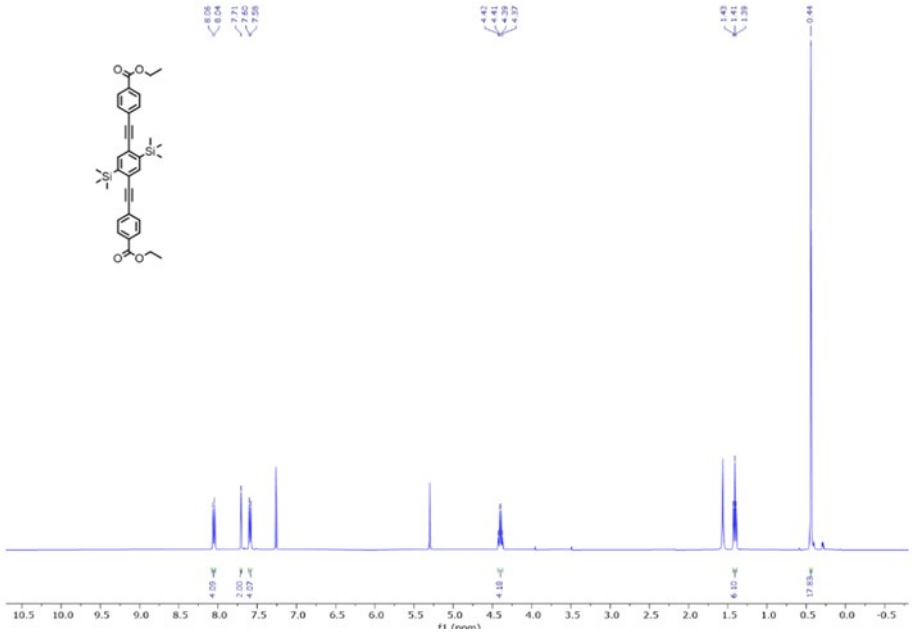

Figure S119. ^{13}C ($CDCl_3$, 25 °C) NMR spectra of **S4**.

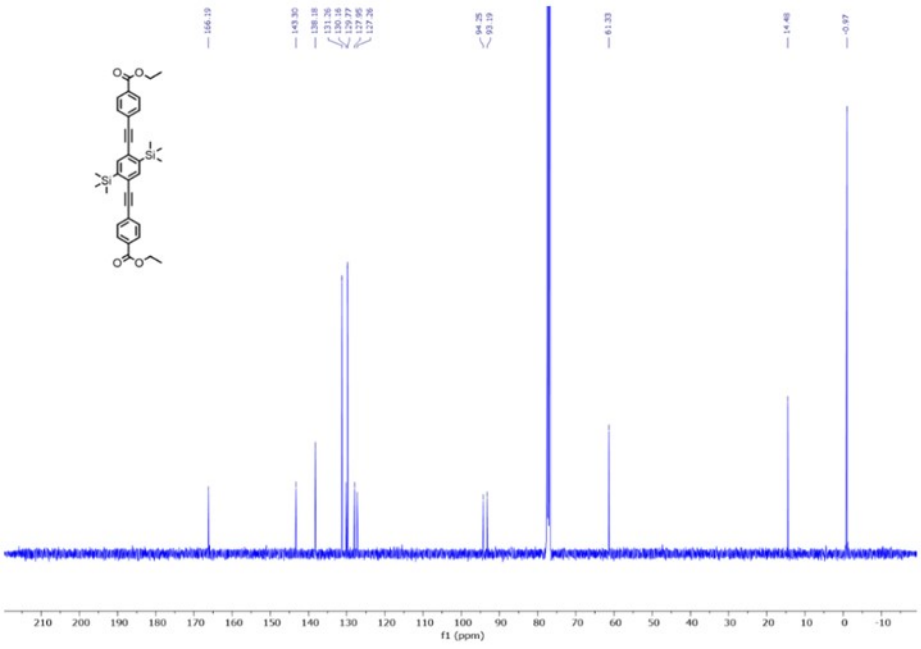

Figure S110. ^{1}H ($CDCl_3$, 25 °C) NMR spectra of **PEPEP-TMS**.

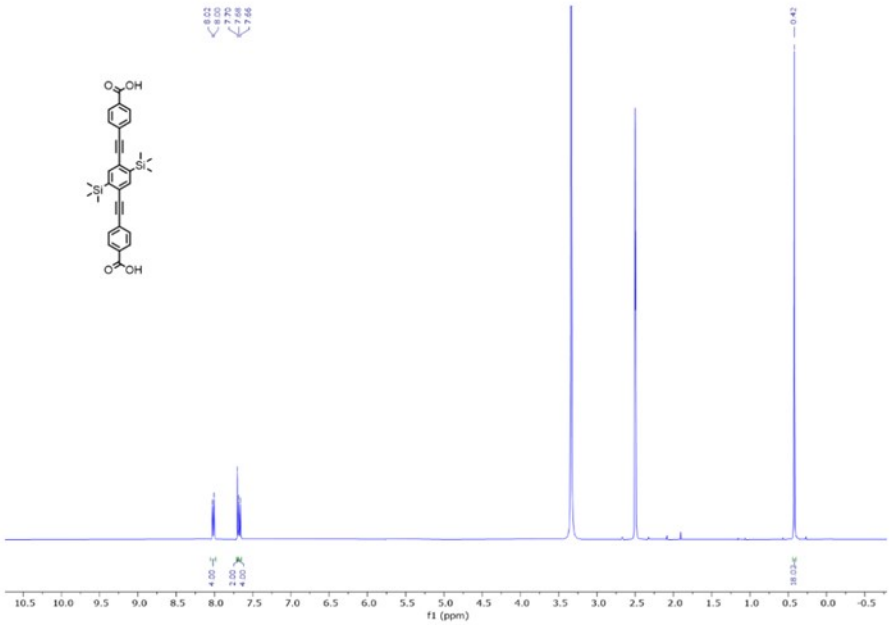

Figure S111. ^{13}C ($CDCl_3$, 25 °C) NMR spectra of **PEPEP-TMS**.

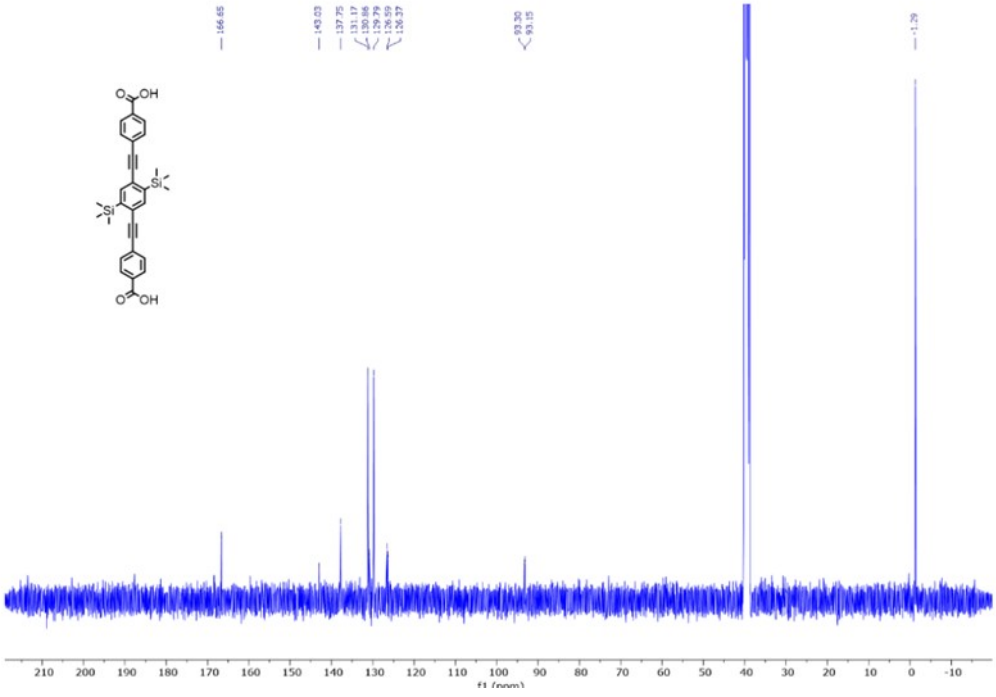

Figure S112. ^{1}H ($CDCl_3$, 25 °C) NMR spectra of **S5**.

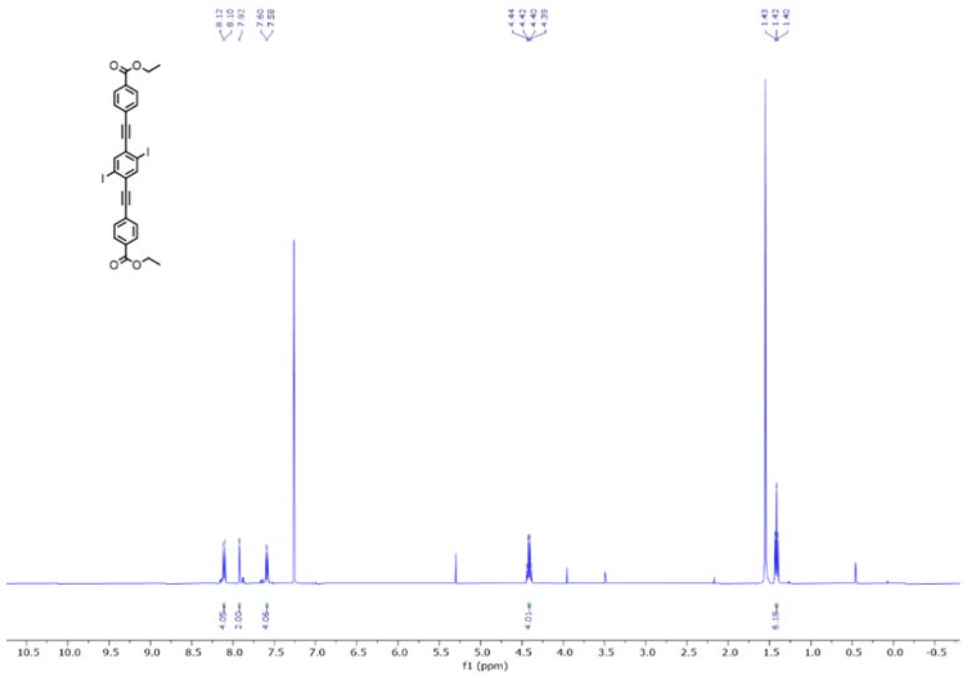

Figure S113. ^{13}C ($CDCl_3$, 25 °C) NMR spectra of **S5**.

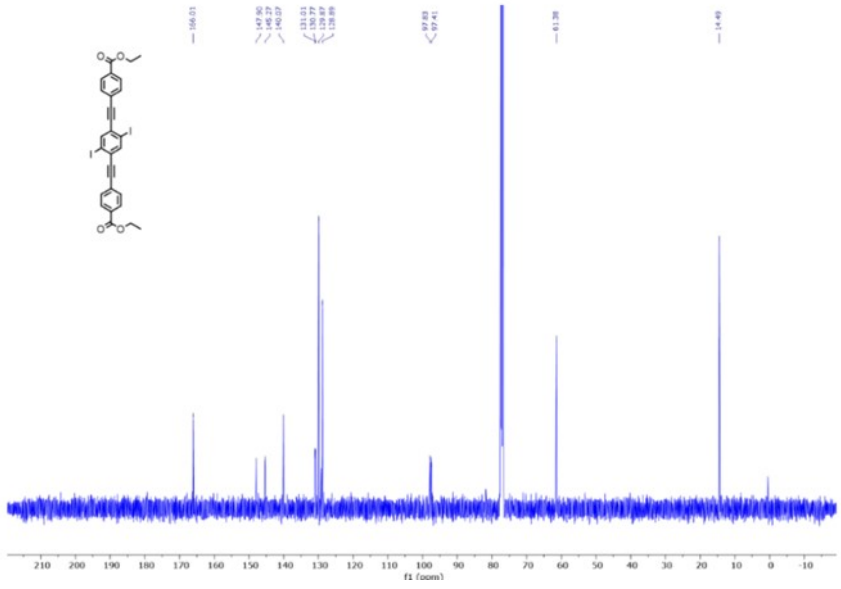

Figure S114. ^{1}H ($CDCl_3$, 25 °C) NMR spectra of **PEPEP-I**.

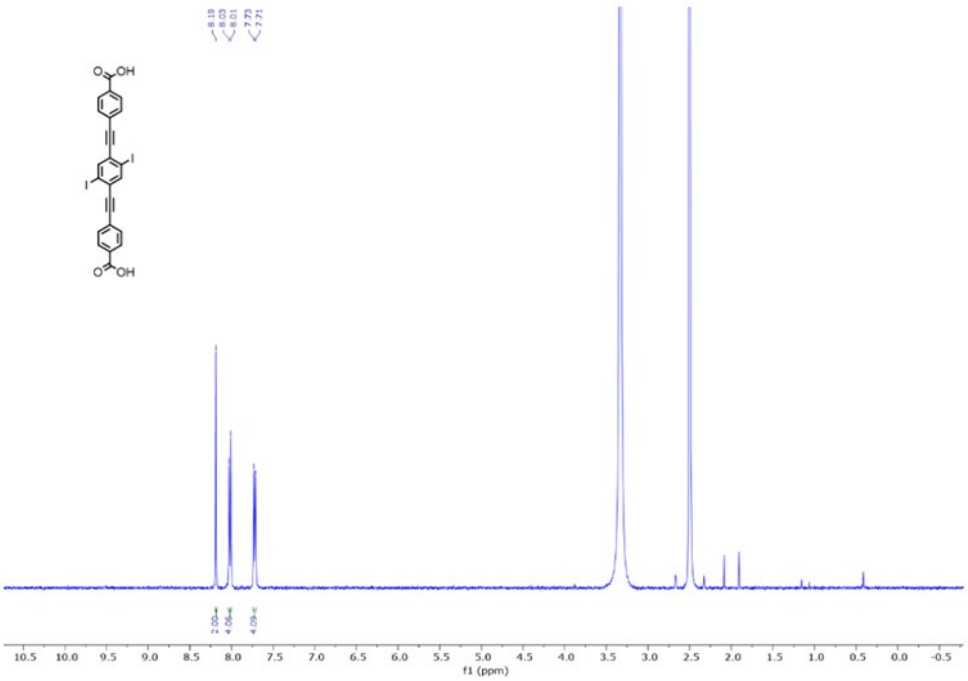

Figure S115. ^{13}C ($CDCl_3$, 25 °C) NMR spectra of **PEPEP-I**.

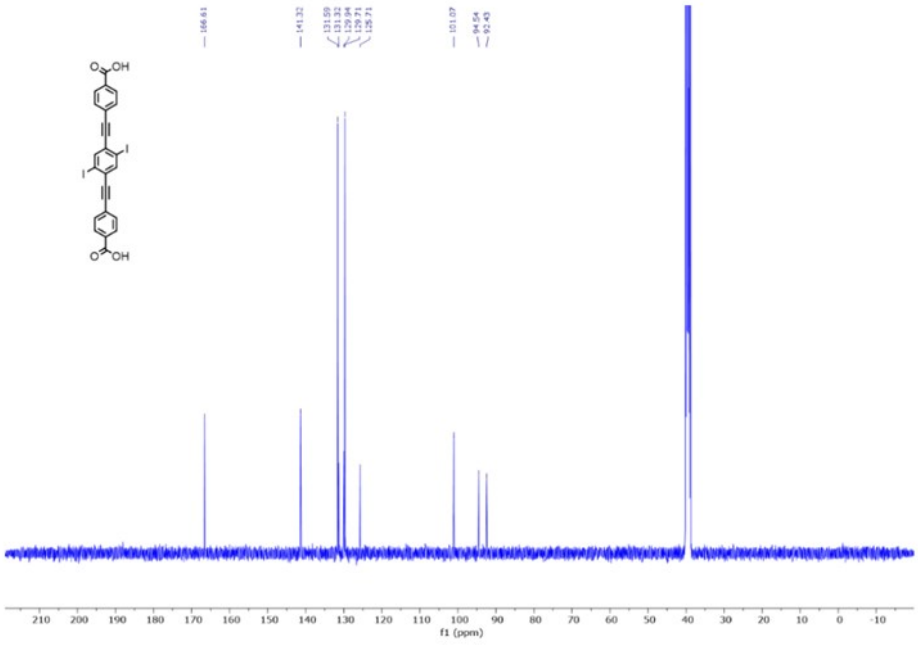

Figure S116. ^{1}H ($CDCl_3$, 25 °C) NMR spectra of **S6**.

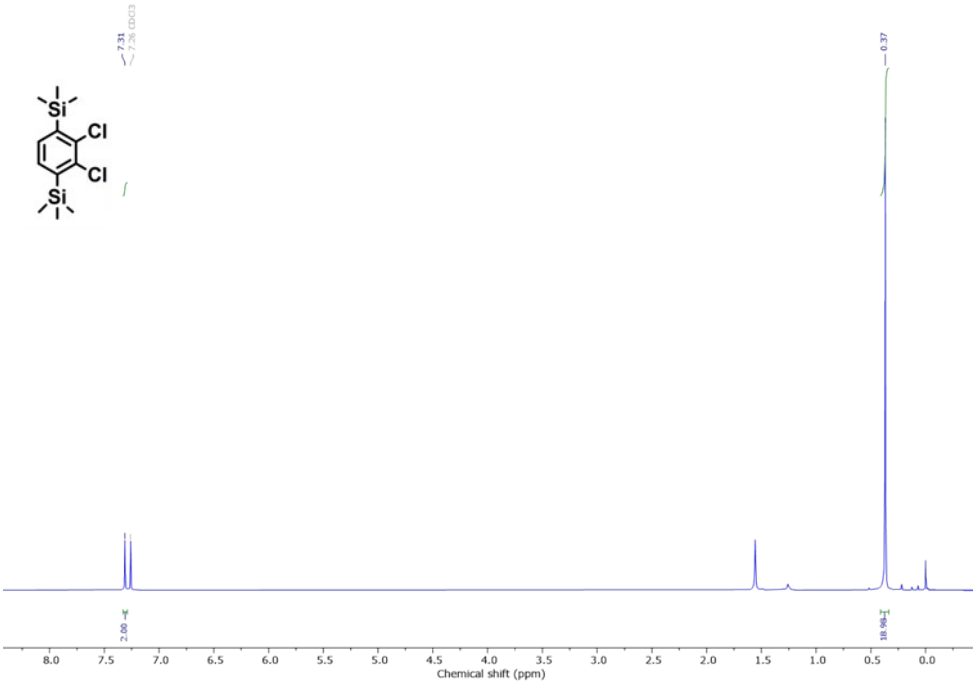

Figure S117. ^{13}C ($CDCl_3$, 25 °C) NMR spectra of **S6**.

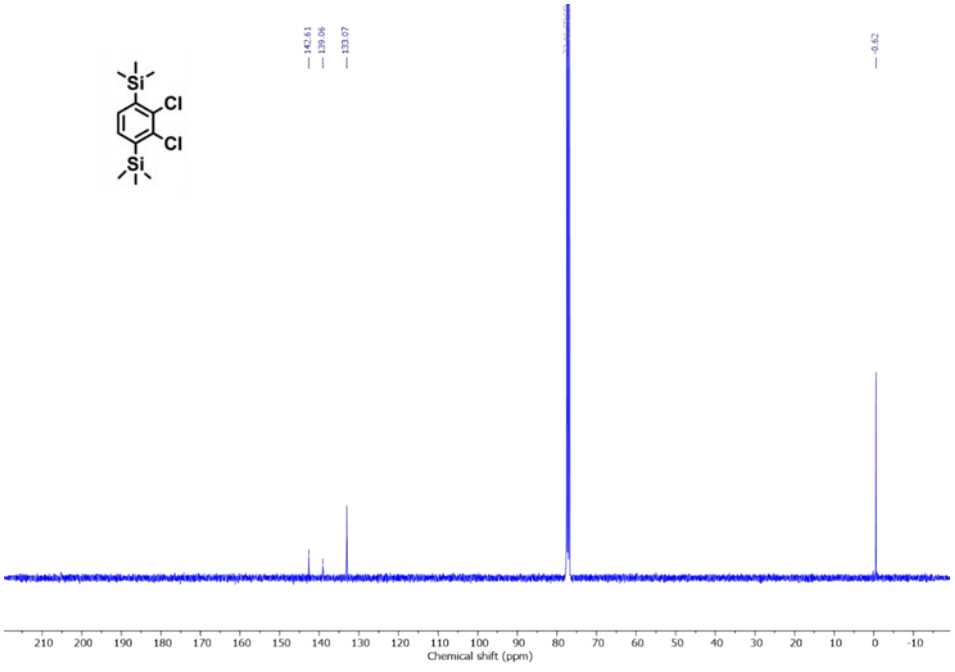

Figure S118. ^{1}H ($CDCl_3$, 25 °C) NMR spectra of **S7**.

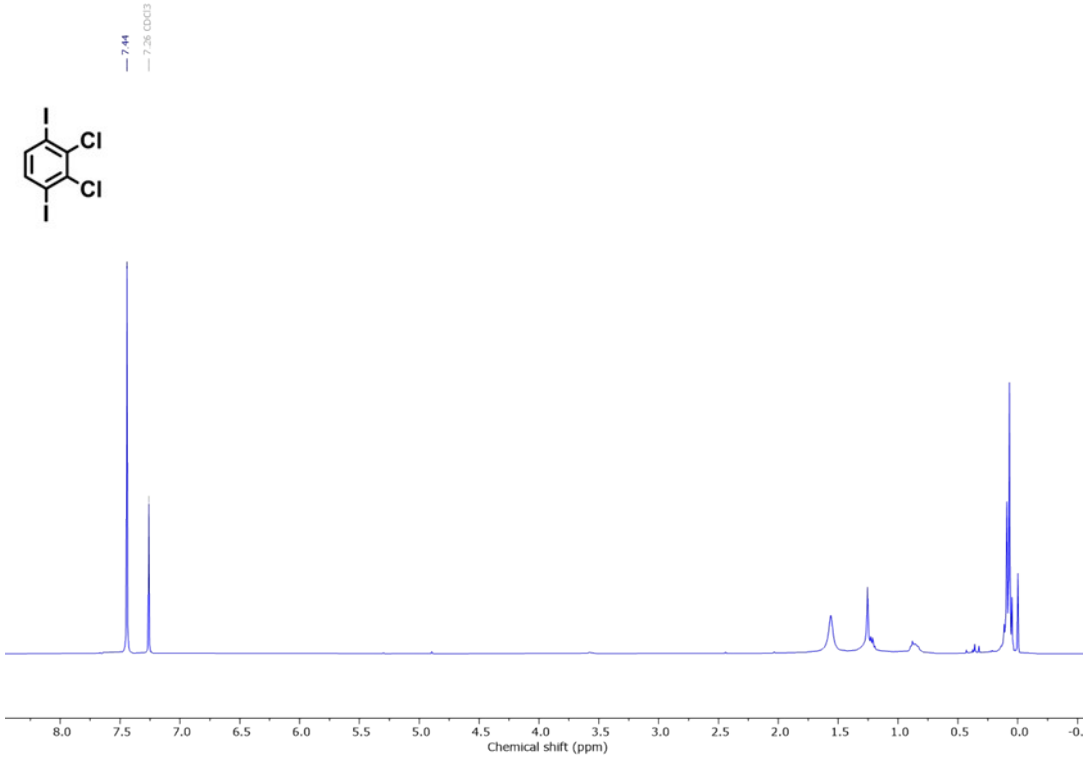

Figure S119. ^{13}C ($CDCl_3$, 25 °C) NMR spectra of **S7**.

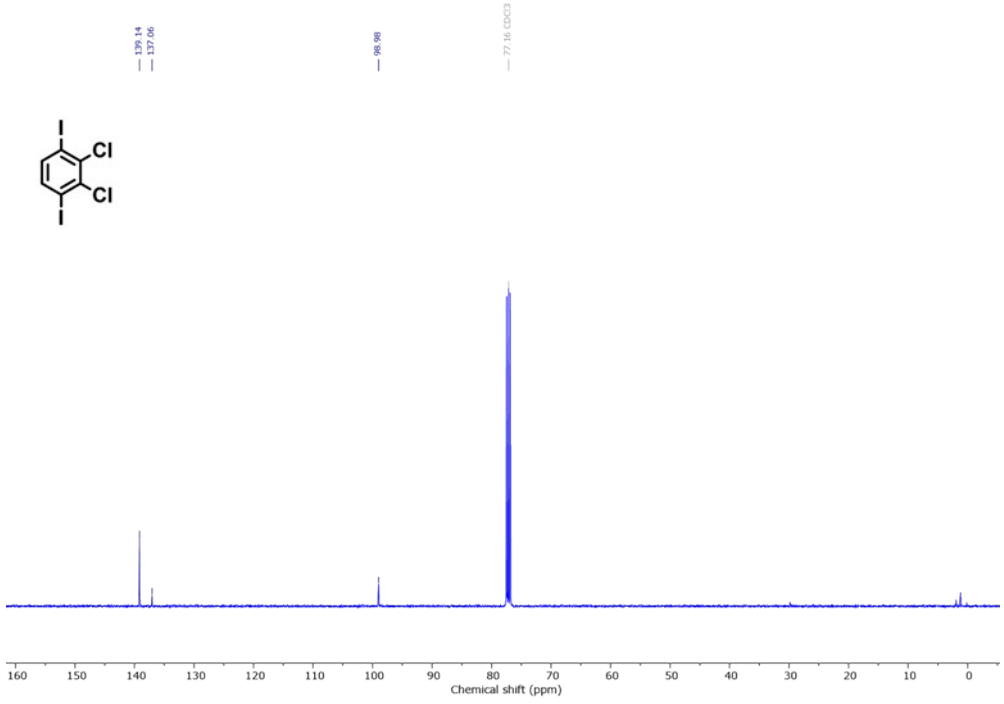

Figure S120. ^{1}H ($CDCl_3$, 25 °C) NMR spectra of **S8**.

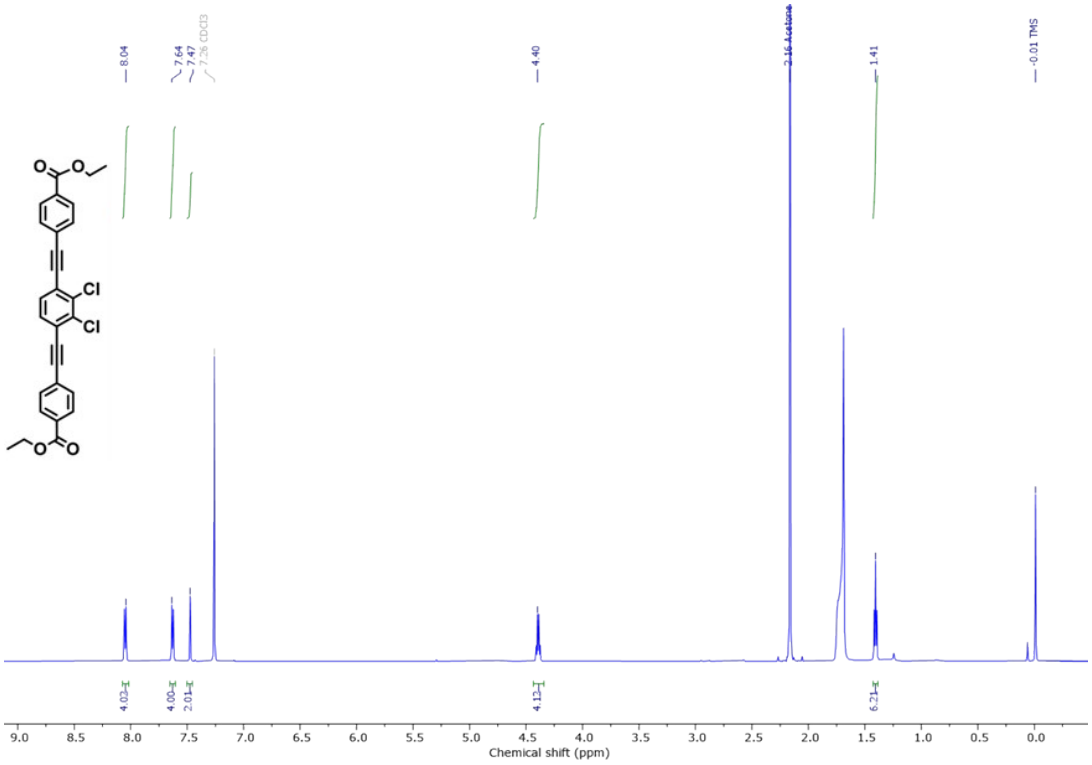

Figure S121. ^{13}C ($CDCl_3$, 25 °C) NMR spectra of **S8**.

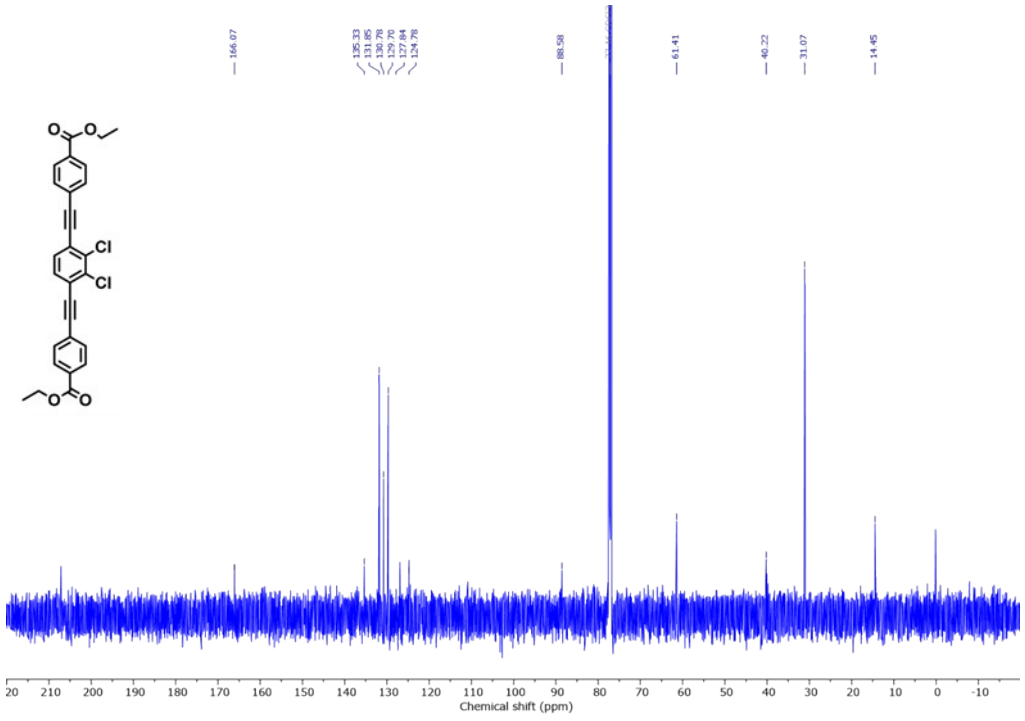

Figure S122. ^{1}H ($CDCl_3$, 25 °C) NMR spectra of **PEPEP-Cl**.

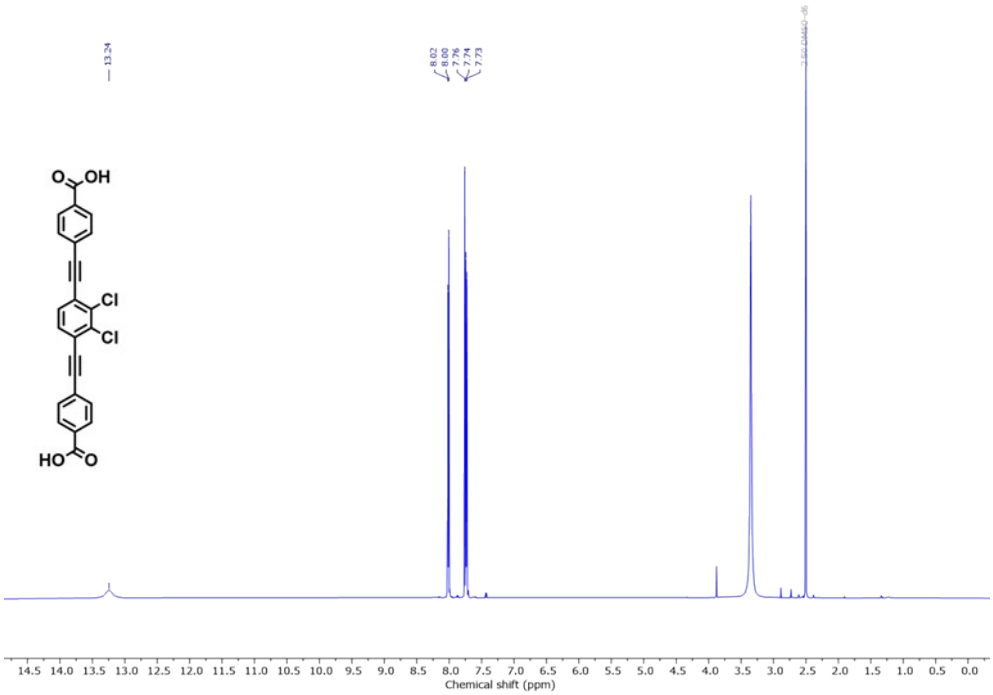

Figure S123. ^{13}C ($CDCl_3$, 25 °C) NMR spectra of **PEPEP-Cl**.

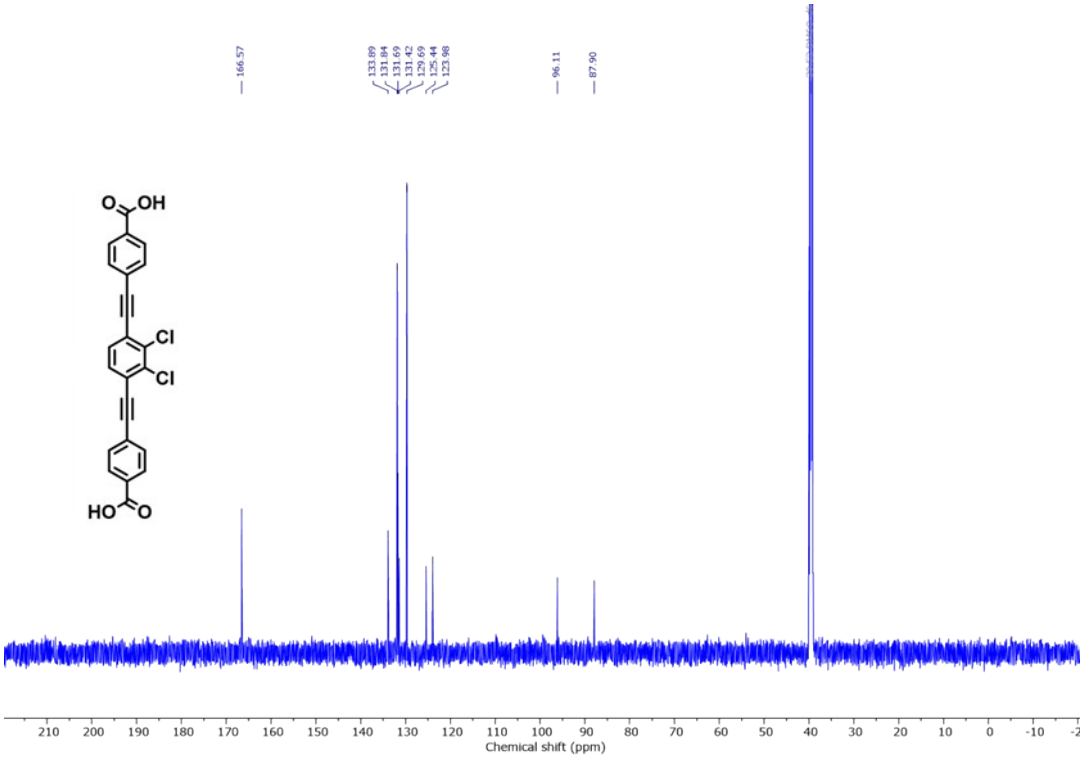

Figure S124. ^{1}H ($CDCl_3$, 25 °C) NMR spectra of **S11**.

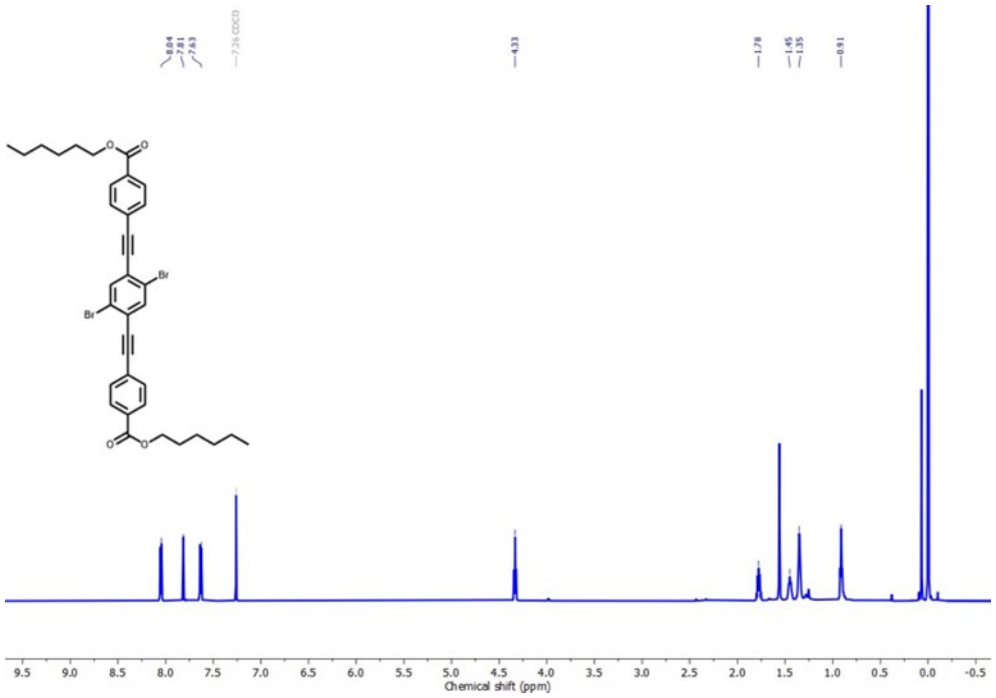

Figure S125. ^{13}C ($CDCl_3$, 25 °C) NMR spectra of **S11**.

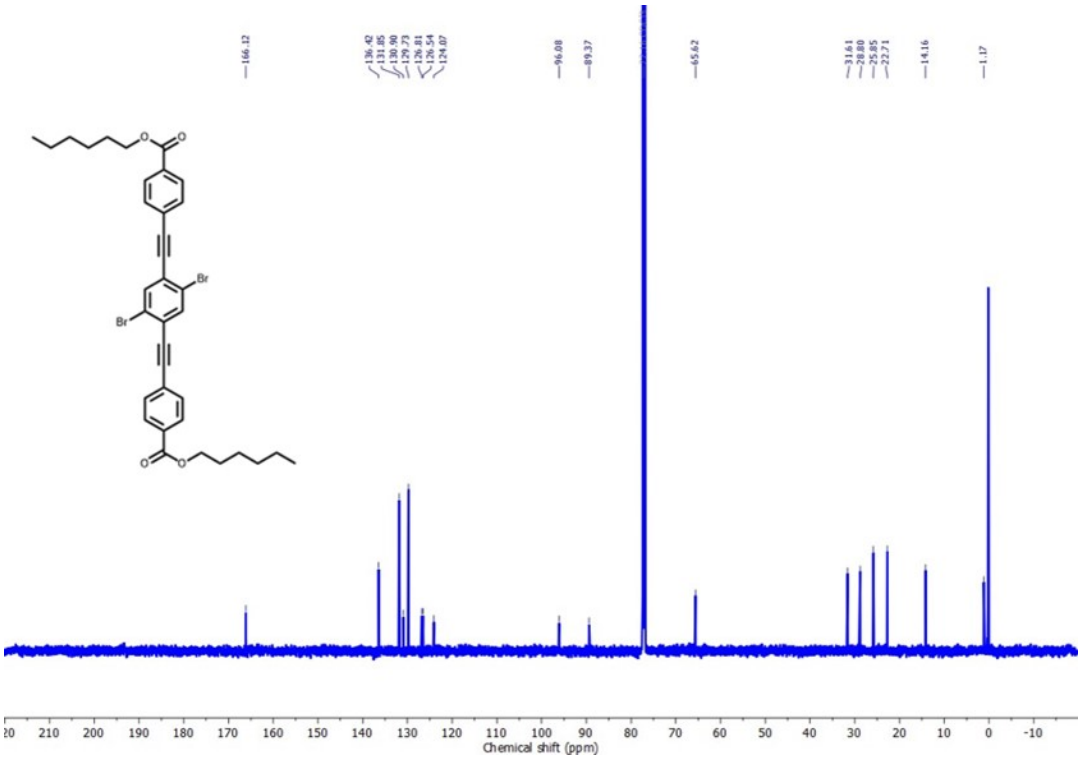

Figure S126. ^{1}H ($CDCl_3$, 25 °C) NMR spectra of **PEPEP-Br**.

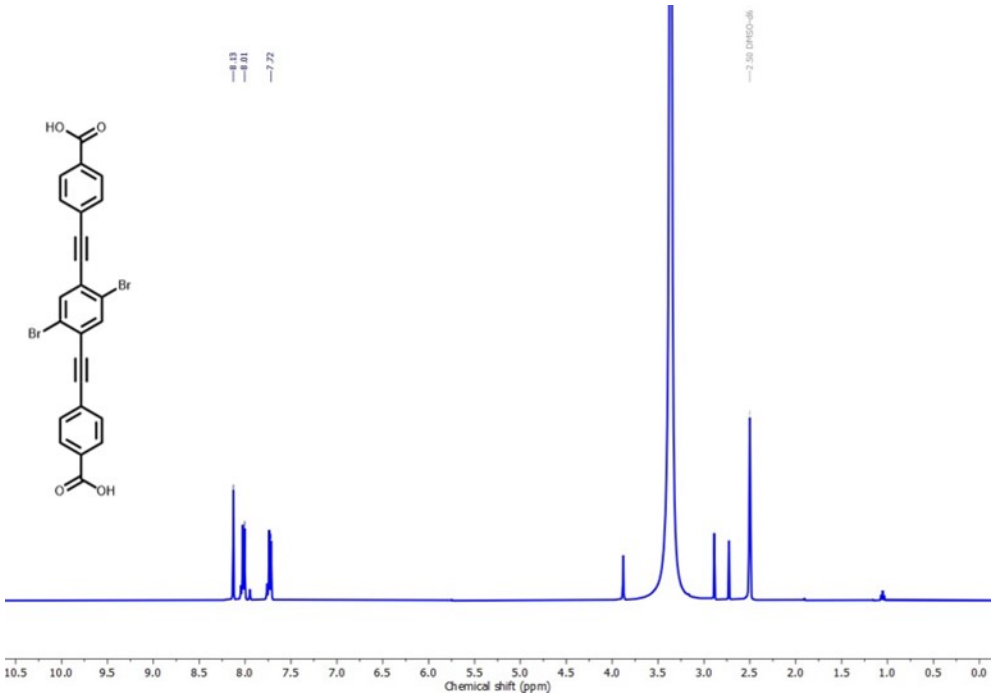

Figure S127. ^{13}C ($CDCl_3$, 25 °C) NMR spectra of **PEPEP-Br**.

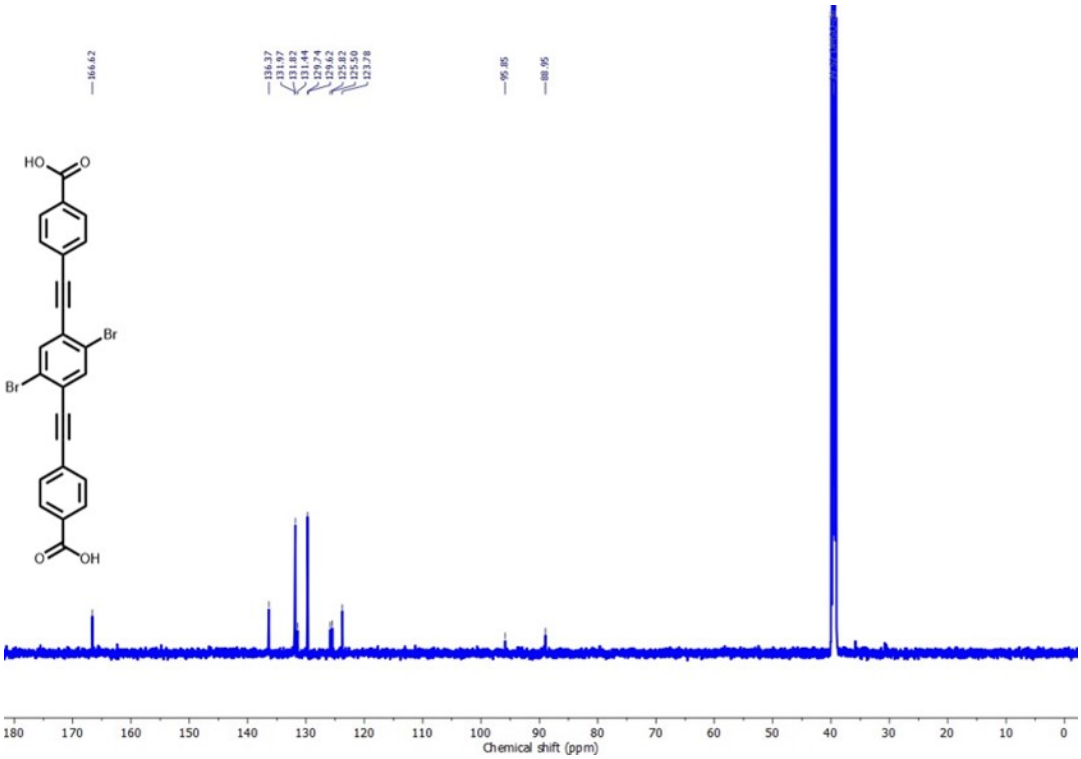

Section S10. **References:**

(S1) Newsome, W. J.; Ayad, S.; Cordova, J.; Reinheimer, E. W.; Campiglia, A. D.; Harper, J. K.; Hanson, K.; Uribe-Romo, F. J. Solid State Multicolor Emission in Substitutional Solid Solutions of Metal–Organic Frameworks. *Journal of the American Chemical Society* **2019**, *141* (28), 11298-11303. DOI: 10.1021/jacs.9b05191.
(S2) Newsome, W. J.; Chakraborty, A.; Ly, R. T.; Pour, G. S.; Fairchild, D. C.; Morris, A. J.; Uribe-Romo, F. J. J-dimer emission in interwoven metal–organic frameworks. *Chemical Science* **2020**, *11* (17), 4391-4396, 10.1039/D0SC00876A. DOI: 10.1039/D0SC00876A.
(S3) Mohammad-Pour, G. S.; Hatfield, K. O.; Fairchild, D. C.; Hernandez-Burgos, K.; Rodríguez-López, J.; Uribe-Romo, F. J. A Solid-Solution Approach for Redox Active Metal–Organic Frameworks with Tunable Redox Conductivity. *Journal of the American Chemical Society* **2019**, *141* (51), 19978-19982. DOI: 10.1021/jacs.9b10639.
(S4) Fairchild, D. C.; Hossain, M. I.; Cordova, J.; Glover, T. G.; Uribe-Romo, F. J. Steric and Electronic Effects on the Interaction of Xe and Kr with Functionalized Zirconia Metal–Organic Frameworks. *ACS Materials Letters* **2021**, *3* (5), 504-510. DOI: 10.1021/acsmaterialslett.1c00077.
(S5) Schaate, A.; Roy, P.; Preuße, T.; Lohmeier, S. J.; Godt, A.; Behrens, P. Porous Interpenetrated Zirconium–Organic Frameworks (PIZOFs): A Chemically Versatile Family of Metal–Organic Frameworks. *Chemistry – A European Journal* **2011**, *17* (34), 9320-9325, https://doi.org/10.1002/chem.201101015. DOI: https://doi.org/10.1002/chem.201101015 (acccessed 2023/06/02).
(S6) Luliński, S.; Serwatowski, J. Bromine as the Ortho-Directing Group in the Aromatic Metalation/Silylation of Substituted Bromobenzenes. *The Journal of Organic Chemistry* **2003**, *68* (24), 9384-9388. DOI: 10.1021/jo034790h.
(S7) Wang, D.; Michinobu, T. One-step synthesis of ladder-type fused poly(benzopentalene) derivatives with tunable energy levels by variable substituents. *Journal of Polymer Science Part A: Polymer Chemistry* **2011**, *49* (1), 72-81. DOI: https://doi.org/10.1002/pola.24419 (acccessed 2024/01/29).
(S8) Krause, L.; Herbst-Irmer, R.; Sheldrick, G. M.; Stalke, D. Comparison of silver and molybdenum microfocus X-ray sources for single-crystal structure determination. *Journal of Applied Crystallography* **2015**, *48* (1), 3-10. DOI: doi:10.1107/S1600576714022985.
(S9) Gómez-Gualdrón, D. A.; Moghadam, P. Z.; Hupp, J. T.; Farha, O. K.; Snurr, R. Q. Application of Consistency Criteria To Calculate BET Areas of Micro- And Mesoporous Metal–Organic Frameworks. *Journal of the American Chemical Society* **2016**, *138* (1), 215-224. DOI: 10.1021/jacs.5b10266.
(S10) Osterrieth, J. W. M.; Rampersad, J.; Madden, D.; Rampal, N.; Skoric, L.; Connolly, B.; Allendorf, M. D.; Stavila, V.; Snider, J. L.; Ameloot, R.; et al. How Reproducible are Surface Areas Calculated from the BET Equation? *Advanced Materials* **2022**, *34* (27), 2201502. DOI: https://doi.org/10.1002/adma.202201502 (acccessed 2024/03/31).
(S11) Toby, B. H.; Von Dreele, R. B. GSAS-II: the genesis of a modern open-source all purpose crystallography software package. *Journal of Applied Crystallography* **2013**, *46* (2), 544-549.
(S12) Coelho, A. Indexing of powder diffraction patterns by iterative use of singular value decomposition. *Journal of Applied Crystallography* **2003**, *36* (1), 86-95. DOI: doi:10.1107/S0021889802019878.
(S13) BIOVIA, D. S. Materials Studio 2016: Forcite. *Reflex, CASTEP* **2016**.